Modelling the oceanic meridional overturning circulation: challenges and insights

Julie Deshayes

Sorbonne Université
Ecole doctorale des Sciences de l'Environnement

Modelling the oceanic meridional overturning circulation: challenges and insights

Habilitation à Diriger des Recherches[1]

2022
Paris, France

Julie Deshayes

[1]version préliminaire du 10/01/22

Résumé

L'objectif de ce manuscrit est d'examiner en parallèle les avancées récentes dans la compréhension de la circulation méridienne moyenne (MOC) et la modélisation océanique. Même si la MOC est une structure océanique complexe, des modèles simples apportent un éclairage utile sur ses mécanismes de variabilité. Ainsi je mets en évidence que le courant profond qui exporte les masses d'eau formées par convection, et constitue la branche profonde de la MOC, reflète les fluctuations des courants de bord de la gyre subpolaire, plutôt que du taux de formation d'eau dense.

Des modèles beaucoup plus complexes, car représentant toute la dynamique océanique à l'échelle globale, remettent aussi en question le lien entre MOC et formation d'eau dense, à condition que la résolution spatiale soit suffisante pour bien représenter les courants de bord ouest. Malheureusement la production de tels modèles est coûteuse et empêche de quantifier les incertitudes liées aux choix numériques. Afin d'estimer ces incertitudes, j'ai développé un ensemble de programmes pour inter-comparer les transports dans différents modèles d'océan, de manière robuste et efficace. En inter-comparant plusieurs modèles haute résolution dans l'Atlantique Sud, j'ai montré que la MOC est actuellement dans un état "bistable", et pourrait donc diminuer brusquement si les apports d'eau douce augmentent dans l'Atlantique Nord. Par contre les modèles de climat, de plus basse résolution spatiale, ne reproduisent pas ce comportement, et auraient donc tendance à surestimer la stabilité de la MOC. J'ai montré aussi que les modèles d'océan à haute résolution convergent pour les échelles spatio-temporelles de variabilité de l'Agulhas leakage, au sud-ouest de l'Afrique du Sud, même si leurs structures dynamiques et thermohalines diffèrent. De nouveau, les modèles de climat ne parviennent pas à représenter ces échelles de variabilité, à cause de leur résolution spatiale trop faible.

Depuis 2015, je travaille à améliorer la composante océanique (de resolution 1°) du modèle IPSL-CM6. Après la production des simulations pour CMIP6, j'ai poursuivi mes investigations sur les incertitudes de ce modèle, en développant une version du modèle de resolution $1/4^\circ$ dans l'océan. La structure et l'intensité de la MOC dans les deux modèles est similaire, malgré des différences en lien avec la formation d'eau dense autour de l'Antarctique. Le résultat le plus important est que l'incertitude liée à la calibration des deux modèles est aussi importante que celle liée à la résolution spatiale. Ceci nous pousse à envisager de nouvelles manières de calibrer les paramètres des modèles d'océan et de climat, en même temps qu'améliorer les paramétrisations des processus de fine échelle spatiale dans les modèles de basse résolution.

Contents

Acknowledgements

Michèle Fieux, Juliette Mignot, Hélène Planquette, Rym Msadek, Alexandra Bozec, Fiammetta Straneo, Stéphanie Jenouvrier, Stéphanie Desprat, Ruth Curry, Anne-Marie Tréguier, Aline Blanchet,
Isabelle Ansorge, Juliet Hermes, Marjolaine Krug, Jennifer Veitch, Eva Bucciarelli, Yunne-Jai Shin,
Marie-Alice Foujols, Claire Lévy,
Anna-Lisa Bracco, Anne-Laure Dalibard, Dorotea Iovino, Sonya Legg, V. Balaji, Stéphane

à mes filles, Anita et Céleste

Chapter 1

Introduction

Circulation in the upper North Atlantic ocean primarily consists of large-scale gyres, anticyclonic (clockwise) at mid-latitudes and cyclonic (anti-clockwise) at higher latitudes (Fig.1.1). The gyres are asymmetric in nature, with widespread and relatively weak currents to the east, and rather narrow and strong return currents to the west. For this reason, the latter have a generic given name, the western boundary currents, while their counterparts in the eastern side of gyres only have geographical denominations.

The Gulf Stream is the most famous western boundary current. It transports roughly 30 Sv of subtropical water masses, northward, within 100 km offshore along the coast of Florida, before it detaches from the coast and becomes highly turbulent (purple lines in Fig.1.1). Then it entrains adjacent waters and feeds many local recirculations, so that the total transport to the south of Nova Scotia reaches up to 150 Sv.

The northeastward extension of the Gulf Stream, named the North Atlantic drift, can be tracked from Nova Scotia to Iceland and into the Nordic Seas. To the north of this flow, the upper layers are dominated by the cyclonic subpolar gyre, transporting colder and fresher water. Although they loose heat and gain freshwater as they cross the Atlantic, the waters of the North Atlantic drift are still fairly warm and saline when they reach the submarine ridge from Greenland over Iceland and Faroes to Scotland – the Greenland-Scotland Ridge.

Most of the warm and salty inflow into the Nordic Seas continues northward along the Norwegian coasts, then branches into the Barents Sea and the Arctic Ocean. On the way, it is further cooled by the atmosphere and receives additional freshwater from river runoff, precipitation, and ice melt, which transforms it into two main types of water. Roughly 30% of the warm inflow is converted into water that is very cold, but so fresh that it remains close to the surface where it combines with water from the Pacific and flows southward on both sides of Greenland to enter the subpolar gyre. The remaining $\approx 70\%$ are also cooled, but retain sufficient salinity to reach high densities. These dense waters descend and fill up the deep parts of the Nordic Seas and Atlantic ocean (black lines in Fig.1.1). The modified overflow water is supplemented by dense water from deep

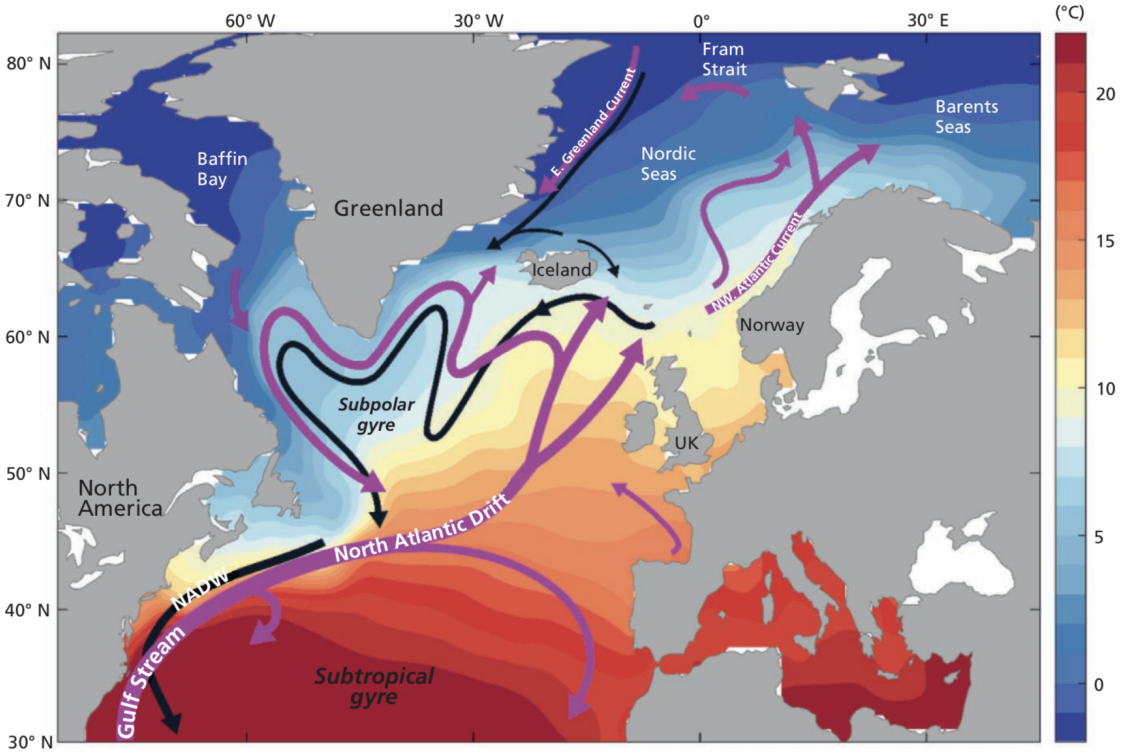

Figure 1.1: Schematic of branches of circulation in the North Atlantic (purple and black arrows indicate surface and deep ocean branches of circulation, respectively), overlaid on mean Sea Surface Temperature (data from the ECCOv4-r3 ocean state estimate). Figure taken from EASAC policy report 42 (2020) which I co-authored.

convection in the Labrador and Irminger Basins. The resulting water mass – termed North Atlantic Deep Water (NADW) – continues southward at depth, feeding the Deep Western Boundary Current (hereafter DWBC) that eventually crosses below the Gulf Stream, circa $35°$N. In the North Atlantic, the combination of all the currents described above constitutes the **Meridional Overturning Circulation** (hereinafter MOC) : **a northward drift of warm, salty water masses, and a southward return current of cold, fresh, dense water masses at depth**.

The MOC is an essential contributor to the energy balance of the Earth system, because the associated heat transport, oriented poleward in the North Atlantic, compensates for the imbalance in radiative forcing received at the surface. Rather than being constant in time, the strength of the MOC varies and abrupt climate change in the past $20,000$ yr seems to be linked to switches of the MOC from intense to weak states. When the MOC is intense like at present, dense North Atlantic Deep Water (hereafter NADW) is formed at high latitude and exported southward, compensated for

by a poleward heat transport in the upper ocean that contributes to sustain mild air temperatures in Europe. Contrastingly, the MOC was nearly or completely eliminated during the coldest deglacial intervals in the North Atlantic region, as suggested by paleo proxies, while rapid accelerations of the MOC were concurrent with the two strongest regional warming events during deglaciation (McManus et al., 2004). Notwithstanding, **little is known about the current status of the MOC and its recent fluctuations** : only few dedicated programs observed the MOC directly (RAPID-MOCHA[1], OSNAP[2], among others). In addition, those highlighted the large variability on weeks to decades, which rises uncertainty on indirect estimates. As a consequence, ocean modelling is necessary to study the MOC mean state, mechanisms of variability and future behaviour.

One essential component of the MOC is the formation of NADW, resulting from the winter densification of the surface water in the northern North Atlantic. Variability of the MOC can be related to changes in the rate of NADW formation in most simulations with oceanic General Circulation models (OGCM) in particular at coarse spatial resolution (e.g., Mignot and Frankignoul, 2005). Yet, observations (Pickart and Spall, 2007) and simulations with high spatial resolution (Talandier et al., 2014) suggest that there is no direct link between the MOC strength and NADW formation rate : meso-scale processes in the subpolar gyre and dynamics within the boundary currents determine the MOC strength and structure. **This imposes to revise "classical" mechanisms of variability** that **assume a direct link between the MOC and NADW formation** (e.g., Swingedouw et al., 2006).

NADW is mostly carried southward by the DWBC (black lines in Fig.1.1), which originates from the southward slopes of the Greenland-Scotland Ridge and in the Irminger and Labrador Seas (Dickson and Brown, 1994). Interannual variability in the DWBC remains poorly documented because of the scarceness of tailored and long-term observations, and so does its link with changes in the rate of NADW formation. The repeated in-situ observations offshore the Grand Banks reveal that the DWBC transport in that region hardly varied in two surveys 6 years apart (Schott et al., 2006, $1993 - 1995$ vs $1999 - 2005$), although hydrographic properties to the north changed substantially in the meanwhile. Downstream of the Grand Banks, the transport in the DWBC seems to be mostly influenced by the Gulf Stream, topographic Rossby waves and recirculation cells, but again the lack of long-term observations impedes to describe precisely the mechanisms of interannual to decadal variability.

Dynamics of the DWBC is expected to be complex, as much as that of the upper ocean western boundary current systems like the Gulf Stream or the Agulhas Current, which closes the subtropical Indian Ocean gyre. Again, ocean modelling is required to encompass all sources of complexity : non-linearities, interactions with topography,

[1] `https://rapid.ac.uk/rapidmoc/index.php`

[2] `https://www.o-snap.org/`

sharp horizontal and vertical density contrasts. Satellite observations provide a useful benchmark to evaluate model representations of western boundary current systems, and highlight that substantial biases remain, for example in the position of retroflection of the Agulhas Current (Penven et al. (2011)). Subsequent efforts addressed those biases in the last decade, and provided new insights on the local dynamics at play (e.g., Renault et al., 2017). It remains to reduce biases in western boundary current systems of global ocean configurations and climate models, in light of these insights.

What about the dynamics of the *deep* western boundary current systems, like the DWBC or the Agulhas Undercurrent (which flows below the Agulhas Current, in opposite direction, and constitutes the main carrier of NADW outside the Atlantic Ocean) ? There will never be the equivalent of satellite observations for their upper counterparts, so they have to be considered differently. Yet, I am convinced that model improvements dictacted by the need to reduce biases in the upper western boundary current systems, will ultimately benefit the representation of the deep counterparts. In parallel, **direct long-term observations are needed to further evaluate hence improve models** in this respect. By then, we should finally be able to model properly hence understand better the role of the MOC in global climate. Although much remains to be done, and some challenges persist regarding ocean modelling, progress has already been made in this direction, and the present manuscript aims at illustrating this.

The MOC, the North Atlantic ocean, western boundary currents and ocean modelling in general, are topics that have inspired many authors over the last 30 yrs (more than 1000 in my own readings). Hereinafter, I have made an effort to reduce the number of references to the minimum required to illustrate my narrative. Apologies to the readers of the present manuscript who feel that their work should have been quoted.

1.1 The Meridional Overturning Circulation

By definition, the MOC is the zonal integral of ocean currents, described through a streamfunction. If the vertical coordinate used to depict the ocean currents follows depth or pressure, then the sign of the MOC reflects whether, in a latitude / depth diagram, the horizontal currents describe a positive (clockwise if North stands to the right of the diagram, as in Fig.1.2) or negative (anticlockwise) overturning. In the Atlantic, two such cells are visible : a positive MOC cell associated with northward surface currents and southward displacement of NADW (around 2000m), and a negative cell associated with northward bottom flow of Antarctic Bottom Water (hereafter AABW) and southward return flow below NADW.

Box 1 : MOC computation for the novice
The construction of the MOC begins with the equation for mass conservation, with the incompressible, Boussinesq and hydrostatic approximations :

$$\frac{\partial u}{\partial x} + \frac{\partial v}{\partial y} + \frac{\partial w}{\partial z} = 0$$

where (u, v, w) are the velocities in cartesian grid (x, y, z). Integrating this equation in the zonal direction, and assuming no current through the lateral boundaries (hence the MOC is calculated in between two continental masses), yields

$$\frac{\partial V}{\partial y} + \frac{\partial W}{\partial z} = 0$$

where $\{V, W\} = \int_{west}^{east} \{v, w\}(x, y, z)dx$. According to the Schwarz theorem, and assuming that the velocities are smooth enough so that functions $V(y, z)$ and $W(y, z)$ are differentiable, there exists $\psi(y, z)$, a streamfunction named the MOC, solution to the system: $\{\frac{\partial \psi}{z} = -V \quad , \quad \frac{\partial \psi}{y} = W\}$. Calculating ψ from V and W is a 2 steps procedure :

$$\psi(y, z_b) = \psi(y_s, z_b) + \int_{y_s}^{y} W(y, z_b)dy$$
$$\psi(y, z) = \psi(y, z_b) - \int_{z_b}^{z} V(y, z)dz$$

where we assume that grid coordinates y and z equal, respectively, y_s at the southern boundary and z_b at the bottom. If we assume no current at ocean floor, ie $W(y, z_b) = 0$ then the procedure simplifies to its 2nd step : one can calculate the MOC based on the horizontal meridional velocities only, ie with no knowledge about the vertical velocities (besides the assumption of no vertical velocity near the bottom, which is only exact if the ocean bottom is flat).
Classically, the MOC strength is defined as the maximum value of $\psi(y, z)$ throughout the North Atlantic basin, or at a given latitude, for example $26°$N where RAPID observations take place since 2004, using a transport unit named Sverdrup (1 Sv$= 10^6$ m^3/s). It can be computed in other basins following the same computation (assuming no current through the lateral boundaries), as well as for the global ocean by integrating meridional velocities along all longitudes.

What remains obscure in such definition, is the connection, if any, between adjacent poleward and equatorward flowing branches. The construction of the MOC starts with the mass conservation equation, which reduces to volume conservation with the incompressible, Boussinesq and hydrostatic approximations (see Box 1.1) that are commonly made in climate models. This imposes continuous connections between

adjacent poleward and equatorward flowing branches, without specifying which type of process is responsible for such connection. In reality, the connection at high latitude is primarily realized by advection (downward), while that at low latitude is primarily due to vertical diffusion. This peculiarity calls for investigating the MOC through a more exhaustive perspective than its sole streamfunction (hence related index), for example looking at the individual currents near the surface and at depth.

Alternatively, the MOC can be constructed on the latitude / density framework : we then cumulate meridional transports in density bins rather than depth intervals (Talandier et al., 2014). In this case, connections between individual branches is more adequately described in terms of dense water formation (at high latitude) and diapycnal mixing (at low latitudes). Confronting the two different computations of the MOC efficiently highlights where the overall overturning circulation is adiabatic, ie exclusively dynamic, and where it is diabatic, ie involving changes in water mass characteristics. Actually, the MOC is a combination of both systems at most latitudes, which calls for combining the two calculations as much as possible.

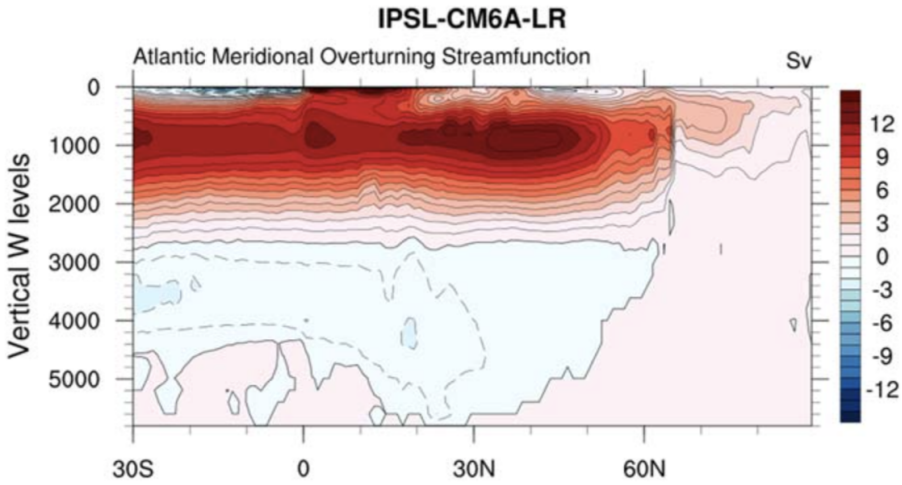

Figure 1.2: MOC streamfunction in the Atlantic Ocean based on IPSL-CM6A-LR historical simulation r1i1p1f1, on average during the period 1980-2005 (from Boucher et al., 2020).

Relevance for global oceans and climate

The MOC plays an important role in climate because of its contribution to distributing heat from the equator poleward. It is important to note here that the horizontal barotropic gyres, at subpolar and subtropical latittudes, contribute to the meridional heat transport as well, the poleward flow being overall warmer than the equatorward return

flow. Actually, in the Atlantic, fluctuations in the gyre strength and MOC strength since 1980 are closely related at interannual to decadal timescales (Deshayes and Frankignoul, 2008), and primarily responding to atmospheric variability. As a result, the MOC and MHT have highly correlated fluctuations, even at longer timescales (Fig.1.3).

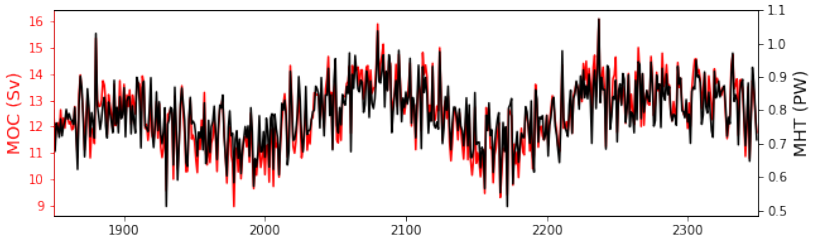

Figure 1.3: MOC strength (blue) and Meridional Heat transport (black) at 26°N in the Atlantic Ocean based on IPSL-CM6A-LR pre-industrial simulation.

There has been numerous studies and reviews on the relevance of the MOC for regional and global climates, namely the impacts of an MOC collapse or substantial weakening (Fig.1.4). On this topic, I recommend the review done by Zhang et al. (2019), which is exhaustive on both the results and their uncertainties. What is important to keep in mind, is that **the influence of the MOC on climate goes through the Atlantic Multidecadal Variability**, which is the dominant feature of North Atlantic SST variability. It has predominant timescale of 50-100 year depending on the climate model : instrumental data are too short to enable exact identification of AMV timescale. AMV anomalies considerably affect the North Atlantic Oscillation (NAO), the jet stream variability and the frequency of atmospheric blocking over the Euro-Atlantic sector, hence multiple features of Northern hemisphere climate : African, North American and Indian rainfall, Atlantic hurricanes, North American and European summer climate, winter sea ice cover and volume in the Arctic, among others. However the mechanisms underlying the AMV remain unknown. Although most climate models suggest the observed AMV reflects internal climate variability (through the MOC and the associated MHT, with the atmosphere providing stochastic forcing or coupled feedback to ocean anomalies), external factors (such as changes in greenhouse gas concentrations, aerosol loading, volcanic eruptions...) could also play a role.

There is an additional role for the MOC on global climate, related to its connection with dense water formation. The latter occurs through vertical mixing at high latitudes, which directly enriches the deep ocean with oxygen, carbon dioxide and all other components that are mostly concentrated in the upper ocean. Hence the North Atlantic is one of the strongest anthropogenic CO2 sinks, a consequence of the large heat loss during winter that leads to dense water formation, as well as the strong biological activity during

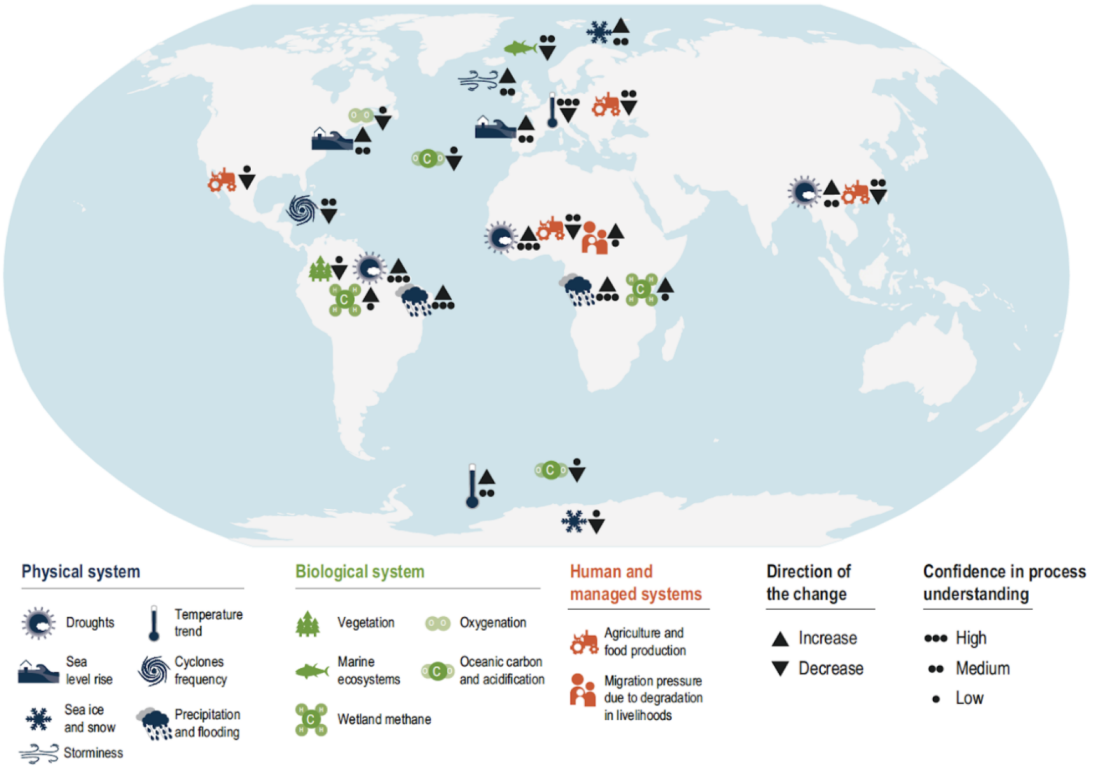

Figure 1.4: Teleconnections and impacts due to an MOC collapse or substantial weakening, taken from IPCC AR6 (2021).

spring and summer (Sabine et al., 2004). Recent observations (Mahadevan et al., 2012) and high-resolution modeling experiments (in idealized configurations Lévy et al., 2014) suggest that mesoscale and sub-mesoscale processes in the subpolar North Atlantic have a direct impact on the amplitude and timing of phytoplankton blooms. Actually, the intricacy of phytoplankton blooms and mesoscale processes related to dense water formation has been suggested a long time ago from observations in the Mediterranean Sea (Lévy et al., 1998).

Recent observations

A number of studies have indicated a weakening of the MOC (e.g., Caesar et al., 2021) although there has been some discussion to what extent they reflect persistent changes rather than a weakening phase of a variable circulation. There has also been some disagreement about which components of the MOC may have weakened.

The total MOC has been monitored along the $26°$N latitude by the RAPID-MOCHA

program since April 2004 and Smeed et al. (2014) reported a weakening over the period from 2007 to 2011, which was followed by a more stable transport (Smeed et al., 2018), and possibly a recovery (Moat et al., 2020). From more indirect evidence, Rahmstorf et al. (2015) suggested an MOC weakening on longer time-scales with a possible contribution from Greenland ice sheet melting, which has been questioned (Böning et al., 2016; de Jong and de Steur, 2016). It has also been suggested that an MOC weakening after 2005 may be a recovery from previous strengthening (Robson et al., 2016; Haine, 2016). But which components of the total MOC, amongst water entrained through the overflows in between Greenland and Scotland and water generated by deep convection in the Labrador and Irminger Basins (Fig.1.1) have weakened, if any ? The generation of Labrador Sea Water (LSW) by deep convection has been shown to be highly variable from year to year with a factor of more than 2 in LSW export rates (Yashayaev and Loder, 2016)). This and a similarly high variability for deep convection in the Irminger Basin (de Jong and de Steur, 2016) makes trend estimates uncertain. Additionally, **analysis of ARGO observations of deep convection, which I contributed to, suggests that deep convection switched from shallow to deep circa 2015, and returned to very deep winter mixing in 2016, as deep as observed in the mid 1990s** (von Schuckmann et al., 2018).

The total volume transport of overflow water is dominated by two main branches: the Denmark Strait overflow and the Faroe Bank Channel overflow, both of which have been monitored by direct current measurement combined with hydrography since mid-1990s and show no sign of weakening (Østerhus et al., 2019). The volume transport of overflow is strongly enhanced by entrainment, but a stable overflow does not necessarily imply a stable entrainment ! Transport estimates of modified overflow (overflow + entrained water) have been reported for different periods where modified overflow water traditionally has been defined in terms of density ($\sigma_\theta > 27.8$ kgm^{-3}). Remarkably, Sarafanov et al. (2012) reported exactly the same value, 13.3 Sv, for the transport of this water mass during the period 2002-2008 as did Dickson and Brown (1994) for a period prior to 1994, although Sarafanov et al. (2012) reported an uncertainty of 1.3 Sv. A direct comparison with the results from the OSNAP measurements reported by Lozier et al. (2019) for a 21-month period 2014-2016 is not as straightforward, but the overturning (in density space) between the southern tip of Greenland and Scotland reported by Lozier et al. (2019), 15.6 ± 0.8 Sv, is consistent with that reported by Sarafanov et al. (2012), 16.5 ± 2.2Sv.

As a consequence, it is crucial to **investigate direct observations and model simulations altogether to determine whether the MOC has already engaged in a significant long-term trend**, such as done by Worthington et al. (2021), who conclude that the MOC shows no decline. This opens directly to introducing what ocean model simulations are, and which uncertainties they carry over.

1.2 Ocean Modelling

In the early days of oceanography, geophysical fluid physicists tried to theorize the characteristics and movements of water masses, based on the fundamental principles of mechanics and thermodynamics. These attempts, conducted from the early 20th century, in parallel with the improvement and multiplication of oceanic observations, focused on establishing then solving the fundamental equations of physical oceanography, namely the Navier-Stokes equations. The analytical resolution of these equations (by hand) was, at that time, consistent with the very limited number of observations of the ocean. Those have led to substantial milestones in our understanding of the ocean dynamics, for example of the abyssal circulation (Stommel and Arons, 1959), currents above bottom slopes in presence of stratification (Anderson and Killworth, 1977), or on the trapping of waves along a discontinuity in topography (Longuet-Higgins, 1968), which are particularly relevant for my scientific questions.

The growing number of observations and the failures of theory to reproduce these observations have revealed the importance of complex phenomena (non-linear processes, factoring in the relief of the seabed, deep stratification), which make the equation system too complex to solve on paper. Moreover, solving these equations numerically provided a response to the emerging interest in future climate projection. In the 1990s, around ten oceanic general circulation models were developed. By distributing these models within user communities, their usage spread and model intercomparison exercises have flourished since then.

In the 2000s, a fully integrated vision of the climate system emerged, with the first models of the Earth system, of which the "blue-white-green" ocean (dynamics, sea ice and marine biogeochemistry) is a major component. Currently, these models are used for future climate projection exercises, which provide information to IPCC reports.

Most importantly, **ocean models are based on the resolution of a set of equations, derived from physical laws**. In this matter, physical oceanography differs dramatically from marine biogeochemistry or biology, where the equations have to be derived from observations or hypotheses on the behaviour of prognostic variables.

Principles

Ocean models are built on the primitive equations, i.e. the Navier-Stokes equations along with a nonlinear equation of state which couples the two active tracers (temperature and salinity) to the fluid velocity, plus additional assumptions made from scale considerations (Table 1.1). This yields the following set of equations, for example :

Spherical Earth approximation	*gravity is locally vertical and independent of latitude*
Thin-shell approximation	*ocean depth is neglected compared to the Earth's radius*
Turbulent closure hypothesis	*the effect of small scale processes, unresolved explicitly, are expressed in terms of large-scale features*
Boussinesq hypothesis	*density variations are neglected except in the buoyancy force*
Hydrostatic hypothesis	*vertical momentum equation is reduced to a balance between vertical pressure gradient and buoyancy force (this imposes to parameterize convective processes)*
Incompressibility hypothesis	*3D divergence of velocities is zero*
Neglect of additional Coriolis terms	*the Coriolis terms that vary with the cosine of latitude are neglected*

Table 1.1: NEMO physical assumptions as of version 4.0 and previous, reproduced from "NEMO ocean engine", Scientific Notes of Climate Modelling Center, 27 — ISSN 1288-1619, Institut Pierre-Simon Laplace (IPSL), doi:10.5281/zenodo.1464816.

$$\frac{\partial u}{\partial t} + \overrightarrow{u}.\nabla u - fv = -\frac{1}{\rho_0}\frac{\partial p}{\partial x} + D^u + F^u \tag{1.1}$$

$$\frac{\partial v}{\partial t} + \overrightarrow{u}.\nabla v + fu = -\frac{1}{\rho_0}\frac{\partial p}{\partial y} + D^v + F^v \tag{1.2}$$

$$\frac{\partial p}{\partial z} = -\rho g \tag{1.3}$$

$$\nabla.\overrightarrow{u} = 0 \tag{1.4}$$

$$\frac{\partial T}{\partial t} + \overrightarrow{u}.\nabla T = D^T + F^T \tag{1.5}$$

$$\frac{\partial S}{\partial t} + \overrightarrow{u}.\nabla S = D^S + F^S \tag{1.6}$$

$$\rho = \rho(S,T,p) \tag{1.7}$$

where $\overrightarrow{u} = (u,v,w)$ is the 3D velocity, p the pressure, T the temperature, S the salinity, ρ the *in situ* density (with ρ_0 as reference), f the Coriolis acceleration and g the gravitational acceleration. D^* are the parameterisations of small-scale physics

for momentum, salinity and temperature, while F^* are the forcing terms. These 7 equations are complemented by boundary conditions, specifying kinematic conditions at the surface and bottom, lateral viscosity and bottom friction. They are formulated here in vector invariant form, in a vector system linked to the Earth such that the two horizontal vectors, tangent to the geopotential surfaces, are perpendicular to the local upward vector. As a result, **the construction of an ocean model begins with the choice continuous equations to be solved, depending on physical assumptions as well as the definition of the vector system**.

If the target is to solve the model numerically, then next step is to employ mathematical algorithms to transform the set of continuous equations into a discretized format, suitable for digital computation - this constitues the basis for OGCM. Otherwise, one may simplify further the set of equations, consistently with the scientific question to be addressed, and eventually solve the problem analytically (see Deshayes and Frankignoul, 2005, and 2.1).

The ensemble of mathematical recipes to discretize a given set of continuous equations, defines an OGCM. Further decisions must be made before producing actual numerical results, such as the grid resolution, forcings and boundary conditions, which constitutes the characteristics of a configuration of that model. Then a numerical simulation is eventually produced, on a specific computational infrastructure (which also has impacts on the results, unfortunately). All three steps defined above carry over their own sources of uncertainties, which can be roughly classified in three types (Table 1.2). **Assessing the validity of a numerical solution to a given scientific problem implies to quantify all these uncertainties**, and it is obviously not straightforward. In addition to technical difficulties, this is related to the uncertainty of observations and to the intrinsic chaotic nature of climate, hence it is likely that a complete quantification of the uncertainties of an ocean numerical simulation is not possible. Intercomparing different numerical solutions to the same problem, gives a more direct yet rough estimate of the overall uncertainties.

Ocean Model Intercomparison Projects

Intercomparing ocean model simulations at global scale was initiated in the early 1990s within the World Ocean Circulation Experiment, a large international program focussed on observations, and identified as the Community Modelling Effort (hereafter WOCE CME). The original goal of this effort was "**to evaluate the performance of state-of-the-art ocean models through direct comparison with observations and to help guide future model development efforts**" (Böning et al., 1996). It is quite puzzling that a 25-yr-old sentence could be published, today, exactly as is !

Many studies were published in the context of WOCE CME and those focussing on the North Atlantic clarified the role played by the outflow of dense water from the Greenland and Norwegian seas onto the mass transports in the subpolar gyre (e.g.

structural uncertainties	*due to the initial choice of equations, hence physical assumptions supposedly relevant to the scientific question, plus the choices of algorithms to discretize the continuous equations*
parametric uncertainties	*involve all the parameters that define a configuration, in particular the representation of subgridscale processes*
intrinsic uncertainties	*gather all factors external to the system (boundary conditions, initial condition...) that are most often partially known*

Table 1.2: Uncertainties associated with the numerical resolution of an ocean model.

Böning et al., 1996). They also highlighted that convective mixing in the Labrador and Irminger Seas, has only little effect on the net sinking of upper-layer water in the subpolar gyre - a result that is now confirmed by observations (e.g. Lozier et al., 2019, a subject that I review in section 3). Finally, Böning et al. (1996) demonstrated that realistic MOC strength can be obtained, provided that adequate horizontal resolution and mixing parameterizations are employed to avoid spurious mixing (a topic that motivated the ANDIAMO project, which I co-lead, see section 5.2).

However, at that time, there was little consensus regarding the design of global ocean-ice experiments, especially those run for centennial and longer time scales. It is remarkable that the atmospheric modelling community was more advanced in this regard, as the Atmospheric Model Intercomparison Project started in the early 1990s (Gates, 1992). Additionally, there was two methods employed to force the models : by imposing fluxes at the surface or employing bulk formulae to factor in ocean surface biases in the flux computation. A preliminary step to intercompare global ocean-ice experiments was to converge to a common forcing strategy (Large and Yeager, 2004), before testing the hypothesis that global ocean-ice models run under the same atmospheric state produce qualitatively similar simulations. Griffies et al. (2009) found that the validity of this hypothesis depends on the chosen diagnostics. **For the North Atlantic MOC, they highlight the large diversity in mean strength and structure, which is due to structural uncertainties (in particular the choice of vertical coordinate) as well as uncertainties in the freshwater fluxes at the ocean surface** (those are compensated for with restoring in sea surface salinity, that happens to have a significant influence on the MOC strength, at least at coarse resolution). The second phase of CORE experiments did not see much progress in the convergence of MOC strength nor shape (Danabasoglu et al., 2014), although the number of contributing models increased from 7 to 18 ! It is roughly the same number of models that participated in

the Ocean Model Intercomparison Project (hereafter OMIP), included in CMIP6 exercice that informed IPCC AR6. Before I participate in this exercice (see section 4.2), I already contributed to ocean model intercomparisons through the development of a new framework, named Physical Analysis of a Gridded Ocean (PAGO, see section 3.2).

Current challenges

Fox-Kemper et al. (2019) revisit the challenges and prospects for ocean circulation models since 2010, encompassing all aspects of ocean modelling : from the equations and mathematical algorithms to discretize, to the inventory of physical processes represented and/or parameterized, via the procedure to assess model simulations against observations. I presented this review to students of LOCEAN in June 2020, and combined figures and schematics from various sources to illustrate each section of the publication [3]. I fully support the conclusion of Fox-Kemper et al. (2019), that progress has been made in many fronts for the last decade : increasing grid resolution, improving numerical algorithms, enriching subgrid scale parameterizations, as well as representing better the interaction with the other climate components (the atmosphere, cryosphere and biogeochemistry). Notwithstanding, I feel like many questions remain unanswered, and those were already identified when I started my PhD :

- We continue **restoring sea surface salinity in ocean-only simulations**, and eventually apply it under sea ice as well, supposedly to compensate for the lack of observations at high latitude, but in reality to contribute to **fine tuning the MOC strength** ! What is the rationale for doing so in long-term simulations ?
- Little is known about how the **initialisation procedure of an ocean model** is impacting the mean state, not to mention processes of variability... This issue is critical when representing ocean cavities under continental ice sheet (see section 4.6).
- When developing a new configuration, ocean modellers are often faced with **numerical instabilities**, which they counteract by reducing the time step. This is an efficient solution, indeed, but it dramatically increases the computational cost, a characteristic that is still rarely factored in when designing numerical experiments. And it eludes the need to re-consider the range of stability of an OGCM, in particular when parameters are otherwise chosen so as to increase energy at small spatial scales.
- **Estimating properly the uncertainties in numerical simulations** is the new prerequisite, to me. To the minimum, the parametric uncertainty should be ac-

[3] https://docs.google.com/presentation/d/1Ls7SyFOUUMxZuxmUnJ6Lg5eOXqHhqMR5_2QbDHkURGw/edit?usp=sharing

knowledged. In other words, a set of parameters that yields to relatively small biases against observations, is not satisfactory ! Intercomparisons of high resolution regional simulations agree on a single conclusion : that they are far from numerical convergence, still.

- Since 2015, I have observed a series of pushes to increase stepwise the horizontal resolution of climate models, including their ocean component, up to kilometric scale. Nowadays, this motivation underlines the "digital twin" fixation, that seems to conceal the added value of coarse resolution long-term simulations, yet crucial for climate applications.

- There is an active research on numerical algorithms, but they seem to exclusively support the trend of increasing spatial resolution, while there is a need to revisit those employed in coarse resolution models, to finally reduce spurious mixing, for example.

1.3 Plan

The objective of this manuscript is to review in parallel recent advances in [i] understanding of the MOC and [ii] ocean modelling. Ocean modelling is often seen as a methodology, producing tools that may be useful to answer a given scientific question. I strongly disagree with this vision, and **I rather consider ocean modelling as a science, merging concepts of applied mathematics, physics for geophysical fluids and computing sciences**. On the other hand, the MOC is such an obscure geophysical object, yet ubiquitous in every discussion about future climate (whether involving climate scientists or general public), that it cannot be discussed independently of the method employed to represent it.

To begin this overview of ocean models, the first chapter reviews studies of the MOC using simple models, that resolve a very simplified set of equations, much simpler than the full primitive equations. These allow in depth understanding of the processes at play in these equations, but their contribution to understanding the real ocean may be limited. In this chapter, I will come back to the link between dense water formation and the MOC, briefly mentioned in introduction.

Second chapter illustrates studies performed with OGCM simulations : as those resolve the full primitive equations, they represent all possible oceanic processes at play in a given spatio-temporal context. As a consequence, in depth analysis of the mechanisms of variability is more challenging. In addition, different OGCM most often produce different simulations, albeit with same (at least similar) external constraints and boundary conditions. Therefore inter-comparison of different simulations is the main focus of this chapter, for the ocean circulation in 3 regions of interest : the North Atlantic, the South

Atlantic and around Southern Africa. These 3 regions, which are equally important for the MOC, host western boundary currents that remain a challenge for ocean modellers.

Finally, climate models are at the center of the third chapter that covers the most recent achievements with NEMO for CMIP6, the ongoing development plans and the challenges and opportunities for future ocean and climate models. In this chapter, the global MOC and its impact on climate are discussed.

In Appendix extra information are gathered, as requested by SU to deliver the habilitation diploma : the list of my publications and the list of Master and PhD students that I supervised. Finally, at the end of the manuscript, the pdf of 5 selected publications is inserted.

Chapter 2

Idealized Models

At the beginning of my PhD, I worked with a $1^{1/2}$ layer model of the MOC, focussing on the adjustment of the upper ocean circulation to dense water formation, represented by changes in the meridional transport at the northern boundary of the domain (Deshayes and Frankignoul, 2005). I also developped simple models during my postdoc, this time to comprehend better the ocean dynamics in the vertical direction, to differentiate vertical advection (aka "sinking") from mixing.

In a convective basin, **dense water formation is induced by fluxes of buoyancy, predominantly heat, from the ocean to atmosphere**. The net annual heat loss is balanced by the convergence of heat by the oceanic circulation, via the surrounding boundary current (Spall, 2004). In this idealized picture of a convective basin, another component has to be introduced to close the heat balance. The exchange of properties between the interior and the boundary current is achieved via turbulent transfers associated with baroclinic instabilities, due to the density gradient between the interior and the boundary current. When adapted to the Labrador Sea, the conceptual model of Straneo (2006b), which employs a parameterization of these turbulent fluxes, reproduces seasonal and interannual fluctuations of the basin stratification and circulation that are similar to observations (Straneo, 2006a). This suggests that **eddies play an essential role in convective basins such as the Labrador Sea** that extends beyond their small spatial scale ($<$20 km) and their short lifetime (of the order of a few months), which is consistent with observations (Lilly et al., 2003) and other modeling studies (Eden and Boning, 2002; Katsman et al., 2004; Chanut et al., 2008). **Wind forcing also acts over the convective basins and may affect dense water formation and export** through various processes: [i] buoyancy forcing through latent heat fluxes, [ii] Ekman transport of heat and freshwater in the upper ocean, [iii] vorticity input by the wind affecting the density distribution, which may precondition (or not) the water column and favor (or inhibit) buoyancy-driven convection (Marshall and Schott, 1999) and [iv] circulation around the convective basin that determines the amount of heat entering the basin. The object of my postdoctoral scholarship at WHOI, was to investigate the

subset [iv] of the possible effects of wind over a convective basin, and I pursued it with the two idealized models of respectively Straneo (2006b) and Spall (2004).

2.1 A conceptual model of the mechanisms of variability in the Labrador Sea

By geostrophy, the large-scale cyclonic circulation around a convective basin is sustained by buoyancy forcing and dense water formation in the interior of the basin, but it is also driven by large-scale wind forcing. Similarly, variability of the boundary currents can be induced by changes in both wind and buoyancy forcings. However, hindcast simulations of the North Atlantic circulation suggest that variability induced by changes in the wind forcing over the subpolar gyre is the main driver of interannual variability of the boundary currents (Eden, 2001). Hence we address one question in Deshayes et al. (2009) : how do changes in the large scale circulation around a convective basin impact dense water formation and export ?

I adapted the model of Straneo (2006b) so as to include an influx of dense water, proportional to the strength of the barotropic component of the boundary current, that is identified as the second forcing in addition to surface buoyancy fluxes in the interior (Fig.2.1). Moreover, while Straneo (2006b) focused on the steady state circulation and its seasonal fluctuations, I considered the variability of the formation and export of dense water due to seasonal to decadal variability in both forcings.

Deshayes et al. (2009) (full text inserted at the end of this manuscript) presents the equations of the revised model, analytical solutions and a numerical framework to apply forcings from the "real" Labrador Sea. **We first show that changes in dense water formation are influenced by changes in surface buoyancy forcing, but are not sensitive to (wind-driven) changes in the barotropic boundary current**. Specifically, the interior tends to integrate the fluctuations in surface buoyancy forcing with a decadal time scale, that is set by eddies (parameterized in this conceptual model). Hence the interior of the basin exhibits most variability at decadal and longer periods, and reduced variability at higher frequency with respect to the variability of the surface buoyancy forcing. That dense water volume in the interior of the Labrador Sea integrates the surface buoyancy forcing is not surprising and consistent with observations of potential energy anomalies in the interior of the basin from 1950 to 1997 Curry and Mccartney (2001). However, **that small spatial scale, short-lived eddies may be responsible for a predominant decadal variability in the Labrador Sea is a major insight of this study**.

The integrating mechanism, which can be seen as a memory of the interior Labrador Sea, does not appear in the dense water export whose variability is instead dominated by changes in the barotropic boundary current forcing via the inflowing transport of

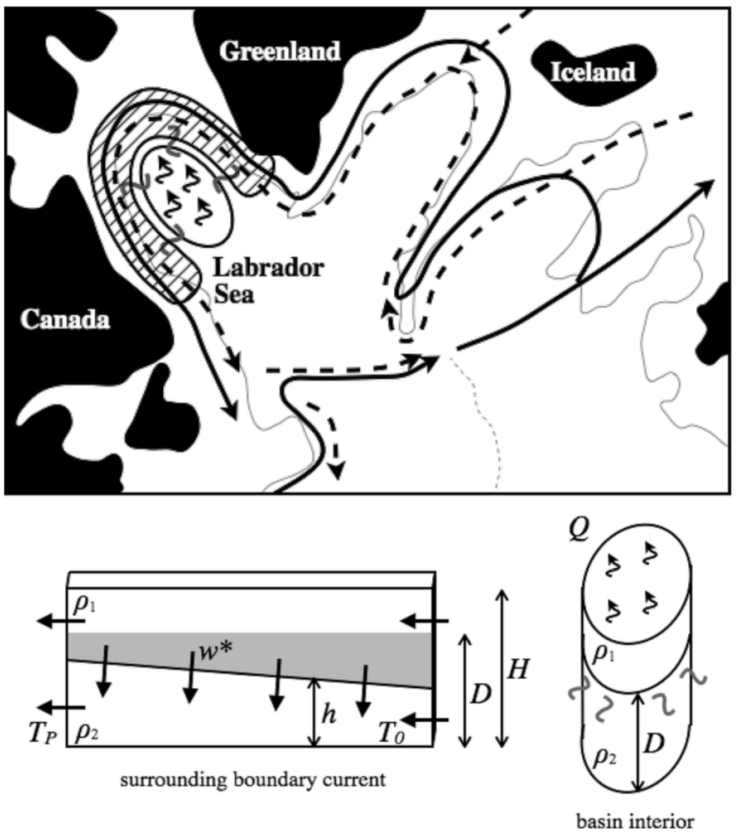

Figure 2.1: Schematic of the circulation in the North Atlantic (top, plain lines for warm water in the upper ocean, dashed lines for cold water at depth) and localization of the region of dense water formation in the central Labrador Sea (thin black line) and the surrounding boundary current (hatched area). The connection between the interior region, where dense water is induced by heat loss at the surface (black winding arrows), and the surrounding boundary current that exports the newly formed dense water, is primarily due to turbulent heat fluxes (gray winding lines). Bottom: schematic of the two regions of the conceptual model, where the forcings are Q the surface buoyancy fluxes in interior and the barotropic boundary current strength that sets T_0, the inflow of dense water. w^* is the diapycnal mass flux within the boundary current, which transport of dense water at exit, T_P, is the prognostic variable of interest.

dense water. Indeed, variations in the barotropic boundary current forcing induce an increase in the variability of dense water export on interannual to decadal time scales, compared to variability of dense water export induced by changes in the surface buoyancy forcing alone (Fig.2.2). This suggests that **interannual variability of dense water transport by the DWBC at the ouflow of the Labrador Sea is primarily induced**

by fluctuations in the wind-driven North Atlantic subpolar gyre. Noteworthy, variability in the diapycnal mixing within the boundary current, i.e. variability in the poleward heat transport in this simple model, has maximum variance at decadal and longer periods and reduced variance at higher frequencies, similarly to variability of dense water formation.

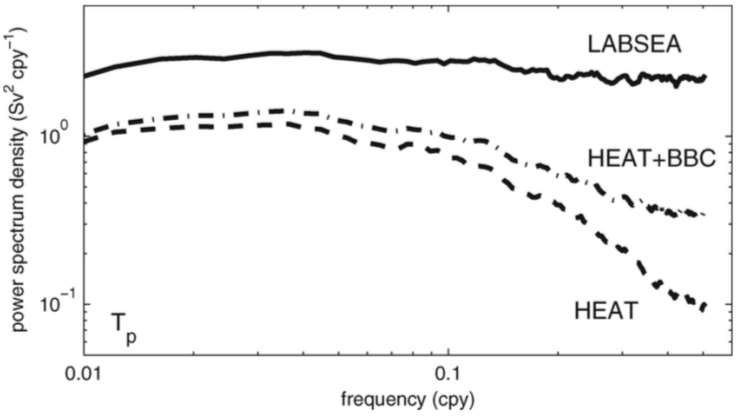

Figure 2.2: Power spectrum density of dense water transport by the DWBC at the outflow in 3 experiments : LABSEA with interannual variability in both forcings of similar amplitude as the "true" Labrador Sea (plain line), an experiment with reduced interannual variability in the barotropic boundary current strength (HEAT+BBC, dash-dotted line) and an experiment with no interannual variability in the barotropic boundary current strength (HEAT, dashed line). Spectra are calculated with the multitaper method using five windows, from ensembles of 100 simulations that start from the same initial conditions (the steady state from a spinup) but use different random time series for the interannual forcings.

2.2 Instabilities in a convective basin

The second project that I developed as a postdoctoral scholar built from Spall (2004) framework to understand better what controls the properties of water mass transformation and the surrounding boundary currents in marginal seas subject to buoyancy loss. This study introduced an idealized configuration of the MIT primitive equation numerical model (Marshall et al., 1997), representing a semi-enclosed circular basin connected to an "open ocean" through a channel, with slopes in the rim of the basin and flat bottom in the interior (Fig.2.3). My objective was to determine the **influence of barotropic instability of the boundary current**, as an additional source to the turbulent exchanges

of heat in between the interior of the basin, subject to surface buoyancy loss, and the surrounding boundary current, which advects heat into the basin.

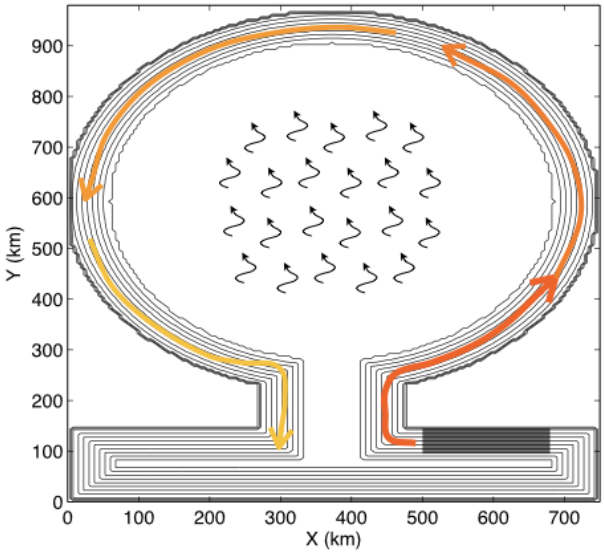

Figure 2.3: Bathymetry of an idealized convective basin (contour interval 100 m, ie the flat area is at 1000m depth), forced by surface buoyancy fluxes in the interior (represented by wiggling arrows) and a barotropic boundary current (applied through restoring in the dark grey shaded area). Coloured arrows represent the circulation of the boundary current around the basin, relatively warm at the inflow and progressively colder as it loses heat due to turbulent exchanges with the interior.

In our configuration, MITgcm solves the momentum and density equations using 10 levels of identical depth, with partial steps algorithm to smooth the bathymetric slopes. The model retains a free surface. A linear equation of state is used so that density is proportional to temperature. The stratification is chosen uniform at the initialization, and such as the internal deformation radius is approximately 17 km (Coriolis parameter is 10^{-4}s^{-1}, constant). The horizontal resolution is 5km, so this configuration is considered eddy permitting. Surface buoyancy forcing is applied identical to Spall (2004) : 20 Wm^{-2} of heat loss are imposed uniformly over the circular basin during 3 months, and then surface fluxes are set to zero for the rest of the year. In parallel, the boundary current is restored to the initial stratification in a region upstream of the inflow to the basin (Fig.2.3, gray shaded area), with a 1 day timescale. This provides an infinite source of buoyancy to the boundary current hence the interior, to compensate for the surface heat loss. Additionally, in this study only, we apply restoring of the barotropic velocities in the same area, so that the barotropic boundary current at the inflow of the basin varies from 0.03 ms^{-1} (which corresponds to no restoring, ie same as in Spall,

2004) up to 0.44 ms^{-1}. All simulations are spunup for 10 to 25 yr, until a statistical steady state is reached.

Enforcing a barotropic component to the boundary current, which is superimposes on that driven by geostrophy only, **has an impact on** the interior solution hence **dense water formation as it modifies the structure of turbulent fluxes in between the boundary current and the interior of the basin**. Close to the inflow, the boundary current is more stable as its barotropic component increases, and the maximum energy center migrates downstream, consistently with the energetics of local instability of barotropic jets (e.g. Mak and Cai, 1989). We apply the diagnostics for eddy energy sources as in Böning and Budich (1992) to further understand the impact of the barotropic boundary current onto the horizontal turbulent fluxes between the interior and the boundary current (Fig.2.4). For the turbulent fluxes due to baroclinic instability, their vertical structure substantially changes with the strength of the barotropic boundary current : while they are limited to the upper part of the basin (0-500m depth) in the case with no restoring, turbulent fluxes below 500m depth increase as the barotropic boundary current increases, and rapidly become predominant (magenta bars in Fig.2.4). This seems to be due to along-slope downwelling that brings heat at depth, increasing the horizontal density gradient hence baroclinic instability. Above, turbulent fluxes due to baroclinic instability also increase with the barotropic boundary current strength, through intensification of the density gradient between the interior and the boundary current (blue bars in Fig.2.4). But this effect rapidly saturates for moderate barotropic boundary currents, and for strong barotropic boundary currents, the turbulent fluxes above 500 m due to baroclinic instability reduce drastically. In the meanwhile, **turbulent fluxes due to barotropic instability develop with increasing barotropic boundary current**, but remain smaller than those due to baroclinic instability (gray bars in Fig.2.4).

These results have not been published yet, because they seem to be strongly related to the along-slope downwelling that developed within the boundary current, and I wanted to evaluate more how this process was affected by modelling choices. In particular z-level models are not the most adequate to resolve bottom boundary layers, so I wonder how much the solution would differ using a sigma-layer coordinate model. Also the presence of "corner" in the coastlines produce significant dissipation, that may have an impact on the dynamics of the boundary current. Note that all the results mentioned above are obtained with "no slip" lateral boundary condition. Controlling better the viscous dissipation along the boundaries would help ensuring that we are mimicking an analog of the Labrador Sea. Finally the horizontal resolution is not sufficient for the model to be eddy permitting, so there may be some dependence on the numerical choices.

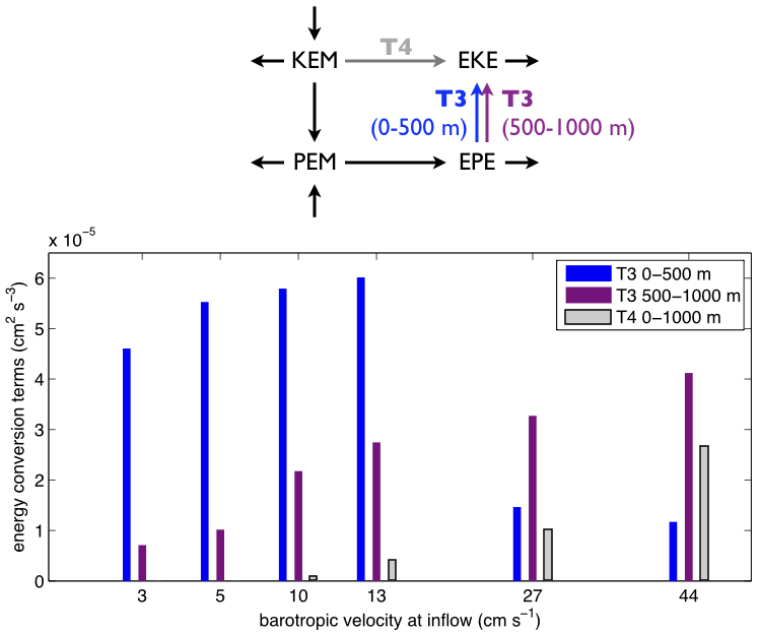

Figure 2.4: Sources of eddy kinetic energy as a function of the barotropic boundary current strength at inflow, due to baroclinic instability in the upper and deep part of the water column (respectively blue and magenta) and from barotropic instability (gray).

2.3 Perspective : on the use of test cases

The use of test cases (idealized configurations with simple boundary conditions and forcings, resolving a given set of equations) has proven efficient in the development process of OGCM : to reveal numerical bugs, determine advantages and pitfalls of certain numerical choices, and highlight remaining challenges. Test cases are also useful for ocean model intercomparisons : complexities and non linearities in boundary conditions and forcings may hide the points of divergence (in the equations solved, the discretization schemes employed and/or the parameterizations introduced).

To begin with, one has to define the set of continuous equations to be solved, simpler than the full primitive equations. These equations represent a specific scientific question that the test case is supposed to address. They can be simple enough to solve analytically, but most of the time they require a numerical resolution. The numerical configuration of a test case is, by definition, simple hence idealized as compared to the real ocean : grid can be rectangular even at high latitude, bathymetry is either absent (so-called flat bottom) or very simple like a linear slope, a canyon or a gaussian sea mount, coastlines are straights, forcings are mostly analytical. With such a simple configuration, numerical resolution can be super fast, and that enables to produce multiple simulations to explore

sensitivity to choices in numerical and physical parameters. The latter is the reason why I claim that test cases are great supports for training, not only in ocean modelling, but more generally in physical ocean dynamics.

In case an analytical solution exists, then the test case can be used as a validation tool when developping ocean general circulation models and eventually incorporated in an ensemble of automatic verification procedures. Because of the simplicity of the configuration, test cases are great for intercomparison of ocean general circulation or hydrodynamic models. They are also useful for training in physical oceanography, beyond ocean modelling exclusively, as they enable producing suites of sensitivity experiments to explore the choices in numerical (e.g. grid spacing) and/or physical (e.g. Coriolis) parameters.

a suite of test cases to comprehend ocean dynamics

To my view, the most simple and fundamental representation of ocean circulation employs a rectangular basin driven by analytical winds. At first, stratification can be very idealized and homogenous over the whole water column or over the moving top layer. This test case then represents the wind-driven gyre, with Sverdrup adjustment in the interior and intensified return current to the west. One can explore how viscosity and friction control the boundary current strength and width, as well as stability. With such a simple test case, one can already comprehend the fundamentals of subtropical gyres, but also explore more recent questions such as the seasonality of the western boundary current (Hutchinson et al., 2018). It can easily be expanded to cover a subpolar gyre as well. And when rotating the grid lines away from Coriolis direction, we can see even more the impact of lateral boundary conditions and straight coastlines on the solution.

Adding buoyancy forcing to the rectangular basin allows to investigate Gulf Stream dynamics, and the respective contribution of eddies to northward heat transport and the meridional overturning. Then one can play with horizontal resolution of the grid, to make sub-meso-scale processes appear, and then test parameterizations of their effects on the large scale. With a slightly more complex stratification, interactions between the upper gyre and the deep circulation will take place, opening up all the questions about variability of the MOC, whether it is wind or buoyancy forced, hence decadal predictability of European climate.

Another simple configuration was developped to study the Gulf Stream, that is the periodic east-west channel with adjacent water masses of different densities to produce baroclinic instability. Later on, this configuration was transposed to the southern ocean, as it also represents the fundamental ingredients of the Antarctic Circumpolar Current. Such a configuration is very useful to explore the direct and inverse energy cascades, in between the basin-scale zonal jet, meso- and sub-meso-scales, all the way to dissipation scales. In particular when adding stochastic wind forcing similar to the well known

southern ocean storms, and irregularities to the flat bottom to enhance dissipation of internal waves.

But the true ocean has no walls and rather a sloping bottom, which has a substantial effect on ocean circulation. The iconic test case to visualize this is the overflow : a dense plume on top of topographic slope, that entrains ambiant water through its descent. This test case can be defined as a zonal slice, or fully 3D. It is mostly used for comparing z-level, isopycnal and sigma models, but also for advection schemes that affect spurious mixing. To my view, this test case mostly reveals the influence that ambient stratification has on propagation and mixing of the dense plume, which makes difficult to extrapolate the sensitivity to numerical choices to realistic ocean configurations.

There exists many other test cases, like the one for convective basins developed by Spall (2004) that I played with during my postdoc, and also a rectangular equatorial basin to represent zonal jets along the equator, the propagation of a soliton over flat bottom, the flow of a barotropic current along topography... There also exists some specific to coastal processes, like wind-driven upwelling, river plumes, or wetting and drying. Some test cases are specifically designed to test numerical features, like the spurious diapycnal mixing induced by advection schemes, errors in the computation of horizontal pressure gradients, or propagation of an eddy throughout nested grids to test local grid refinements. Others are employed to comprehend some aspects of the dynamics at play, and how they depend on external forcings.

what's next ?

Ocean model development is more than developping a numerical tool that can be used by others. Developping test cases at the same time as new codes / schemes / parameterisations seems wise, for validation purposes. Beyond ocean model development, test cases are helpful to training in physical oceanography, not only for ocean modelling, as they allow to comprehend fundamental ocean processes and mechanisms of variability. Also test cases are, by definition, faster and cheaper to run than realistic configurations - this enables to play with all the components of one setting, from numerical to physical aspects, at reasonable human and computing cost. Finally, climate change makes innovation in ocean modelling vital ; all forces, including from other disciplines, are welcome. Test cases can be seen as a playground to collaborate with experts in fluid mechanics, applied mathematics... This is the venue that I am currently exploring within the ANDIAMO project (see section 5.2).

Chapter 3

Ocean hindcasts

The variability of the DWBC, which constitues the deep branch of the MOC in the North Atlantic, is intimately linked at high latitudes to the variability of the subpolar gyre. A better understanding of the mechanisms of variability of the subpolar gyre is therefore essential for understanding the variability of the MOC in the North Atlantic. The interannual variability of the subpolar gyre is largely driven by wind fluctuations (Eden, 2001; Deshayes and Frankignoul, 2008). Atmospheric buoyancy fluxes also force the boundary currents via isopycnal upwelling and dense water formation in the interior of the basins. In addition, the subpolar gyre is influenced by mechanisms of variability at subtropical latitudes via the North Atlantic Drift, and at higher latitudes via exchanges through the Greenland-Scotland sills. In contrast with the simple models illustrated in the previous section, investigating these various processes altogether requires solving an OGCM with as realistic boundary conditions and forcings as possible, and evaluating against all possible observations. Note that this automatically limits the time range of analysis to the last decades. Such a simulation of an OGCM, designed so as **to produce ocean variables as comparable to direct observations as possible**, is called an ocean hindcast.

This chapter aims at illustrating some advantages and pitfalls of manipulating ocean hindcasts for the MOC, while progressing on the understanding of the various dynamics of the MOC. The chapter starts in the North Atlantic, but finishes in the South Atlantic, where the MOC's transport of freshwater is an indicator of its stability. Besides, the Agulhas Current is another western boundary current, analog to the Gulf Stream, in particular for the presence of an underlying current in the opposite direction. I am convinced that improving the numerical representation of the Agulhas Current and Undercurrent will eventually benefit the numerical representation of the Gulf Stream and DWBC.

3.1 Modelling ocean currents in the North Atlantic

In climate models with coarse spatial resolution (of the order of 1°), as well as in realistic OGCM simulations that reproduce the North Atlantic circulation at higher spatial resolution ($20 - 100$ km), the variability of the MOC is directly linked to the variability of the rate of dense water formation in the subpolar gyre. However, in regional observations and simulations of even higher spatial resolution ($1 - 20$ km), the link between MOC variability and fluctuations in the rate of dense water formation is not direct and mesoscale processes, influenced by the circulation and stratification in the subpolar gyre edge currents, play a decisive role (see section 2). Deshayes et al. (2009) suggest that the variability of the DWBC is very little affected by convection fluctuations. This result is consistent with the observation-based study of Pickart and Spall (2007) and recent observations from the OSNAP program (Lozier et al., 2019), who suggest that the formation of dense water in the Labrador Sea has a very small influence on the MOC. Rather, Deshayes et al. (2009) suggest that the variability of DWBC is dominated by fluctuations in the intensity of the boundary currents of the subpolar gyre and the characteristics of water masses advected into the Labrador Sea. Progressing further in understanding the drivers of DWBC variability, which cannot be done investigating observations alone as they are too sparse, requires ocean hindcasts as realistic as possible for both the circulation at the surface and at depth.

from NATL12 to SAKAI

I started to work with NEMO ocean hindcasts in 2007 with the setting up of a $1/12^\circ$ resolution North Atlantic configuration led by Anne-Marie Tréguier (CNRS, LOPS), supposedly the first eddy-resolving configuration produced with NEMO in the North Atlantic. A first long simulation ($1980 - 2000$) was carried out in 2008. This simulation showed a contraction of the subpolar gyre from 1996 onwards with an amplitude that is much too strong compared to observations, hence it was decided to exploit this simulation in regions away from the subpolar gyre only, for example at subtropical latitudes (Maze et al., 2013; Treguier et al., 2012). In parallel, I decided to develop a new regional configuration of NEMO for the subpolar gyre, baptized SAKAI (Fig.3.1). SAKAI configuration covers all boundary currents of the subpolar gyre, but does not reach the eastern boundary of the North Atlantic to limit computational cost. I developed two versions of the configuration, of resolution $1/12^\circ$ and $1/24^\circ$, ie respectively $2 - 3$km and $1 - 2$km, to test sensitivity to grid resolution. Boundary conditions were prescribed, every 5 days, with outputs from either NATL12 simulation or GLORYS12, which is the ocean renalysis at $1/12^\circ$ produced with NEMO by Mercator (ie assimilating observations).

All these experiments did not lead to any publication, because SAKAI suffered from one major bias along its southern boundary. This materializes in the surface dynamics as a plume of EKE penetrating into the domain from the south west boundary, which is not

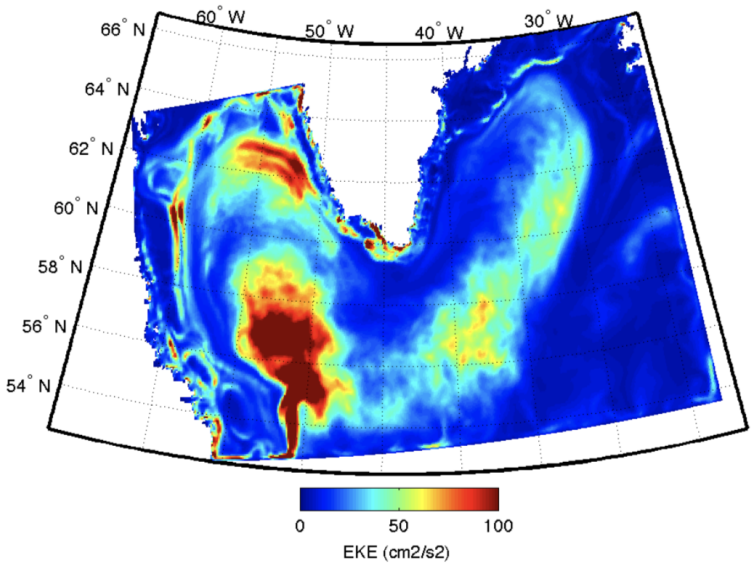

Figure 3.1: Surface eddy kinetic energy in SAKAI configuration for the period 1990-1999.

realistic (Fig.3.1). Indeed, inconsistencies between the internal dynamics and conditions applied at the boundary, create a strong return flow opposite to the Labrador Current that does not exist in reality. Finally, I concluded that **it is not possible to fine tune the dynamics in the interior of the subpolar gyre using a regional configuration and at the same time avoid inconsistencies between the interior dynamics and the boundary conditions at the exit of the Labrador Sea**. This encouraged me with using the nesting capacity of NEMO.

from SAKAI to ERNA

The ERNA configuration (for Eddy Resolving North Atlantic) combines the ORCA05 global configuration (of resolution $1/2°$) with a $1/8°$ horizontal resolution AGRIF zoom (two-way nesting, Debreu et al., 2012) that covers the North Atlantic from $20°$N to $75°$N. In the zoom, the cell sizes range from 12km in the south to 7km in the north. ERNA therefore explicitly resolves mesoscale processes up to about $35°$N. Further north, it is only considered eddy permitting. The ice model is also subject to mesh refinement, and sea ice properties are exchanged between global and zoom configurations. I manually fine tuned the bathymetry along Florida, by hand, so as to avoid an overshoot in the Gulf Stream downstream Cape Hatteras. The improvements in currents with zoom, compared to lower resolution global configurations ($1/2°$ and $1/4°$), are dramatic for the Gulf Stream detachment (Fig.3.2), the position of the North Atlantic drift and the DWBC in the whole North Atlantic (see Fig. 4 of Talandier et al., 2014, inserted at the

end of this manuscript). Note that Fig.3.2 also illustrates that a proper Gulf Stream detachement is not automatic at $1/12°$ resolution.

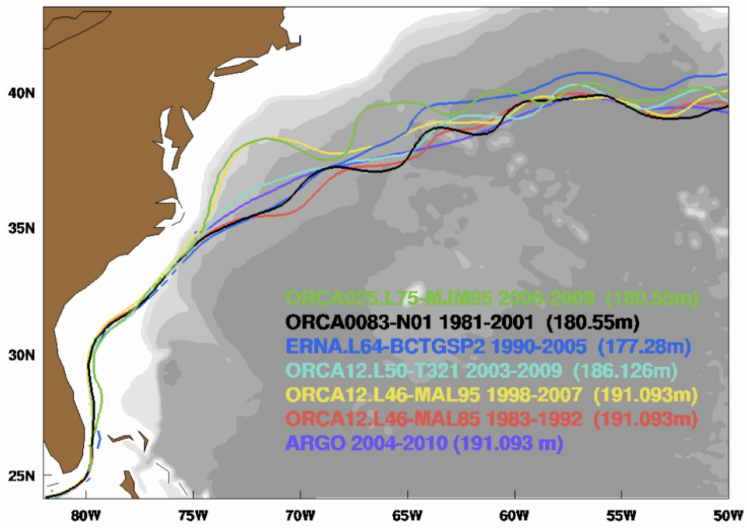

Figure 3.2: Mean position of the Gulf Stream (as indicated by 18C isotherm at 200m depth) in ERNA reference simulation (dark blue), observations (namely ARGO climatology, purple) and various DRAKKAR simulations (at $1/4°$ in green and at $1/12°$ resolution in black, cyan, yellow and red).

Furthermore, the analysis of the intensity of the MOC as a function of latitude, calculated in density or depth, highlights the importance of interactions between currents at different depths (Fig.15 of Talandier et al., 2014). When exiting the Labrador Sea around $53°$N, **the DWBC successively interacts with the upper ocean circulation composed with the North Atlantic Drift, the Northern Recirculation Gyre, and the Gulf Stream near Cape Hatteras**. This surface/deep current interaction seems to induce an increase of the MOC intensity in depth-space, giving rise to a maximum MOC near $35°$N. This process is missing in the configuration with coarse resolution $(1/2°)$, hence with erroneous Gulf Stream position. At $26.5°$N, the MOC is 4 Sv larger in the refined configuration and is in good agreement with observations. Finally, beyond the refined area (i.e. in the coarse resolution area) in the South Atlantic, the MOC maximum at $40°$S is 3 Sv larger at the end of the simulation, meaning that the correction of upper and deep currents is able to propagate outside the grid refinement area without being fully damped. This underlines the benefit of using AGRIF technique for a reasonable computing time compared to a fully global higher resolution configuration.

This strategy revealed also efficient to resolve the issues encountered with SAKAI, as we inserted a second level of grid refinement in ERNA, which covers the Irminger and

Labrador Seas with a horizontal resolution of $1/32°$, i.e. about 2km. In this configuration, which explicitly resolves the mesoscale processes in the subpolar gyre (hence the name FER for "Full Eddy Resolving"), the temperature and salinity drift is significantly less than in ERNA and the surface EKE is comparable to the observed climatology of Reverdin (2003) in the Labrador Sea, which is very encouraging for this innovative configuration. Nevertheless, I did not have the opportunity to explore sensitivity to the numerical choices (advection scheme, lateral conditions, sea ice model...). In addition, there is a positive bias of EKE at the surface in FER to the north of the North Atlantic Drift (near the southern boundary of the 2nd zoom), which should be reduced.

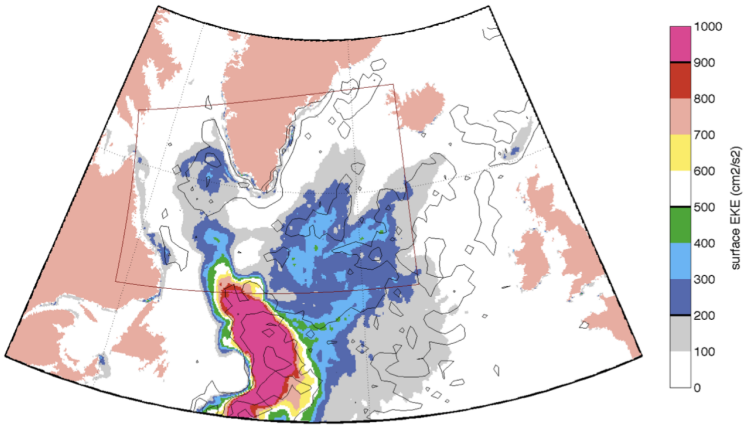

Figure 3.3: Surface eddy kinetic energy in FER configuration (colour shading) and calculated from float observations (black contours) for the period 1993-2006. Contours of the 2nd AGRIF zoom are drawn in maroon.

3.2 Intercomparing ocean transports

Ocean observations are generally insufficient to describe variability on interannual to multi-decadal time scales, especially of currents. The analysis of numerical simulations is very useful in this case, but it is essential to take into account the biases inherent in the model used. To do this, the joint analysis of simulations from different models is relevant. However, comparing currents at depth produced by models with different grids (horizontal or vertical) is not easy. I have developed a set of diagnostic programs, called PAGO for Physical Analysis of a Gridded Ocean, for this purpose. PAGO works with ocean data from multiple models (NEMO, MOM, POP, MPIOM, ROMS, HYCOM, MICOM, OFAM), no matter the choice of horizontal and vertical grid discretization (note that PAGO has not been adapted yet to work on unstructured grids, but it would

not represent any major challenge to adapt it to other shapes than rectangles). It also diagnoses hydrographic databases, which is useful for validating the mean state of thermohaline structures.

PAGO analyses the vertical structure of the ocean along user-selected sections according to geographical criteria, with minimum interpolation of dynamic variables to best reproduce the conservation properties of the models (Fig.3.4). It computes a set of transport indices normal to these sections (volume, heat, salt and freshwater transport): net transport, overturning and gyre components (see Box 2), transport in an isopycnal layer or between two depths (Mignot et al., 2013). It can also be used to simply visualize the normal velocities and hydrographic properties along any user-defined section (Talandier et al., 2014). Because PAGO respects conservation properties of the model as much as possible (depending on the sampling strategy for output variables), it enables the reconstruction of heat and freshwater budgets within enclosed volume (Deshayes et al., 2014; Barrier et al., 2015).

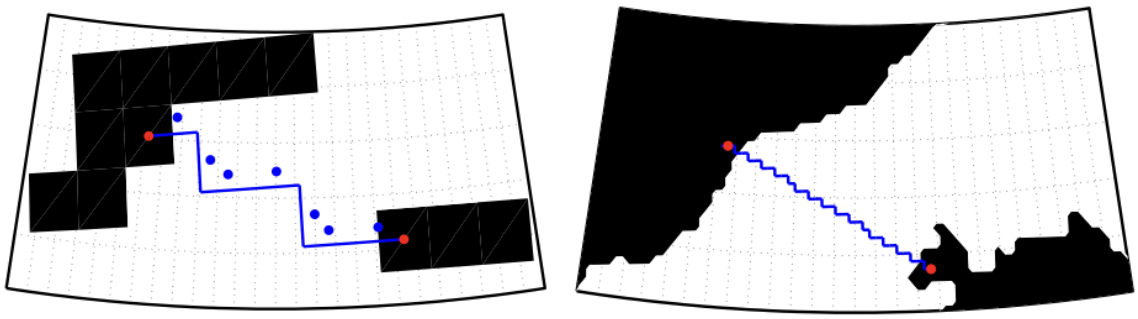

Figure 3.4: Example of PAGO section in between Greenland and Iceland in a coarse (left) and high (right) resolution model. Dark shading represents land. The blue dots (left) are indicators to check that all velocities normal to the section orientate in the same direction (they can be seen as the head of arrows crossing the section, and should locate on the same side of the section).

The programs are available in two computing language : Matlab (since September 2012 through `https://www.whoi.edu/science/PO/pago/`) and Python, thanks to contribution of Nicolas Barrier (`https://github.com/barriern/PyPago`), a PhD student that I co-supervised. I have personally trained apporoximately 30 scientists to the use of PAGO, in particular during a 1 week course organized by the Bjerknes Center in Bergen (Norway, 03/2015). From the many publications that employ PAGO, I chose to briefly summarize two of them, that I contributed to while at UCT.

Box 2 : physical decomposition of the ocean transports

The objective of this physical decomposition is to interpret transports through a user-defined section, positioned from land to land, in a physical framework. All ocean 3D variables along this section, and in particular velocities, can be written as the sum of physical components orthogonal to each other :

$$\underset{(t,z,l)}{v} = \underset{(t)}{\overline{v}^{z,l}} + \underset{(t,z)}{\overline{(v-\overline{v}^{z,l})}^{l}} + \underset{(t,l)}{\overline{\left(v-\overline{v}^{z,l}-\overline{(v-\overline{v}^{z,l})}^{l}\right)}^{z}} + \underset{(t,z,l)}{...}$$

net overturning barotropic baroclinic

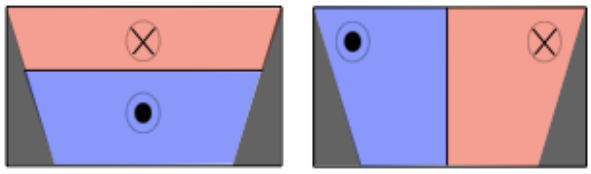

where the overbar symbolize the average operator on the specified dimension(s). The last term to the right hand side is simply calculated as a residual, and interpreted as the baroclinic component of the variable. It is also possible to perform this decomposition using density coordinates rather than depth as the "vertical" dimension. In this case, I usually gather the barotropic and baroclinic terms into a single "horizontal" component. Applying this decomposition on velocities across the section, and then intergrating over the whole section area (in the vertical plane), produces the strength of the overturning and barotropic circulations through the section.
In order to decompose the transport of heat through the section, I normally decompose velocities and temperature separately, and then multiply the overturning velocity by the overturning temperature, and the barotropic velocity by the barotropic temperature. Note that, by doing so, the structures of overturning velocity and temperature (respectively of the barotropic velocity and temperature) do not exactly superimpose. As a result, the cross components of the heat transport (ie overturning transport of barotropic temperature, and barotropic transport of overturning temperatures) do not necessarily vanish. For this reason, I always compute the baroclinic heat transport as a residual from all other terms, hence it includes the cross components as well as.
Decomposing transports of salinity is not as frequent as transports of freshwater, commonly defined as

$$\frac{S - S_{ref}}{S_{ref}}$$

where S_{ref} is a chosen reference salinity, that is constant. Note that the choice of S_{ref} has an impact on the amplitude of each components of the freshwater transport, hence it should be done consistently with the scientific question addressed.

Decadal changes in the subpolar gyre

Variations in the intensity of the subpolar gyre on interannual time scales are strongly linked to fluctuations in the NAO index, with a maximum circulation intensity associated with positive NAO phases in winter (Deshayes and Frankignoul, 2008). The same applies to convection variations in the Labrador Sea interior, which are mainly driven by fluctuations in winter heat fluxes, themselves very strongly correlated with the NAO index (Deshayes et al., 2007). Thus, following the succession of winters with positive NAO anomalies from 1990 onwards, the subpolar gyre reached a maximum intensity in the mid-1990s and convection in the Labrador Sea was deepest in 1994. Thereafter, the NAO was for several winters in a neutral phase and the intensity of the subpolar gyre rapidly decreased. This signal is clearly visible in satellite observations Hakkinen (2004). In addition, it appears that the subpolar gyre has "contracted" from the mid-1990s until 2004 : the eastern boundary of the subpolar gyre has migrated westwards, allowing subtropical water masses to penetrate further into the Northeast Atlantic and the Nordic Seas (Hatun, 2005). The mechanism responsible for this contraction of the subpolar gyre is unclear: is it a local response to atmospheric forcing, a response to a subtropical ocean anomaly, or a response to an ocean anomaly in the western part of the subpolar gyre?

The study of Barrier et al. (2015) (full text inserted at the end of this manuscript) provides some answers to this question, via reconstructions of the heat budget in a series of realistic ocean hindcasts in the North Atlantic, ranging from $1/4^\circ$ to $1/12^\circ$ horizontal resolution. In the western subpolar gyre, the 1995 warming event is the decadal, baroclinic ocean response to positive NAO conditions from 1988 to 1995. The latter induced increased surface heat loss in the Labrador Sea that intensified deep convection hence strengthened the MOC and the associated poleward heat transport. In the eastern subregion, a concomittant warming is induced by an interannual, barotropic adjustment of the gyre circulation to an abrupt switch from positive NAO conditions in winter 1995 to negative NAO conditions in winter 1996. Indeed, the gyre response to negative NAO conditions is a cyclonic intergyre-gyre that increases northward volume and heat transports at the southeastern limit of the subpolar gyre. Therefore, Barrier et al. (2015) suggest that **the atmospheric drivers, the mechanisms at stake and the associated timescales are different to the east and to the west of Reykjanes Ridge**.

Meridional salt transport in South Atlantic

While all climate models predict an increase in the amount of freshwater in the North Atlantic, due to Greenland melting and intensified hydrological cycle, there is no consensus on whether this induces an abrupt change in the MOC: a necessary condition is that the MOC is in a bistable state (where "on" and "off' states coexist, Rahmstorf, 1996).

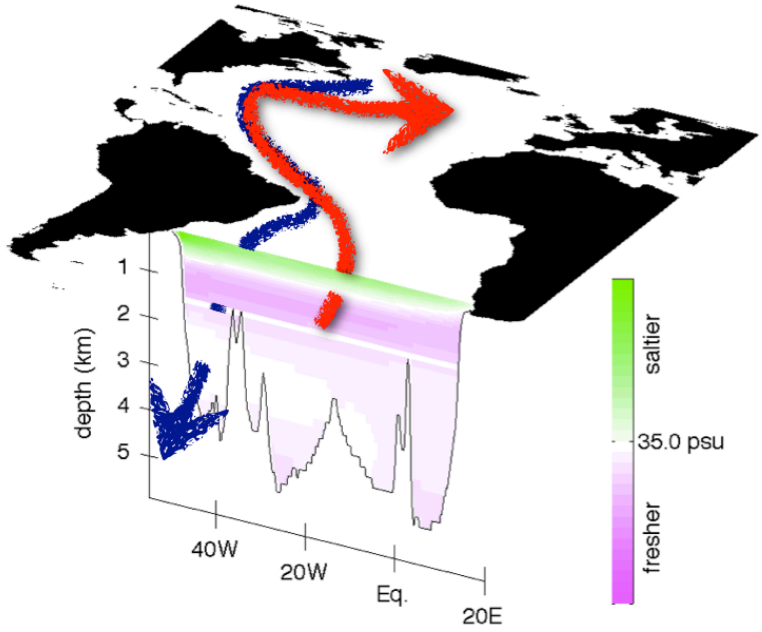

Figure 3.5: Mean salinity in the South Atlantic (color shading relative to 35.0psu) and positioning of the depth where the local MOC is maximum (circa 1000 m depth).

The amount of freshwater transported by the MOC in the South Atlantic seems to be a relevant indicator of the MOC's bistability. Nevertheless, observations, ocean reanalyses and coupled models produce very different values of this indicator (Hawkins et al., 2011; Weaver et al., 2012). I took advantage of the new NEMO ORCA12 simulations (global simulations at $1/12^{\circ}$ resolution) produced by the DRAKKAR group to calculate this indicator and revise this issue. These simulations explicitly reproduce the Agulhas eddies in southern Africa, which transport heat and salt from the Indian Ocean to the Atlantic Ocean.

According to ORCA12 simulations, the transport of freshwater by the MOC is currently southward, meaning that the northward flowing branch, in the upper ocean, is saltier than the southward flowing one, at depth (Fig.3.5). This would act as a positive feedback if the amount of freshwater increases in the North Atlantic and the MOC suddenly decreases : the MOC would transport less salinity northward in the South Atlantic, hence reducing further density in the upper North Atlantic. Note that the relatively high salinity transported by the Agulhas leakage to the South Atlantic (the leakage of warm and salty subtropical water masses from the Agulhas Current as it retroflects to the south Indian Ocean), actually feeds into the upper branch of the MOC being saltier than its deeper branch, hence contributes to the MOC being in the bistable regime. **The fact that the MOC is in the bistable regime, according the freshwater transport**

index, is confirmed by the 4 independent simulations of the ORCA12 model, based on different choices of model parameters and forcings (Deshayes et al., 2013, full text inserted at the end of this manuscript). Note that 1 of the 4 simulations has no restoring of sea surface salinity, yet behaves similarly to the other ones, hence sea surface salinity restoring does not seem to play a role in this context.

Comparison with similar lower resolution simulations shows that the freshwater transport by the MOC depends on the model resolution, via the depth and strength of the MOC. At coarser resolution than $1/12^{\circ}$, the MOC maximum locates deeper in the water column, hence the upper branch transports more fresh Antarctic Intermediate water masses northward, and eventually becomes fresher than the deep branch of the MOC. In such situation, if the amount of freshwater increases in the North Atlantic and the MOC suddenly decreases, there would be less northward transport of freshwater in the South Atlantic, which would favor a recovering of the MOC. This explains why climate models do not predict abrupt changes in the MOC : they tend to overestimate the stability of the MOC in the present climate.

Spatio-temporal characteristics of the Agulhas Leakage

Because of its impact on the global circulation of heat and salt, it is essential to better understand the mechanisms of variability of the Agulhas Leakage, which refers to the advection of warm, salty water of Indian origin into the South Atlantic, and in particular to be able to distinguish the response to atmospheric conditions from the signature of intrinsic oceanic variability processes. The Agulhas leakage is the product of the unstable retroflection of the Agulhas Current, which generates large eddies in southern Africa (Fig.3.6). These eddies, the Agulhas Rings, with their relatively warm and salty cores, make up the bulk of the Agulhas leakage. Estimates of the Agulhas leakage, in observations and regional models, do not seem to converge. On the one hand, the methods used to estimate this transport, in observations and models, differ widely, which makes it difficult to compare published estimates. On the other hand, the retroflection of the Agulhas current is a complex and non-linear process, as is the production of Agulhas rings and, ultimately, the Agulhas leakage.

Assuming that the variability of the Agulhas Leakage is dominated on interannual time scales by intrinsic processes of variability, different models, which correctly reproduce these processes, can be expected to converge in their spatio-temporal variability characteristics. On the contrary, low spatial resolution models, such as climate models, would be biased in these variability characteristics and, therefore, would not correctly reproduce the variability of the Agulhas Leakage and its impact on the global ocean and climate. This was verified through an inter-comparison of the Agulhas Leakage in 3 OGCM (NEMO, HYCOM and ROMS) in several configurations of different spatial resolution (from $1/12^{\circ}$ for ORCA12 to 2° for the ocean component of the climate model IPSLCM5). The first step was to develop a new method for estimating the Agulhas

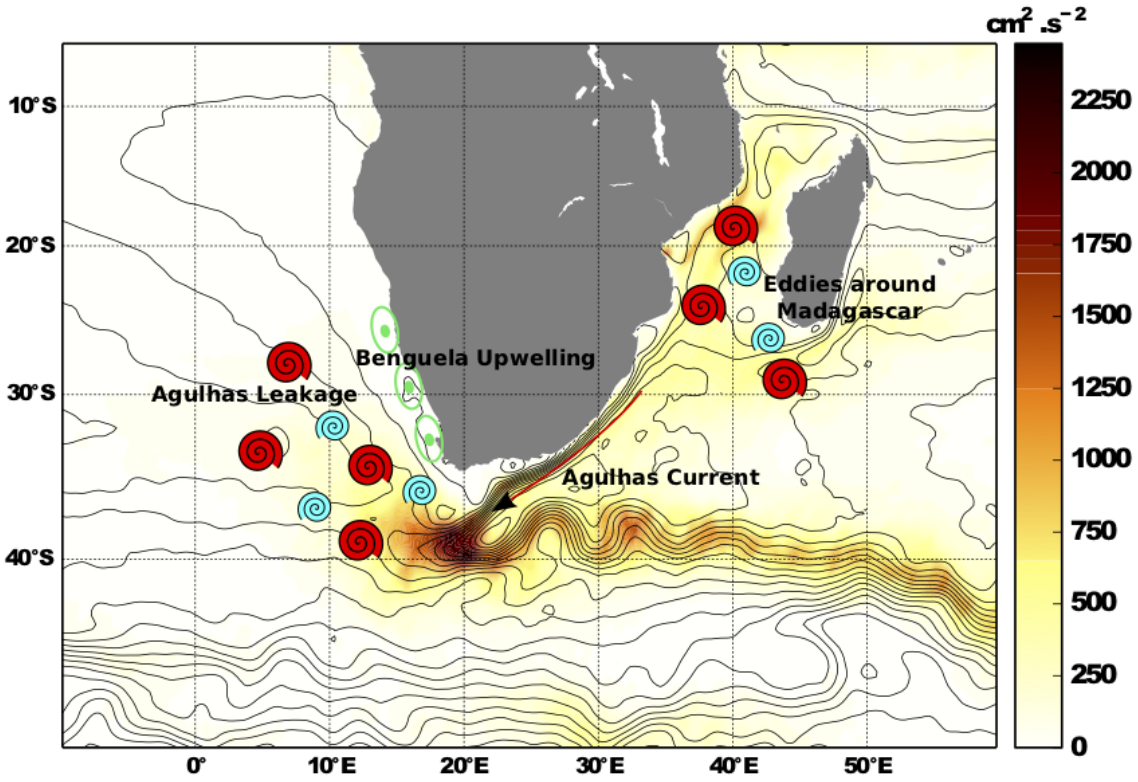

Figure 3.6: Key ocean features of the marine environment around Southern Africa, mean dynamic topography (1 contour / 10 cm, black lines) and mean eddy kinetic energy (colour shading), both being estimated from AVISO observations over the period 1993-2017 (unpublished material, prepared with P. Penven).

Leakage that would allow the analysis and inter-comparison of several models of different configuration and resolution, and PAGO was the perfect tool for this. Then, we performed a spectral analysis of the spatio-temporal variability for each available model. Note that I taught spectral analysis during my visit to the University of Cape Town, as I observed students did not know how to interpret power spectra, hence I introduce in this manuscript a box for the novice (Box 3).

Power spectra of the Agulhas leakage show that the variability is dominated by the passage of Agulhas Rings, whatever the model considered, as long as the horizontal resolution is sufficient to reproduce eddies at this latitude, and despite biases, for some models, in the trajectories of these eddies. However, the IPSLCM5 model does not reproduce these variability processes and, consequently, does not correctly represent the variability of the Agulhas Leakage nor its impact on the global climate (Holton et al., 2017).

Box 3 : interpreting power spectra for the novice

Estimating power spectral density is a very powerful way to characterize the time scales of variability of a signal. First, one has to verify that the figure plotting power spectral density, as the example provided below, is correct : [i] frequencies on the x-axis must be consistent with duration of the time series (δt is the time step and N is the number of time steps) and the rate of sampling, [ii] at low frequency, the spectra must flatten (provided that mean and eventual trends have been removed prior to calculating the spectra), [iii] the area above the curve equals half of the variance (in case of variance conserving spectra).

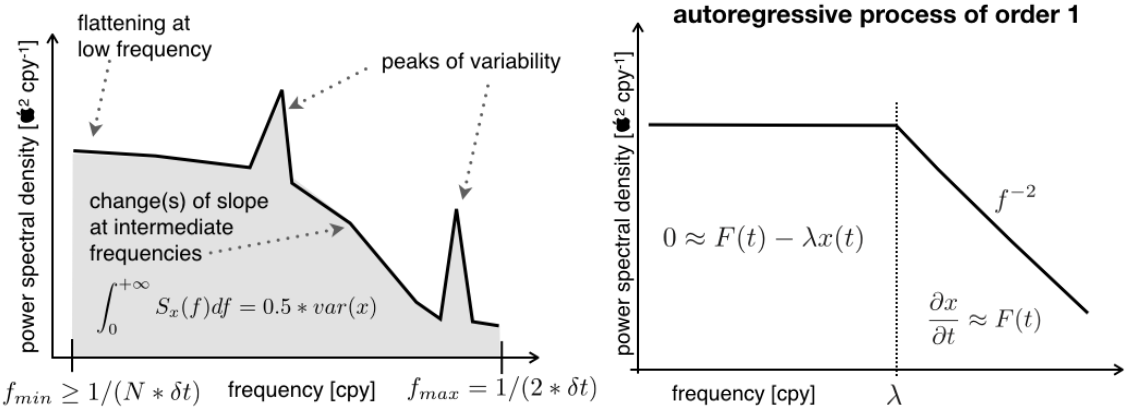

As reading a power spectrum, one has to observe distinctly peaks of variability, indicating a periodic process in the signal, from changes of slope. In both cases, it is important to take into account the uncertainty in the power spectral estimate (not indicated on the schematic above).

Changes of slope in power spectrum indicate changes in the predominant process(es) in the signal. To illustrate, let's consider the case of an autoregressive process of order one, aka Markov process :

$$\frac{\partial x}{\partial t} = F(t) - \lambda x(t) \tag{3.1}$$

where the variable to analyse x only depends on time t, while F is a forcing and $1/\lambda$ the time scale for damping. It is simple to derive the equation for power spectral densities :

$$S_x(f) = \frac{S_F(f)}{\lambda^2 + f^2}$$

where S_x and S_F are the power spectra for the signal and the forcing, respectively, and f the frequency. At frequencies smaller than λ, S_x and S_F have the same shape, and most often a flat spectra (the forcing usually represents the atmosphere, which is seen as white noise process by oceanographers). On the other hand, at frequencies larger than λ, ie at periods shorter than the time scale for damping, S_x will follow an f^-2 slope, due to the integrative process on the left hand side of eq. 3.1.

Numerical representations of the Agulhas Undercurrent

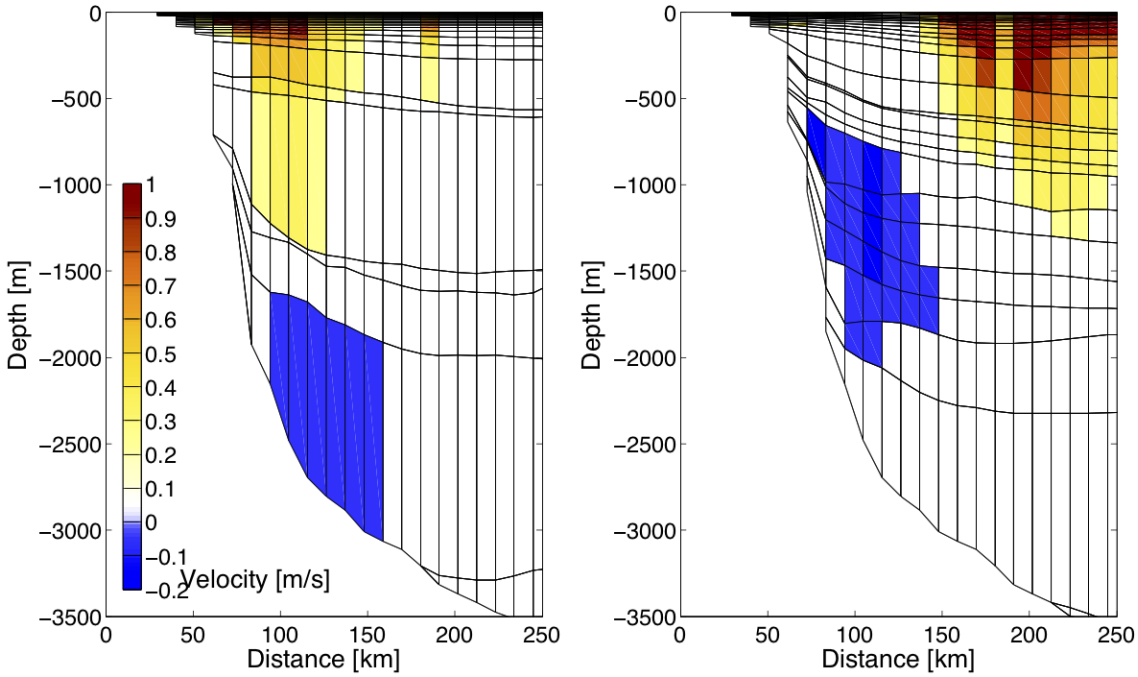

Figure 3.7: Snapshot of the vertical velocity structure (m/s) in two regional experiments to the south of Africa, at $32.5°$S across the Agulhas Current. The thin black lines show the horizontal and vertical grid cells. Positive velocities are directed to the south-east, ie in the direction of the Agulhas Current, while negative velocities are flowing in the opposite direction, equatorward.

If the dynamics of the Agulhas Current are still unknown, the dynamics at depth are even more uncertain. There is a deep current between 1000 and 2000m along the topography, oriented to the north-east, under the Agulhas Current. The so-called Agulhas undercurrent, which has been observed on a few occasions, is often poorly represented in models of the region. Consequently, there is as yet no study of its influence on the dynamics of the Agulhas Current. Bjorn Backeberg (UCT) had produced two very close simulations of the regional circulation with the HYCOM model, differing only in one numerical choice: the density of the isopycnal layers at depth in the model. We undertook to compare these simulations for the characteristics of the Agulhas undercurrent and to determine whether this has consequences for the dynamics of the Agulhas Current. Most of the work was carried out by a Master student (ENSTA-Bretagne), visiting UCT, using PAGO to extract hydrodynamic conditions across the Agulhas Current. The choice of isopycnal layers at depth has a strong impact on the representation of intermediate

water masses of low salinity, of Antarctic origin, on the intensity and structure of the Agulhas undercurrent and the Agulhas Current (Fig.3.7), and finally on the position of the retroflection. Reconstructions of sources and sinks of potential vorticity indicates that the underlying dynamics involve many highly non-linear processes that partially compensate each other. The publication we prepared on these results was rejected several times, mainly because we do not have online diagnostics of potential vorticity trends to confirm our hypothesis. The development of such online diagnostics of potential vorticity is not straightforward, and motivated for the AFRICA project described below.

3.3 Perspective

AFRICA project

The objective of the AFRICA project (Addressing ocean FRonts, energy Routes, Impacts and Couplings around Africa) is to better understand the dynamics of the Agulhas Current, clarify its impacts on biogeochemical cycles and ecosystems, as well as on the larger spatial scale ocean circulation and climate. This is the marine environment that provides protein resources to a large population of the African continent ($> 100,000,000$ people), so this project is highly relevant to society, and particularly timely in the current context of global climate change. It is also an ambitious project as it addresses a major challenge for oceanographers, namely the modelling of western boundary currents. Several recent initiatives have succeeded in significantly reducing model biases in the Agulhas Current, but these improvements have been achieved independently, by different groups developing different models. Another added value of the project is to develop diagnostics of potential vorticity, consistent between the two models, in order to compare them with each other and with the theory of western boundary currents. **The motivation of the AFRICA project is to coordinate a set of developments, simulations and diagnostics using CROCO and NEMO, to combine these improvements and assess which biases are left in numerical simulations of the Agulhas Current**.

In practice, AFRICA consists of coordinating modelling activities of L. Renault (IRD, LEGOS), P. Penven (IRD, LOPS), S. Pous (MNHN, LOCEAN) and myself, regarding hydrodynamics around southern Africa. Since 2018 we receive French funding (CNRS LEFE-GMMC program) to meet, discuss and valorise our collaborations. My personal contribution is to lead the group, organize discussions and synchronize model developments (especially online diagnostics of potential vorticity and energy routes, which are already partially done by different packages) and simulations produced (e.g. to standardise the boundary conditions of regional configurations, for example), and also to participate in the development and analysis of the simulations. Project AFRICA is also an opportunity to maintain the collaboration between South Africa and France regarding ocean modelling, that was mostly active during the ICEMASA joint laboratory

(2010-2018, IRD funded).

Caribbean archipelago

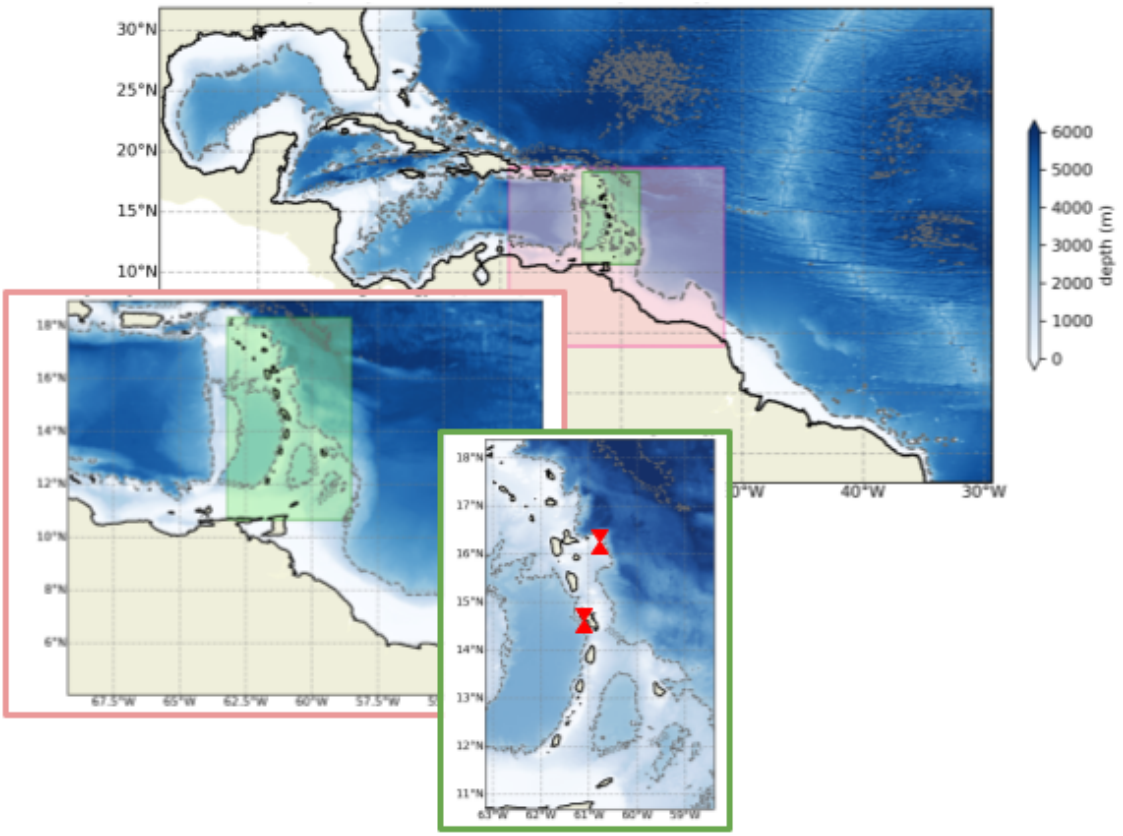

Figure 3.8: Bathymetry of the embedded NEMO configurations for hydrodynamic modelling of the Caribbean archipelago : the configuration with the largest imprint has $1/12°$ resolution (contribution of J. Jouanno, IRD, LEGOS), the first AGRIF zoom (red shading) has $1/36°$ resolution, and the second AGRIF zoom (green shading) has $1/108°$ resolution. Red symbols represent the location of ADCP measurements in 2017 and 2020 (continuous observations during 6 months each).

Hydrodynamic modelling of the Caribbean archipelago, including the French West Indies, is primarily motivated by academic objectives: to better understand the oceanic and atmospheric phenomena that take place there (interactions between rings of the North Brazil Current and circulation around the islands, deep atmospheric convection, etc.) and the mechanisms of interactions between large and fine scales that occur there (e.g. onshore/offshore oceanic exchanges, which are also relevant for other regions of

the world). Nevertheless, a better knowledge of ocean circulation and hydrodynamic conditions will also enable to respond directly to societal issues of major importance: anticipation of flooding, forecasting of sporadic Sargasso beaching, improvement of cyclone trajectory forecasts, and forecasting of climate change impacts, in addition to contributing to questions of marine biology (Chérubin and Richardson, 2007). Currently, 3 large international projects aim to better describe the atmospheric and oceanic conditions of the region: EUREC4 (`http://eurec4a.eu/`, EU + US funding, field campaign in 2020), CARIB-COAST (EU funded, through INTERREG program, 2018-2022) and FORESEA (French ANR project, 2020-2022). For these three projects, we proposed to develop a hydrodynamic model of kilometric resolution of the Caribbean archipelago, which will be used to support regional models of finer spatial resolution or coupled ocean-atmosphere models.

To model the Caribbean archipelago at kilometric resolution, we had the choice of using the NEMO or CROCO models, both of which are widely used and developed at LOCEAN. Rather than choosing one or the other of these two models, we have chosen to develop the same regional configuration in both models in parallel. This will allow us to satisfy the needs of the 3 major projects mentioned above (CROCO for EUREC4 and FORESEA, NEMO for CARIBCOAST), in addition to having the opportunity to perform a robust intercomparison study of NEMO and CROCO for tropical ocean dynamics. Intercomparison studies between these two models have already been carried out, but rarely with exactly similar configurations. Therefore, it remains to be determined whether NEMO and CROCO represent tropical regional dynamics in a similar way with comparable numerical performance.

The work with NEMO has already began, and I have developed a new regional configuration of the French west indies, embedding AGRIF zooms in a pre-existing configuration at $1/12^\circ$ that covered the entire west tropical Atlantic (same configuration as in Jouanno et al., 2008, see Fig.3.8). The first AGRIF zoom, at $1/36^\circ$, is used to disentangle the various processes of mesoscale variability (influence of North Brazil rings, Rossby waves coming from tropical Atlantic, local instabilities). A second AGRIF zoom, at $1/108^\circ$, will support process studies in the vicinity of the islands, in particular where observations are available (ADCP moorings for 6 months in the bay of Fort de France and offshore to the east of Guadeloupe). At the time of writing this document, this second configuration runs smoothly as independent regional configuration, but is very unstable in AGRIF two-way nesting mode. This is the configuration that will support intercomparison between NEMO and CROCO, as a stand-alone regional configuration, forced by boundary conditions extracted from the configuration with 1 AGRIF zoom.

Chapter 4

Climate models

When I joined the LOCEAN NEMO R&D team in 2015, it was in charge of preparing ocean configurations for the IPSL-CM6 model within CMIP6 exercice, but without an identified project leader. I took on this role to coordinate the team's actions, at first, in particular for the development and distribution of eORCA1 and eORCA025, the two iconic configurations of NEMO for climate applications at present. Then I developped interest in climate modelling for my own scientific projects, in particular to clarify the role of freshwater in circulation changes. This is a question that I started to investigate when developping the model inter-comparison tool PAGO (section 3.2) and applied it to CMIP5 models.

4.1 Role of freshwater on MOC variability : a first insight from CMIP5 models

In the North Atlantic, observations show decadal to multi-decadal fluctuations in the subpolar gyre and its freshwater content, but the observational period of about 50 years is insufficient to fully investigate these fluctuations (Curry, 2005). The period of direct observations of the MOC is even shorter, and does not allow to clearly identify a link with subpolar variability. A large number of studies of observations and numerical simulations have addressed different aspects of this issue, but they have not yet led to a coherent view of this ocean system. In fact, interpretations of the causes of simulated and observed variability in the MOC and freshwater content of the North Atlantic are so divergent that they appear contradictory. Observations and hindcast simulations suggest that from the early 1970's to the mid-1990's, the subpolar gyre became fresher while the gyre and meridional circulations intensified (see, for example Frankignoul et al., 2009, which I produced all analysis and figures). This is opposite to the relationship of freshening causing a weakened circulation, most often reproduced by climate models.

As a first application of PAGO, I intercompared the freshwater budget of 5 preindustrical climate simulations (using the GFDL, NCAR, CNRM, IPSL and MPI-M models prepared for CMIP5 exercice, see Deshayes et al., 2014, full text inserted at the end of the present manuscript). Mean and standard deviation of all terms in the freshwater budget are very different among models (they vary by more than a factor 2). Freshwater convergence through lateral boundaries mostly reflects the transport at the southern boundary of the subpolar gyre, for both the mean and the variability, which suggests that subtropical influence on subpolar freshwater budget overcomes that of polar regions. In GFDL, IPSL, and CNRM, its fluctuations have comparable variance and are highly correlated with freshwater content changes, whereas surface fluxes and diffusion have a much smaller impact. In NCAR and MPI-M, surface fluxes gain importance in the freshwater budget. The high correlation between freshwater content changes and freshwater convergence is consistent with hindcast simulations (e.g. Frankignoul et al., 2009) and the preindustrial control run of another climate model Wu and Wood (2008). Direct observations of oceanic full-depth circulation are too rare to evaluate freshwater convergence to the subpolar gyre and check whether this result is realistic. One preliminary step would be to compare the range of variability of freshwater content in these models with esti mates from a compilation of available observations in the subpolar gyre, but the latter must come with an estimate of the error because of the interpolation in space and time of sparse observations.

Relationships between freshwater content changes and the subpolar gyre strength and the AMOC are also very different. In the GFDL model, the subpolar gyre intensifies as freshwater content increases, on an interannual time scale, while freshwater content decreases as the subpolar gyre intensifies on a multidecadal time scale. In IPSL, freshwater content increases as the MOC is more intense, on an interannual time scale, while freshwater content decreases as MOC is more intense on decadal and multidecadal time scales. The other models show inconclusive results that do not allow us to identify whether freshwater fluctuations are passive to circulation changes or play an active role in modifying the subpolar gyre strength and MOC. As a conclusion, Deshayes et al. (2014) highlights that **changes in salinity in the subpolar can be both active and passive, regarding the circulation changes, depending on the model and time scale of variability**.

All models mentioned above suffer from important biases in their representations of freshwater cycle, in particular the crude contribution of the cryosphere, and lack of dynamical continental ice sheets in both hemispheres. It is a direction of model improvement that has seen little progress from CMIP5 to CMIP6, unfortunately.

4.2 Preparing NEMO for CMIP6

The contribution of LOCEAN NEMO R&D team to the development of the ocean component of IPSL-CM6 started with the preparation of a new revision of NEMO, version 3_6_stable, which includes a number of code improvements over previous versions : an explicit representation of the free surface that implies variable volume of grid cells (Levier et al., 2007), the new TEOS10 equation of state (Roquet et al., 2015) and the new version of the sea ice module, LIM3 (Rousset et al., 2015), among others. The management of freshwater inflow has also undergone several changes, including depth distribution and parameterisation based on observations of ice sheet melt flows around Antarctica and iceberg melt flows in the Southern Ocean (Mathiot et al., 2017), and this is one of the new features of the code to which I have contributed directly. We also decided to include the new representation of deep mixing from Lavergne et al. (2019) and I took care of the validation of these developments for the IPSL-CM6A-LR ocean configuration. As a last but not least piece of development, I was in charge of modifying NEMO so that it produces output variables as recommended in Griffies et al. (2016). In particular, I lead the discussion about the time average of variables considering changes in grid cell volume, which is non trivial.

The principal configuration of NEMO used in CMIP6 is eORCA1, the quasi-isotropic global tripolar grid with a 1° nominal resolution, extended to the south so as to better represent the contribution of Antarctic under-ice shelf seas to the Southern Ocean freshwater cycle. The grid has a latitudinal refinement of $1/3^\circ$ in the equatorial region. Vertical discretization uses a partial step formulation (Barnier et al., 2006), which ensures a better representation of bottom bathymetry, with 75 levels. The initial layer thicknesses increase nonuniformly from 1 m at the surface to 10 m at 100 m depth and reaches 200 m at the bottom (Fig.4.1); they are subsequently time dependent (Levier et al., 2007).

The bathymetry of eORCA1 inherited from CNRM-CM5 (Voldoire et al., 2013) but I personally revised several regions of interest for the deep circulation : Denmark Strait, in between Iceland and Faroe islands and to the south of Faroe islands, the Drake passage, Romanche and St Pauls fracture zones, and many more. In doing so, I extracted then compared the bathymetry used in ORCA2, the nominal 2° global configuration of NEMO that G. Madec fine tuned extensively, but also MOM and GOLD 1° global configurations used in CMIP5. Bathymetry in the coastal regions turned out to be problematic as well, as pre-industrial control integrations of IPSL-CM6A-LR suffered from explosions in ice-covered regions close to the shore. We ran several tests imposing a minimum depth of 30 m and 50 m, the latter having a huge stabilizing effect but affecting the realism of coastlines dramatically. In the end, we kept for IPSL-CM6A-LR a minimal depth of 30 m, as I identified a bug in the temperature of the river runoffs that also contributed to reduce the instabilities.

Choices for ocean dynamics and tracers for eORCA1 of IPSL-CM6A-LR are detailed

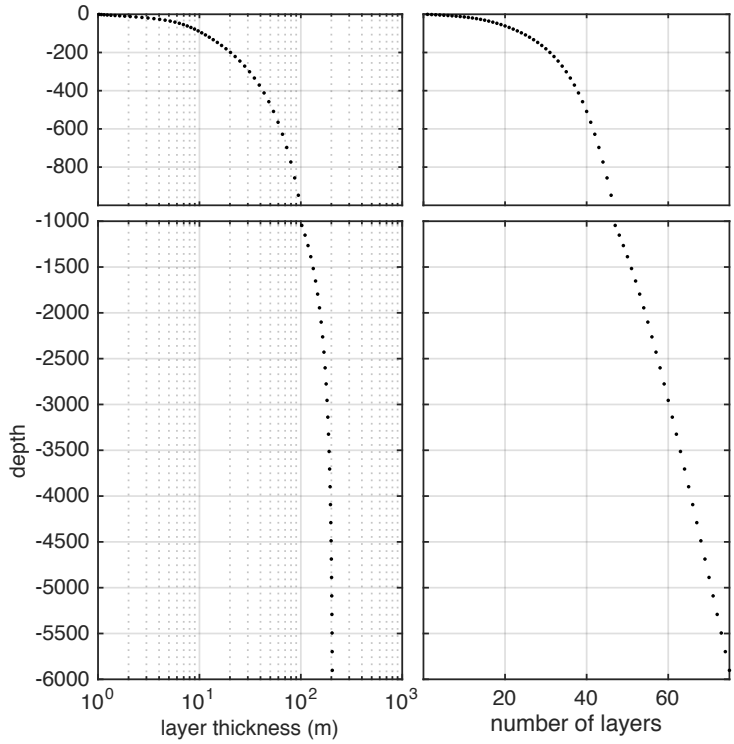

Figure 4.1: Positioning of the 75 levels in eORCA1 configuration of NEMO, widely used in CMIP6.

in Boucher et al. (2020). They were informed by a large number of simulations, in ocean-only mode and in coupled mode, comparing to observations when available, of hydrodynamic and sea-ice variables, as well as biogeochemical variables (Mignot et al., 2021). Indeed, the tuning strategy of IPSL-CM6A was motivated by ensuring realistic dense water formation, which is crucial for biogeochemical cycles (in particular the injection of oxygen and nutrients in the deep ocean). Given the relative high vertical stratification in the Southern Ocean (Boucher et al., 2020) and the coarse spatial resolution over shelf around Antarctica, Antarctic Bottom Water formation had to be sustained by opening large polynyas. This was done by reducing to 95% the maximal area covered by sea ice, which corresponds to a prescribed increase in the frequency of leads. AABW formation was also increased by injecting freshwater coming from the continental ice-sheet, at depth along the coastline. This strengthened the density gradient from the coast offshore, hence the geostrophic circulation along the coast, preconditioning for dense water formation offshore.

Other CMIP6 climate models than IPSL-CM6, use NEMO as their ocean component: CNRM, Hadley Center MetOffice, EC-Earth, NOC, ECMWF, BSC and CMCC. A forge

project dedicated to this collaboration has been set up (named shaconemo for SHAred Configurations for NEMO) : it allows the sharing of specific files (initialization files, namelists, etc.) that are not distributed with the NEMO code, but also the exchange of information about the simulations that each group carries out. It is important to specify that, although starting from a common base, each group makes specific choices for their configurations according to the other components of the climate model and their specific scientific interests. Together with J. Mignot and T. Khulbrodt (NCAS), we initiated a study inter-comparing all choices made for the different NEMO eORCA1 configurations employed in CMIP6, and started with closely comparing the choices in between IPSL-CM6A-LR and UK-GC3.1. A postdoc supervised by J. Mignot and myself, namely M. Menary, ran additional simulations to draw links between specificities and climate features. None of these two studies has been published yet, because neither of these efforts was conclusive. Rather, this motivated the QUEST project described below (section 4.5), to quantify parametric uncertainties in IPSL-CM6A-LR.

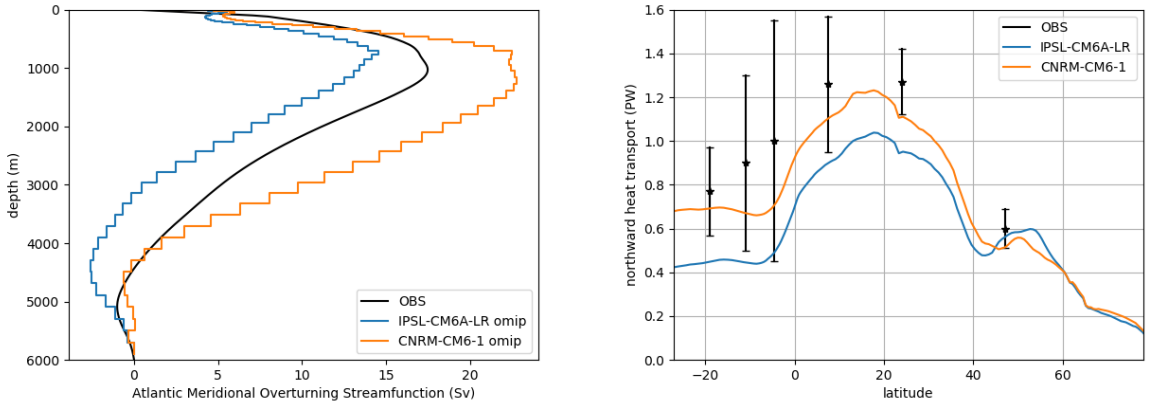

Figure 4.2: MOC streamfunction at $26°$N (left) and meridional heat transport in the Atlantic as a function of latitude (right) in IPSL-CM6A-LR (blue) and CNRM-CM6-1 (orange) OMIP simulations (last cycle, ie 1950-2009) and in observations (black, for period 2004-2017). Observations of MOC come from the RAPID project, while observations for the meridional heat transport are taken from Ganachaud and Wunsch (2003).

To demonstrate the range of diversity in NEMO eORCA1 MOC shape and strength, Figure 4.2 compares results from OMIP simulations (section 1.2) realized using IPSL-CM6A-LR and CNRM-CM6-1 configurations (ocean-only simulations, forced by CORE atmospheric dataset). **Neither of the two models are close to observations of MOC strength and shape at $26°$N in the Atlantic**, where direct observations are available since 2004 thanks to the RAPID project. MOC strength is overall too weak in

the IPSL-CM6A-LR, while it is generally too strong in CNRM-CM6-1. The shape of the mean MOC streamfunction also suffers from substantial biases : the maximum is too shallow in IPSL-CM6A-LR, while CNRM-CM6-1 exhibits two local maxima below and above $1,000$ m depth, which differs from observations. The meridional heat transport in the Atlantic, that is closely connected to the MOC at $26°$N (see Fig. 1.3), is also too weak in IPSL-CM6A-LR but falls within observational estimates in CNRM-CM6-1. This illustrates that biases in MOC strength and shape superimpose on hydrographic biases, eventually compensating each other (or not) so as to produce climate variables of interest more or less close to observations.

Note that there is no range of significance in MOC shape as estimated from observations (Fig. 1.3, left), as it is the temporal average of direct observations, while the meridional heat transport estimates are provided with error bars as they come from combined hydrographic campaigns (Fig. 1.3, right). And it is important to keep in mind that the MOC has only been observed since 2004, which remains insufficient to depict its full range of states. As a conclusion, mismatches between model and observations of MOC shape at $26°$N must be interpreted with caution : they indicate inaccuracies in the simulated ocean dynamics, for sure, but do not imply that the role played by the MOC in overall climate is erroneous.

4.3 IPSL-CM6A-LR

Boucher et al. (2020) present the IPSL-CM6A-LR model in details, in particular the couplings between different components (see Box 4 for the list of couplings affecting the ocean component of a climate model), and compare its metrics to previous contributions of IPSL to CMIP exercices, namely IPSL-CM5A-LR and IPSL-CM5A-MR that both used the iconic NEMO ORCA2 as ocean configuration (LR and MR refer to spatial resolution of the atmospheric component). Overall, IPSL-CM6A-LR suffers from excessive stratification in the thermocline and too weak stratification near the surface, and it remains to clarify whether this comes from the tuning of eORCA1 configuration, or a robust characteristic of the mean state given the other components of the climate model. The excessive thermocline stratification at mid-latitudes translates into a pinching of the upper limb of the MOC in the Atlantic Ocean (Fig.4.3, left). Indeed, at $26°$N, the RAPID observations suggest a maximum overturning around $1,000$ m depth, while it is reached at 700 m depth in IPSL-CM6A-LR. In this respect, the vertical profile was more realistic in IPSL-CM5A configurations, but with a lower magnitude. Note that all versions of IPSL-CM exhibit an underestimation of the MOC maximum at $26°$N (by about 25% in IPSL-CM6A-LR), a bias that is common to many coarse resolution climate models in the absence of overflow parameterization (Danabasoglu et al., 2014). This may in part be explained by the difference in time period used in this comparison (2004–2017 for the observations as compared to 1980–2005 for the models). However, it is more likely

to be due to biases in precipitation in the North Atlantic and/or the representation of overflows and western boundary currents, which remains a challenge in coarse resolution climate modeling.

Differences with previous versions of the model are most likely related to differences in dense water production in the North Atlantic. In IPSL-CM5A, deep mixed layers are found south of Iceland and south of Greenland, a bias associated to an over extended winter sea ice in the Labrador and Nordic Seas. In IPSL-CM6A-LR, deep mixed layers are confined to the Labrador Sea and the Nordic Seas, which is close to observed locations. However, when looking at other members of the historical ensemble, it appears clearly that there is substantial variability in the North Atlantic deep convection in this model.

The MOC profile at $26°$N also illustrates an excessive volume of cold abyssal water masses : the streamfunction changes sign at a depth of around $2,800$ m in IPSL-CM6A-LR versus $4,500$ m in observations. This is most likely due to deep convection in the Southern Hemisphere, that is very intense in IPSL-CM6A-LR, much more than in IPSL-CM5A models. Although there are important observational uncertainties related to the mixed layer depth estimates, in particular in the Southern Ocean where convection sites are most often surrounded by sea-ice, this convection is possibly overestimated in IPSL-CM6A-LR. This provides cold water masses that invade the deep ocean and strengthens the meridional density gradients in the Southern Ocean, inducing a very strong Antarctic Circumpolar Current (around 151Sv at Drake passage, to be compared to 137 ± 7Sv in observations).

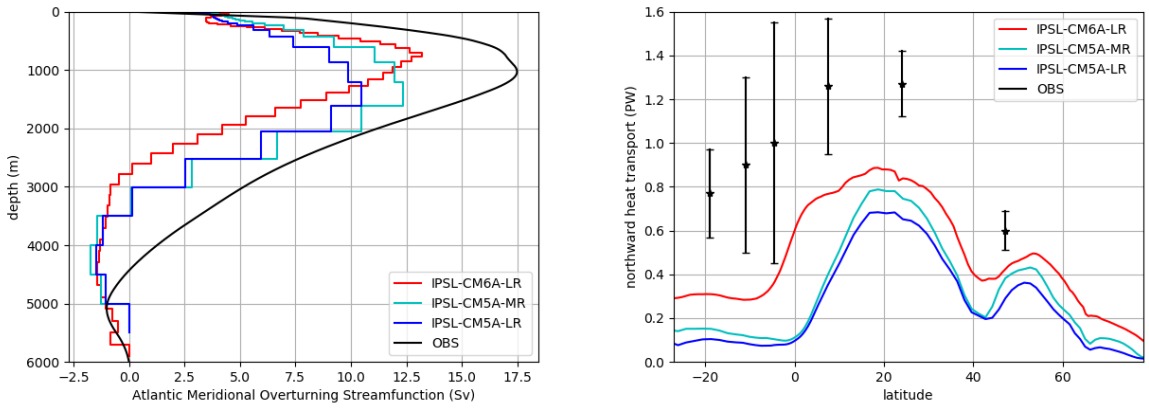

Figure 4.3: MOC streamfunction at $26°$N (left) and meridional heat transport in the Atlantic as a function of latitude (right) in IPSL-CM6A-LR (red), IPSL-CM5A-MR (cyan) and IPSL-CM5A-LR (blue) on average for the period 1980-2005 (historical simulation r1i1p1f1) and in observations (black, same as in Fig. 4.2).

Box 4 : Ocean couplings in a climate model for the novice
In the list below of all possible interactions involving the ocean component, we assimilate sea ice together with ocean dynamic and thermodynamic modules :

ocean - atmosphere couplings

- radiative heat fluxes, shortwave (downward to the ocean surface, independent of ocean state, penetrating at depth below the surface) and longwave (from the ocean surface upward, depending on ocean sea surface temperature)
- sensible heat fluxes associated with contrasts in temperature at interfaces
- freshwater and latent heat fluxes associated with evaporation (strongly dependent on ocean and atmospheric conditions)
- freshwater and heat fluxes associated with precipitations (in liquid and snow form, independent of ocean state)
- momentum fluxes via winds (with possible thermal and dynamical feedback from the ocean on winds)

ocean - cryosphere couplings

- iceberg calving from ice shelf and melting (freshwater and heat fluxes, with indirect ocean feedback for calving, via destabilization of the ice shelf, but direct ocean feedback for melting)
- melting and refreezing under ice shelf (freshwater and heat fluxes, dependent on ocean and ice shelf)
- subglacial discharges (freshwater and heat fluxes, independent of ocean conditions)
- pressure effect of ice shelf onto the ocean close to grounding line (as ice sheet is considered to be floating further offshore)

ocean - land couplings

- runoffs (freshwater and heat fluxes independent of ocean conditions but plume dynamics depend on ocean state and winds)
- geothermal vents at ocean floor (heat fluxes mostly, independent of ocean conditions)

The dependencies mentioned above are reflecting the current understanding of the physical interactions. In a numerical climate model, the level of interaction that is effectively represented in each coupling term, is most often limited by computational constraints. Indeed, including feedbacks in coupling terms is costly : it involves transferring information in between different spatio-temporal grids, which is non trivial (due to conservation and stability issues), in addition to the cost of exchanging data in between processors.

One of the major influence of the ocean to the global climate is through the meridional heat transport. This quantity is closer to observations in IPSL-CM6A-LR compared to previous versions, in the Atlantic ocean (Fig.4.3, right) as well as on global scale (not shown). This presumably contributes to reducing sea and air surface temperature biases over Europe and northern Africa in IPSLCM6 (Boucher et al., 2020).

IPSL-CM6A-LR is characterized by a multicentennial variability of MOC in the piControl simulation (Fig.1.3), driven by delayed freshwater accumulation and release in the Arctic (Jiang et al., 2021) (suggesting that salinity has an active role in the MOC of IPSL-CM6A-LR, as for IPSL-CM5, cf 4.1). To account for the intrinsic uncertainty associated with ocean and atmospheric states in 1850, an ensemble of 32 historical simulations was produced, each simulation starting from a chosen date of the piControl simulation. From this ensemble, Bonnet et al. (2021) pre-select members that are the closest to the observed global near-surface air temperatures : these members are also those with a large internally-driven weakening of the MOC since 1940's. From the 21st century onwards, however, external forcings have an increasing influence on internal variability, and dominate the decline in MOC. Consequently, the MOC weakening suggested in Caesar et al. (2018) 's reconstruction might be mainly internally-driven rather than externally forced (Bonnet et al., 2021). Note that this study does not factor in the potential role played by Greenland melting, as historical simulations of IPSL-CM6A-LR do not include an active cryosphere. The latter has been considered in Devilliers et al. (2021) described below.

4.4 Role of Greenland melting

Greenland has experienced intensive melting over the last century, particularly in the 1920's and in recent decades. The additional freshwater input to the North Atlantic is likely to affect the regional and large scale circulation: at the same time, some signs of a recent weakening of the MOC have been reported. In order to better understand the possible impact of Greenland melt on North Atlantic circulation, salinity and temperature trends, we developed an observation-based estimate of freshwater fluxes from 1840 to 2014 associated with runoff fluxes from the Greenland ice sheet and surrounding glaciers (Devilliers et al., 2021). Inputs from melting icebergs are also included and spatially distributed over the North Atlantic according to an observed climatology. Then we run an ensemble of historical simulations of the coupled IPSL-CM6A-LR climate model, adding these reconstructed additional freshwater fluxes, from 1920 to 2014.

The average of all ten members shows cooler and fresher water masses around Greenland, which spread into the subpolar gyre and then to the subtropical gyre and the Nordic seas. Over the whole period, convection is reduced in the Labrador Sea and the Nordic Seas, while it is slightly increased in the Irminger Sea, and the MOC is reduced by 0.32 ± 0.35 Sv at $26°$N. The multi-decadal trend in North Atlantic surface

temperature obtained with the additional freshwater forcing is slightly more consistent with observations than in the standard historical simulations. However, the two trends only differ at a 90% confidence level. A slight reduction of the bias to observations in the subpolar gyre region suggests that some of the surface temperature variability in recent decades may have been forced by the release of freshwater from Greenland and surrounding regions since the 1920's. Finally, we point out that the decrease in MOC due to Greenland melt remains modest in these simulations and can only explain a very small part of the 3 ± 1 Sv weakening suggested by Caesar et al. (2018).

One of the limitations of this study, conducted with IPSL-CM6A-LR, is the low spatial resolution of the ocean model around Greenland. Indeed, the circulation in the fjords, with a spatial scale of 1-10 km, and the associated oceanic mixing processes, have a strong impact on the export of freshwater to the open ocean. In addition, sensitivity studies have shown that the above results depend on the chosen strategy for distributing meltwater. Furthermore, the simulations produced do not represent the impact of the ocean on the Greenland ice sheet, which has yet to be introduced into our current climate models. With this in mind, I participated in the GRISO workshop (12/2018, USA) which brought together international experts in high-latitude ocean modelling. I personally moderated the discussion on the essential steps to be taken to ensure that ocean-Greenland ice sheet interactions are properly represented in future climate models.

4.5 Quantifying uncertainties in IPSL-CM6A-LR

Right after IPSL-CM6A-LR production for CMIP6 was finished, J. Mignot, F. Hourdin (LMD) and myself decided to continue exploring the uncertainties of this model. We envisioned a suite of simulations, with this model and two companion versions with increased spatial resolution in the ocean and/or the atmosphere. Our proposal, named QUEST (Quantifying Uncertainties and Enhancing the Speed of climate model Tuning), which I led as PI, was granted 45M computing hours by PRACE in 2019.

Climate change is no longer a possible threat for the future, it has become a reality. Robust and cost-efficient mitigation and adaptation policies require assessments of current and future risks for natural and human systems. This risk assessment relies on projections of the future climate relying on physically-based numerical simulations of the global climate that couple oceanic circulation, atmospheric dynamics, convection and clouds, together with continental hydrology, the carbon cycle and its interaction with marine biogeochemistry etc. Because of the global nature and complexity of the climate system, and because of the length of the simulations required, the approximations made in such models are numerous. Improving those simulations and quantifying the associated uncertainties are of prime importance for society. The QUEST project targets the quantification and understanding of uncertainties in the present-day climate representation and Equilibrium Climate Sensitivity estimation using IPSL-CM6.

We first explored the parametric uncertainty in IPSL-CM6A-LR configuration, by testing other tunings of the model free parameters. The question of climate model tuning has been given more importance recently in the literature (Hourdin et al., 2017). After 3 years of a long iterative process of tuning IPSL-CM6A-LR, which I led with J. Mignot for the ocean component, it appears now crucial to find a faster and more objective way of tuning climate models. At present, IPSL is focussing on the history matching approach of Williamson et al. (2013, 2017), which has already been adapted for the atmospheric component (Couvreux et al., 2021; Hourdin et al., 2021). Thanks to a sequence of atmosphere-only simulations for tuning, and then ocean-atmosphere coupled simulations to quantify the Equilibrium Climate Sensitivity, we address the following question : what are the smallest and largest climate sensitivities that could come from possible alternative choices of cloud and convective parameters, under crucial energetic constraints that are imposed in the tuning of the standard configurations of our coupled model? Analysis of the simulations is ongoing, and is the centerpiece of a publication in preparation.

In addition, we developped and performed selected simulations with two new configurations, with increased resolution in the atmosphere only (MR1, increasing resolution in the atmosphere from about 1.9° to 1.2°) and in the atmosphere and ocean (MR025, increasing also resolution in the ocean from 1° to 0.25°). With these two new configurations, **we can finally have access to the structural uncertainty in IPSL-CM6A-LR associated with grid resolution**. Although the 0.25° grid remains too coarse to represent explicitly the predominant fine scale structures in the ocean, it allows a far better representation of the mean barotropic currents and general thermodynamic structure of the ocean interior, by notably better representing topography and its effect on oceanic currents. This is expected to improve horizontal and vertical mixing within the ocean, a key process for taking up heat from the warming atmosphere. Besides, a crucial additional argument in favor of not increasing the resolution higher in the ocean, is to allow running several centennial scale climatic simulations, to explore variability up to multi-decadal scale and quantify uncertainties associated with the tuning of these configurations. Overall, the three configurations yield very similar climates, as illustrated for their annual mean biases in sea surface temperature that are almost indistinguishable from each other (Fig. 4.4).

Developping an eddy-permitting version of IPSL-CM6

I started the development of a 0.25° ocean configuration for IPSL-CM6 in 2015, and QUEST proposal gave me the opportunity to finalize these efforts. Originally, the ORCA025 configuration was developped by the DRAKKAR group, so as to highlight the role played by small scale oceanic features, mostly mesoscale eddies. I have updated this emblematic configuration to be suitable for IPSL-CM6, and created the eORCA025 configuration (extended to the south, similarly to eORCA1), in the framework of the

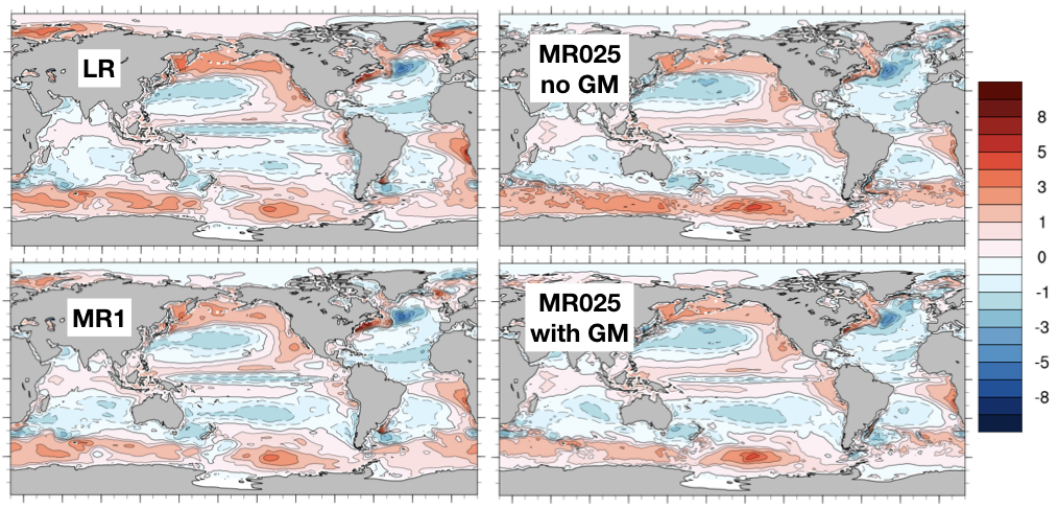

Figure 4.4: Annual mean bias in sea surface temperature in IPSL-CM6A-LR (top left), IPSL-CM6A-MR1 (bottom left), and IPSL-CM6A-MR025 without (top right) and with (bottom right) mesoscale parameterisation (see section 4.5). All simulations performed under present-day control conditions (stable external forcings, with modified albedo to account for the ongoing heat uptake of the present day oceans, see Mignot et al., 2021, for explanation on this specific protocole), and averaged over 100 years, a few hundred years after initialisation.

IsENES-2 project in collaboration with the MEOM team of the IGE, the DRAKKAR group, and for the needs of the CRESCENDO project (H2020) among others. Several scientific arguments motivate the increase of ocean resolution in climate models (to better represent bathymetry, to improve the mean ocean circulation, the spatial distribution of biogeochemical tracers, some variability mechanisms...) but it is important to keep in mind that the $0.25°$ resolution remains insufficient to explicitly resolve oceanic mesoscale processes. Hence, for the purposes of coupling with atmosphere dynamics, represented at even coarser resolution, it may be preferable to parameterise these processes rather than represent them only partially.

The perspective of coupling to marine biogeochemistry also motivates to parameterise mesoscale processes at $0.25°$. Since the EMBRACE project (H2020), I contributed to develop and test a technical solution to run the biogeochemical module at coarser resolution than the ocean dynamics. If physical processes have a high spatial variance at the 1 or 2 mesh scale (which is the case for vertical velocities in all ORCA025 configurations of DRAKKAR), then the grid change will have a strong impact on the coupling between physics and biogeochemistry. This impact may be positive, for example if the spatial variance is the signature of numerical noise that we want to get rid of, but it

is not obvious to disentangle grid scale noise from physical processes. Consequently, I think that it is preferable to control the spatial variance at small spatial scales, and this requires a decrease in the explicit part and an increase in the parameterised part of fine-scale processes. To move in this direction, it was necessary to perform a large number of simulations, with and without coupling to the marine biogeochemical model, and to carry out detailed analyses of the spatial and temporal variability of physical and biogeochemical variables.

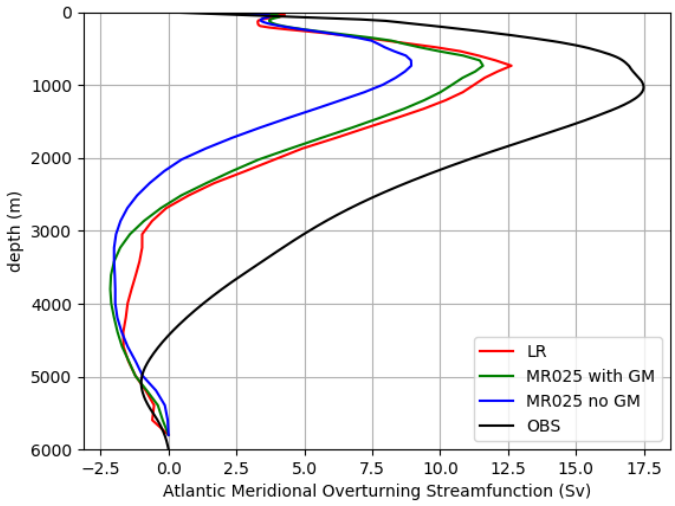

Figure 4.5: MOC streamfunction at $26°$N in IPSL-CM6A-LR (red), IPSL-CM6A-MR025 with eddy parameterisation (green) and without eddy parameterisation (blue) and in observations (black, same as in Fig. 4.2). Model simulations are averaged over 100 yr after 450 yr of integration under present-day control conditions (as in Fig.4.4).

Tuning the parameterisation of mesoscale processes in eORCA025 was done in collaboration with M. Ilicak, as he visited LOCEAN in 2016. Starting from the original GM parameterisation (Gent and Mcwilliams, 1990), we tested different values for the maximum eddy induced velocities, added a criteria on the local Rossy radius of deformation to activate the mesoscale parameterisation (Hallberg, 2013), evaluated the contribution of a mixed-layer parameterisation (Fox-Kemper et al., 2011) and modified the isoneutral diffusivity. These simulations were done in ocean-only mode, as running in coupled mode was too expensive computationally. These experiments informed the characteristics of the coupled IPSL-CM6A-MR025 configuration with eddy parameterisation shown in Fig. 4.5 (green line). As a comparison, we also ran a companion IPSL-CM6A-MR025 configuration with no eddy parameterisation (Fig. 4.5, blue line). The northward-flowing branch of the MOC, near the surface, remains too shallow in IPSL-CM6A-MR025, as in

IPSL-CM6A-LR, and mesoscale parameterisation does not seem to have any impact on this bias. However, **removing the mesoscale parameterisation drastically reduces the maximum value of the overturning**, hence making worse the already negative bias of IPSL-CM6A-LR as compared to observations. The mesoscale parameterisation also has an impact on the MOC streamfunction at depth, below $2,000$m, where the maximum overturning cell for abyssal water locates shallower with no GM than with GM. This seems to be related to dense water formation in the Southern ocean, as the two simulations exhibit substantial differences in mixed layer depth around Antarctica, and polynyas seem to be reduced with GM, as expected. To the contrary, differences in mixed layer depth are very small in the North Atlantic, which is not expected. It seems that the MOC is stronger with GM because the boundary currents in subpolar gyre are more intense, but this remains to be clarified.

4.6 Perspective

As we progress in understanding the role of small scale ocean processes in climate, in particular through inverse energy cascades, the need to represent their effect despite the coarse spatial resolution increases. This imposes revising the parameterisations of sub-grid-scale processes, and also augmenting the complexity in ocean configurations for climate models, such as ice-shelf-covered areas around Antarctica. I am involved in several initiatives to progress in this direction, which I briefly introduce below. Those do not exclusively concern the MOC, but aim at improving the numerical representation of ocean dynamics, hence will benefit to models of the MOC and its role in climate, as well.

Increasing complexity in ocean - ice shelf interactions

Together with Ute Hausmann, postdoc funded by the WAPITI project (P.I. J.-B. Sallée, `http://wapiti-project.com`) whom I co-advised, we developed a high-resolution numerical configuration of the southwestern Weddell Sea, which, with its continental shelves and huge adjacent sub-glacial cavities such as the Filchner-Ronne iceshelf, represents one of the main links between the Antarctic ice sheet and the rest of the globe. Running simulations with and without tides, we were able to demonstrate that tides increase the kinetic energy of the currents in contact with the ice shelf, and thus the rate of melting, which must be balanced by increased heat transport into the cavity (Hausmann et al., 2020).

I also participated in the study led by Katherine Hutchinson, other postdoc of NEMO R&D which I am the principal advisor, based on novel hydrographic observations offshore Larsen C iceshelf (Hutchinson et al., 2020). Using a water mass decomposition technique, we highlighted the high level of mixing taking place offshore the iceshelf front,

and the large spatial disparity in water mass characteristics. In addition, she could not exclude the hypothesis that warm water masses on the continental shelf impact under ice-shelf cavity and, possibly, melting of Larsen C iceshelf. These results underline the need to improve the representation of water mass transformations in these areas, in climate models that aim at representing ice sheet - ocean interactions.

As a step forward in this direction, Katherine is now working on the eORCA1 configuration that I prepared for CMIP6, in order to evaluate how to improve the representation of these processes at 1° resolution. As a preliminary step, we played with a test case of under ice-shelf cavity to illustrate the impact of spatial resolution and other numerical choices (including initial conditions), on the representation of circulation and water mass transformations within the cavity. We have also tested optimal numerical choices when representing explicitly the cavities in eORCA1, so as to improve water mass transformations and circulation around Antarctica. Hopefully this will improve dense water formation hence the global circulation consequently, but that remains to be proven.

Introducing Machine Learning techniques in IPSL-CM

Notwithstanding the improvements achieved with eORCA025 when including a parameterization of mesoscale processes, the latter remains imperfect : some characteristics of meso-scale processes are not represented (in particular the vertical structure of associated heat and salt fluxes), some drivers are eluded (for example the influence of topography), and they include non-scale aware parameters that have to be tuned. In order to by-pass these constraints, I have started to envision using other types of parameterizations, based on Machine Learning algorithms (e.g. Bolton and Zanna, 2019), so as [i] to ensure a better transfer of information from high to low resolution models (Couvreux et al., 2021) and [ii] to adjust automatically the non-scale aware parameters (e.g. Williamson et al., 2017).

In the perspective of advancing the IPSL climate modelling community with regard to ML techniques, together with V. Balaji, MOPGA laureate at IPSL, we organize since 2018 monthly discussions on the benefits of Machine Learning for climate modeling. The community that we gather with these discussions is national, as it includes collaborators in Grenoble, Lyon and Brest beyond Paris, and sometimes international when US colleagues join us. In addition, I co-advised with V. Balaji two postdocs : Anna Sommer (during 6 months in 2019) and Redouane Lguensat (since march 2020). Redouane is currently exploring D. Williamson's technique of automatic tuning using Lorenz (1996) simple model, before switching to NEMO. I also joined the M2LInes consortium led by L. Zanna (NYU, `https://m2lines.github.io/`), which aims at developing new parameterisations of sub-grid-scale processes for climate models.

Chapter 5

Conclusion

5.1 Insights on the MOC

Even if the MOC is a complex oceanic structure, as it superimposes contributions from several currents that are highly non linear, some knowledge can be gained from simple oceanic models. During my postdoc, I have developed two simple models to investigate the relationship between dense water formation in convective areas, and the boundary currents that constitute the MOC. Deshayes et al. (2009) suggest caution when estimating variability of the MOC from observations of the DWBC in the subpolar gyre. Indeed, interannual variability of the transport of dense water by the DWBC at the outflow of the Labrador Sea is not related to changes in dense water formation, but reflects variability in the boundary currents of the subpolar gyre, which are primarily forced by the wind. This is primarily due to the fact that the interior of the convective basin and the surrounding boundary currents are connected by turbulent heat fluxes. I have also shown that the latter result from both baroclinic and barotropic instability of the boundary current, hence are also affected by wind forcing.

As a consequence, it is compulsory to produce ocean hindcasts as realistic as possible, for both the wind-driven circulation and the buoyancy driven water mass transformations, so as to make further progress in understanding the variability of the MOC in the North Atlantic. Unfortunately, producing such hindcast is not straightforward, as high resolution is requested to represent western boundary current dynamics adequately. Rather than increasing spatial resolution at the global scale (I concluded that regional configurations are not compatible with MOC investigations), I demonstrate in Talandier et al. (2014) that embedding AGRIF nests enables to increase resolution locally hence improve the surface and deep ocean currents in the North Atlantic. In this study, we also show that reducing biases in simulated ocean currents reduces the influence of dense water formation in the subpolar gyre onto the MOC. This challenges analyses of the MOC drivers in models that do not represent ocean currents correctly.

Notwithstanding, I explored the role of salinity in MOC changes in 5 climate models contributing to CMIP5, and developed in the meanwhile PAGO, a tool to inter-compare transports in ocean models, in a robust and efficient way. Deshayes et al. (2014) illustrate that freshwater budget in the North Atlantic and its link to the MOC differs widely between models, forcing to revise the relationship of freshening causing a weakened circulation, as usually expected.

Meridional transport of freshwater in the South Atlantic provides other type of information about the MOC, as it seems to indicate whether it is likely to change abruptly or not. AInter-comparing a suite of global simulations at high and coarse spatial resolution, Deshayes et al. (2013) found that an abrupt change in the MOC is possible at present, if the amount of freshwater in the North Atlantic increases. On the other hand, climate models with coarse spatial resolution tend to overestimate the stability of the MOC, according to this criteria.

Investigating high and coarse ocean models around the tip of South Africa, indicates that different models resolving eddies converge in the spatio-temporal scales of variability of the Agulhas leakage, despite substantial differences in the synoptic currents and thermohaline structures. However, climate models suffer again from their coarse resolution, and miss to represent these characteristics of variability.

Since 2009, I have tried to incorporate my expertise of the MOC and ocean modelling into the preparation of the ocean component of IPSL-CM6. Because other models shared the same version of NEMO at same spatial resolution (namely 1°), we exchanged expertise and information on this configuration of NEMO, so-called eORCA1. As illustrated when comparing IPSL and CNRM models, we observe points of similarity in the MOC and meridional heat transport, but substantial differences as well, even in ocean-only simulations forced by the same atmospheric conditions (due to the fact that calibration was performed for the coupled model). This confirms that we are still missing convergence in MOC strength and structure, as already pointed after the previous CMIP exercice.

I explored further the structural and parametric uncertainty in the MOC as represented by IPSL-CM6A-LR, developing a version of the model with increased resolution in the ocean (up to $1/4^\circ$) and atmosphere. Again, I found similarities in the MOC strength and shape, but also substantial differences, in particular regarding dense water formation around Antarctica. Meanwhile, I demonstrate that the global $1/4^\circ$ configuration of NEMO, which only partially resolves mesoscale processes, produces results more consistent with the observations if a parameterization of these eddies is activated.

5.2 Future plans in ocean and climate Modelling

Ongoing evolution of OGCM is oriented primarily towards resolving finer scale processes, via an increase in the spatial resolution of configurations, even at global scale (Fox-

Kemper et al., 2019). This motivation to increase the complexity of OGCM (for example representing non-hydrostatic processes, or wet and dry areas hence shoaling) comes with a need to understand better how the models are functioning, so as to quantify all sources of uncertainties (structural, ie associated with numerical choices and parametric, related to unresolved processes). Unfortunately, increasing spatial resolution increases the computational cost of a given configuration, hence limiting our capacity to run multiple sensitivity experiments to assess uncertainties. It also impedes to realize long term integrations, which are necessary to explore ocean processes at climate scale. Additionally, increasing spatial resolution does not diminish spurious diapycnal mixing induced by numerical schemes (Holmes et al., 2021), which is one of the most critical weaknesses of OGCM for climate integrations.

Similarly, discussions about the future of climate modelling has been tied up with incitements to increase spatial resolution, at least since CMIP5. The most iconic manifestation of this trend is an everlasting flagship enterprise to develop a climate model with 1km wide ocean and atmospheric grid cells (Bauer et al., 2021). Such a model will certainly give insights on some aspects of climate modelling that remain to be clarified, most importantly the meso-scale interactions between ocean and atmosphere. It will also stimulate technological developments that might benefit to all configurations even at coarser resolution, through optimizing computational efficiency and adjusting to new HPC infrastructures. Notwithstanding, in the kilometric scale climate configuration, there will remain parameterizations of sub-grid-scale processes and couplings to be calibrated, yet quantifying uncertainties will become more difficult, not to say impossible. Hence this new perspective for climate modelling may not facilitate the realization of long-term integrations (> 1000 yr), compulsory to explore different MOC and climate equilibrium states, nor the production of large ensembles of simulations, which is the unique solution to grasp the intrinsic chaotic nature of climate.

Besides increasing spatial resolution, the trend in ocean model development at present is to increase the order of numerical schemes (Lemarié 2020 [1]). As for increased spatial resolution, this does not help with rendering ocean models more interpretable, and it remains to be proven that increasing the order of advection schemes will reduce spurious diapycnal mixing. Indeed, with a finer discretization comes a finer resolution of small-scale features, in particular in the velocity fields. Such irregular velocity fields are harder to handle for the advection of tracers, which are in turns much more diffused. While the research axis based on finer discretization and higher order schemes is well-covered by various modelling groups, the ANDIAMO project (led by S. Téchené, N. Aguillon and myself, supported by Sorbone Universite's ISCD since 2020) proposes to adopt a different point of view, based on low order numerical methods that have by design some desirable properties (see Fig. 5.1). It is worth noticing that coarse grids is the framework where smart first order methods may perform better than high order ones

[1] https://hal.inria.fr/hal-03153619/file/Talk_MOI_June2020.pdf

(Mailler et al., 2021). Also, such an approach makes it possible to assess the mathematical properties of OGCMs, such as existence, unicity and characteristics of equilibrium state(s).

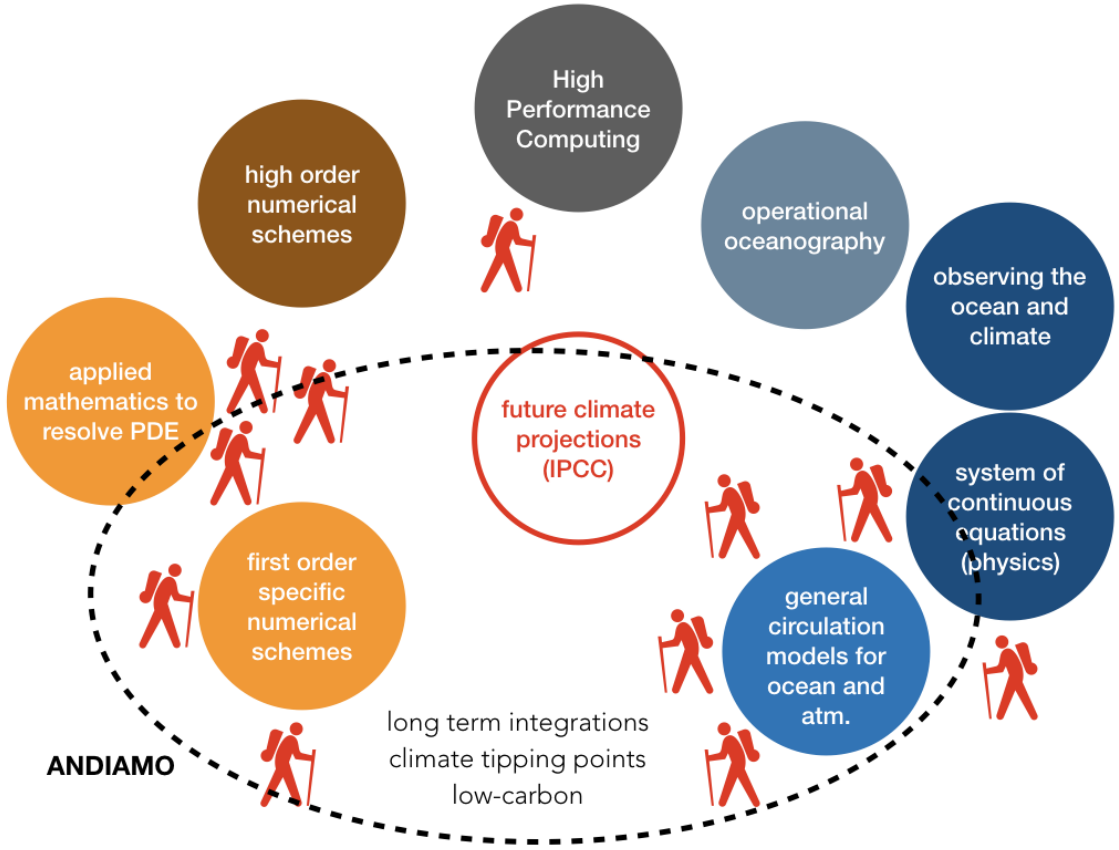

Figure 5.1: Positioning of the ANDIAMO community by subject, in the landscape of mathematics for ocean and climate modelling.

Paramaterizations of sub-grid-scale processes in OGCMs need a revolution, to adjust automatically to the effective resolution of model grids hence reduce the need to tune model parameters for configuration. This revolution has started already, as MOM6 includes scale-aware parameterizations (Adcroft et al., 2019). In parallel, machine learning techniques have become promising tools to improve sub-grid-scale parameterisations, as they enable to automatically transfer information through different scales. This is the focus of M2Lines project funded by the Virtual Earth System Research Institute of Schmidt Foundation, for the period 2020-2024, to which I contribute.

Although climate projections that inform IPCC reports are exclusively based on GCM, the development of these tools relies on other types of models, namely Large Eddy

Simulations that inform parameterisations, Regional Climate Models useful to validate processes at regional scale, and Earth System Models of intermediate complexity, to name a few (Fig.5.2). The latter offer the unique opportunity to produce millennial scale simulations, which are compulsory to explore climate tipping points. Even with such a hierarchy of models in hands, it remains challenging to transfer information from one model to the other, as complexity and spatial resolution are very different from one to the other. Using a hierarchy of models seems particularly appropriate to accelerate spinup and explore uncertainties in the representation (explicit or parameterized) of some processes or interactions between processes. It is also important to keep in mind that each application of future projections requires a tailored degree of complexity and spatial resolution of each component of the climate system, so as to minimise structural and parametric uncertainties. This encourages the development of multi-purpose platforms (with modular number of components, complexity and resolution), to be derived in fit-for-purpose configurations, that will provide answers to specific questions in the most efficient way, rather than unique configurations with maximal complexity and resolution (Balaji, 2021).

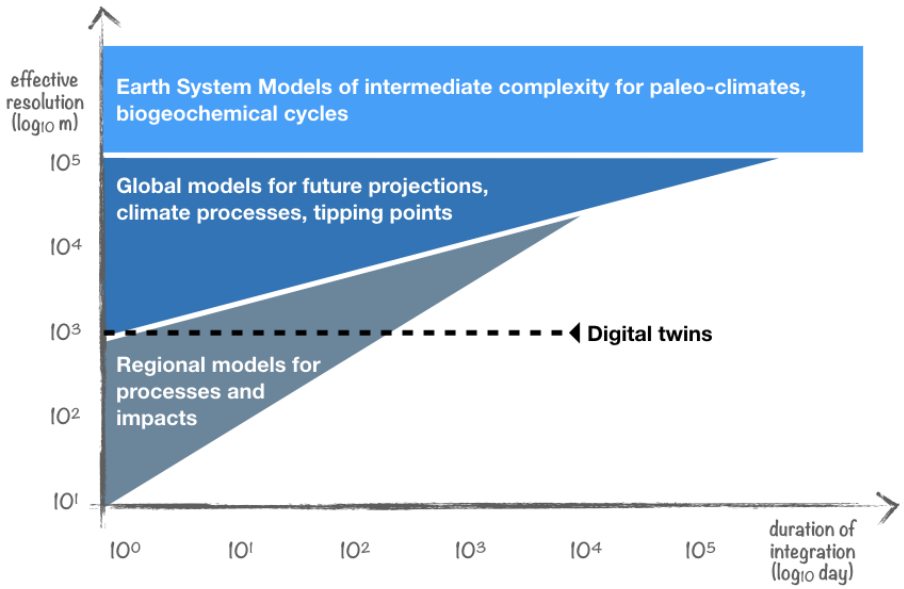

Figure 5.2: Illustration of different types of ocean and climate models by spatial resolution and duration of integration.

Appendix

List of publications

- Bonnet R., D. Swingedouw, G. Gastineau, O. Boucher, J. Deshayes, F. Hourdin, J. Mignot, J. Servonnat, et A. Sima 2021: Increased Risk of near Term Global Warming Due to a Recent AMOC Weakening, Nature Communications 12, 6108, doi:10.1038/s41467-021-26370-0.

- Mignot J., F. Hourdin, J. Deshayes, O. Boucher, G. Gastineau, I. Musat, M. Vancoppenolle, J. Servonnat, A. Caubel, F. Chéruy, S. Denvil, J.-L. Dufresne, C. Ethé, L. Fairhead, M.-A. Foujols, J.-Y. Grandpeix, G. Levavasseur, O. Marti, M. Menary, C. Rio, C. Rousset et Y. Silvy 2021: The Tuning Strategy of IPSL-CM6A-LR, Journal of Advances in Modeling Earth Systems 13, 5, doi:10.1029/2020MS002340.

- Devilliers M., D. Swingedouw, J. Mignot, J. Deshayes, G. Garric, et M. Ayache 2021: A Realistic Greenland Ice Sheet and Surrounding Glaciers and Ice Caps Melting in a Coupled Climate Model, Climate Dynamics, 57, 2467–2489, doi:10.1007/s00382-021-05816-7.

- Bricaud C., J. Le Sommer, M. Gurvan, C. Calone, J. Deshayes, C. Ethé, J. Chanut, and M. Levy 2020: Multi-grid algorithm for passive tracer transport in NEMO ocean general circulation model: a case study with NEMO OGCM (version 3.6), Geoscientific Model Development, 13, 3347–3371, doi:10.5194/gmd-13-3347-2020.

- Hausmann U., J.-B. Sallee, N. C. Jourdain, P. Mathiot, C. Rousset, G. Madec, J. Deshayes and T. Hattermann 2020: The role of tides in ocean-ice shelf interactions in the Southwestern Weddell Sea, Journal of Geophysical Research - Oceans, 125, doi:10.1029/2019JC015847.

- Colombo P., B. Barnier, T. Penduff, J. Chanut, J. Deshayes, J.-M. Molines, J. Le Sommer, P. Verezemskaya, S. Gulev, and A.-M. Treguier 2020: Representation of the Denmark Strait overflow in a z-coordinate eddying configuration of

the NEMO (v3.6) ocean model: resolution and parameter impacts, Geoscientific Model Development, 13, 3347-3371, doi:10.5194/gmd-13-3347-2020.

- Boucher O., J. Servonnat, A. L. Albright, O. Aumont, Y. Balkanski, V. Bastrikov, S. Bekki, R. Bonnet, S. Bony, L. Bopp, P. Braconnot, P. Brockmann, P. Cadule, A. Caubel, F. Cheruy, F. Codron, A. Cozic, D. Cugnet, F. D'andrea, P. Davini, C. de Lavergne, S. Denvil, J. Deshayes, M. Devilliers, A. Ducharnee, J.-L. Dufresne, E. Dupont, C. Ethé, L. Fairhead, L. Falletti, S. Flavoni, M.-A. Foujols, S. Gardoll, G. Gastineau, J. Ghattas, J.-Y. Grandpeix, B. Guenet, L. E. Guez, E. Guilyardi, M. Guimberteau, D. Hauglustaine, F. Hourdin, A. Idelkadi, S. Joussaume, M. Kageyama, M. Khodri, G. Krinner, N. Lebas, G. Levavasseur, C. Lévy, L. Li, F. Lott, T. Lurton, S. Luyssaert, G. Madec, J.-B. Madeleinee, F. Maignan, M. Marchand, O. Marti, L. Mellul, Y. Meurdesoif, J. Mignot, I. Musat, C. Ottlé, P. Peylin, Y. Planton, J. Polcher, C. Rio, N. Rochetin, C. Rousset, P. Sepulchre, A. Sima, D. Swingedouw, R. Thiéblemont, A. K. Traore, M. Vancoppenolle, J. Vial, J. Vialard, N. Viovy and N. Vuichard, 2020 : Presentation and evaluation of the IPSL-CM6A-LR climate model, Journal of Advances in Modeling Eearth Systems, 12, e2019MS002010, doi:10.1029/2019MS002010.

- Hutchinson K., J. Deshayes, J.-B. Sallée, J. A. Dowdeswell, C. de Lavergne, I. Sansorge, H. Luyt, T. Henry, S. E. Fawcett, 2020: Water masse characteristics and distribution adjacent to Larsen C ice shelf, Antarctica, Journal of Geophysical Research Oceans, 125, doi:10.1029/2019JC015855.

- Gourrion J., J. Deshayes, M. Juza and T. Szekely, 2019: Temperature and salinity anomalies in the North Atlatnic subpolar gyre, in Copernicus Marine Service Ocean State Report, Issue 3, Journal of Operational Oceanography, 12, doi:10.1080/1755876X.2019.1633075.

- Séférian R., P. Nabat, M. Michou, D. Saint-Martin, A. Voldoire, J. Colin, B. Decharme, C. Delire, S. Berthet, M. Chevallier, S. Sénési, L. Franchisteguy, J. Vial, M. Mallet, E. Joetzjer, O. Geoffroy, J.-F. Guérémy, M.-P. Moine, R. Msadek, A. Ribes, M. Rocher, R. Roehrig, D. Salas-y-Mélia, E. Sanchez, L. Terray, S. Valcke, R. Waldman, O. Aumont, L. Bopp, J. Deshayes, C. Éthé, G. Madec, 2019: Evaluation of CNRM Earth-System model, CNRM-ESM 2-1: role of Earth system processes in present-day and future climate, Journal of Advances in Modeling Earth Systems, 11, 4182-4227, doi:10.1029/2019MS001791.

- Voldoire A., D. Saint-Martin, S. Sénési, B. Decharme, A. Alias, M. Chevallier, J. Colin, J.-F. Guérémy, M. Michou, M.-P. Moine, P. Nabat, R. Roehrig, D. Salas y Mélia, R. Séférian, S. Valcke, I. Beau, S. Belamari, S. Berthet, C. Cassou, J. Cattiaux, J. Deshayes, H. Douville, C. Ethé, L. Franchistéguy, O. Geoffroy,

C. Lévy, G. Madec, Y. Meurdesoif, R. Msadek, A. Ribes, E. Sanchez-Gomez, L. Terray, R. Waldman, 2019: Evaluation of CMIP6 DECK Experiments With CNRM-CM6-1, Journal of Advances in Modeling Earth Systems, 11, 2177-2213, doi:10.1029/2019MS001683.

- Deshayes J., J. Gourrion, M. Juza, T. Szekely and J. Tintore 2018 : Deep convection in the Labrador Sea, in Copernicus Marine Service Ocean State Report, Journal of Operational Oceanography, 11, doi:10.1080/1755876X.2018.1489208.

- Gourrion J., J. Deshayes, M. Juza, T. Szekely, J. Tintore 2018 : A persisting regional cold and fresh water anomaly in the Northern Atlantic, in Copernicus Marine Service Ocean State Report, Journal of Operational Oceanography, 11, doi:10.1080/1755876X.2018.1489208.

- Menary Matthew B., T. Kuhlbrodt, J. Ridley, M. B. Andrews, O. B. Dimdore-Miles, J. Deshayes, R. Eade, L. Grayt, S. Ineson, J. Mignot, C. D. Roberts, J. Robson, R. A. Wood, P. Xavier, 2018: Pre-industrial control simulations with HadGEM3-GC3.1 for CMIP6, Journal of Advances in Modeling Earth Systems, 10, 3049-3075, doi:10.1029/2018MS001495.

- McInnes M. A., P. G. Ryan, M. Lacerda, J. Deshayes, W. S. Goschen, L. Pichegru 2017: Small pelagic fish responses to fine-scale oceanographic conditions: implications for the endangered African penguin, Marine Ecology Progress Series, 569, 187–203, doi:10.3354/meps12089.

- Treguier A.-M., C. Lique, J. Deshayes, J.-M. Molines 2017: The North Atlantic eddy heat transport and its relation with the vertical tilting of the Gulf Stream axis, Journal of Physical Oceanography, 47, 1281–1289.

- Holton, L., J. Deshayes, B.C. Backeberg, B.R. Loveday, J.C. Hermes and C.J.C. Reason 2017: Spatio-temporal characteristics of Agulhas leakage: a model intercomparison study. Climate Dynamics, 48, 2107-2121, doi:10.1007/s00382-016-3193-5.

- Griffies, S. M., Danabasoglu, G., Durack, P. J., Adcroft, A. J., Balaji, V., Böning, C. W., Chassignet, E. P., Curchitser, E., Deshayes, J., Drange, H., Fox-Kemper, B., Gleckler, P. J., Gregory, J. M., Haak, H., Hallberg, R. W., Heimbach, P., Hewitt, H. T., Holland, D. M., Ilyina, T., Jungclaus, J. H., Komuro, Y., Krasting, J. P., Large, W. G., Marsland, S. J., Masina, S., McDougall, T. J., Nurser, A. J. G., Orr, J. C., Pirani, A., Qiao, F., Stouffer, R. J., Taylor, K. E., Treguier, A. M., Tsujino, H., Uotila, P., Valdivieso, M., Wang, Q., Winton, M., and Yeager, S. G. 2016: OMIP contribution to CMIP6: experimental and diagnostic protocol for the physical component of the Ocean Model Intercomparison Project, Geosci. Model Dev., 9, 3231-3296, doi:10.5194/gmd-9-3231-2016.

- Barrier N., J. Deshayes, A.-M. Treguier et C. Cassou 2015 : Heat budget in the North Atlantic subpolar gyre: Impacts of atmospheric weather regimes on the 1995 warming event, Progress in Oceanography, 130 75–90, doi:10.1016/j.pocean.2014.10.001.

- Thomas M., A-M. Treguier, B. Blanke, J. Deshayes and A. Voldoire 2015 : Isolating the impacts of mixed layer subduction on the meridional overturning circulation in a numerical model, Journal of Climate, 28, 7503-7517.

- Treguier A.-M., J. Deshayes, J. Le Sommer, C. Lique, T. Penduff, J.-M. Molines, G. Madec, C. Talandier, R. Bourdalle-Badie 2014 : Meridional transport of salt in the global ocean from an eddy-resolving model, Ocean Sciences, doi:10.5194/os-10-243-2014.

- Deshayes J., R. Curry, R. Msadek 2014 : CMIP-5 model intercomparison of freshwater budget and circulation changes in the North Atlantic, Journal of Climate, 27 (9), 3298-3317.

- Talandier C., J. Deshayes, A.-M. Treguier, X. Capet, R. Benshila, L. Debreu, R. Dussin, J.-M. Molines, G. Madec 2014 : Improvements of simulated Western North Atlantic current system and impacts on AMOC, Ocean Modelling, 76, 1-19, doi:10.1016/j.ocemod.2013.12.007.

- Barrier N., C. Cassou, J. Deshayes et A.-M. Treguier 2013 : Response of North Atlantic ocean circulation to atmospheric weather regimes, Journal of Physical Oceanography, 44, 179- 201, doi:10.1175/JPO-D-12-0217.1.

- Mignot J., D. Swingedouw, J. Deshayes, O. Marti, C. Talandier, R. Seferian, M. Lengaigne, G. Madec 2013 : On the evolution of the oceanic component of the IPSL climate models: from CMIP3 to CMIP5, Ocean Modelling, 72, 167-184, doi:10.1016/j.ocemod/2013/09/001.

- Deshayes J., A.-M. Treguier, B. Barnier, A. Lecointre, J. Le Sommer, J.-M. Molines, T. Penduff, R. Bourdalle-Badie, Y. Drillet, G. Garric, R. Benshila, G. Madec, A. Biastoch, C. Boning, M. Scheinert, A. C. Coward, J. J.-M. Hirschi 2013: Oceanic hindcast simulations at high resolution suggest that the Atlantic MOC is bistable, Geophysical Research Letters, 40, 3069-3073, doi:10.1002/grl.50534.

- Maze G., J. Deshayes, J. Marshall, A.-M. Treguier, L. Vollmer et A. Chronis 2013 : Surface vertical PV fluxes and subtropical mode water formation in an eddy-resolving numerical simulation, Deep Sea Research 2, 91, 128-138, doi:10.1016/j.dsr2.2013.02.026.

- A. Voldoire, E. Sanchez-Gomez, D. Salas y Mélia, B. Decharme, C. Cassou, S.Sénési, S. Valcke, I. Beau, A. Alias, M. Chevallier, M. Déqué, J. Deshayes, H. Douville, E. Fernandez, G. Madec, E. Maisonnave, M.-P. Moine, S. Planton,

D.Saint-Martin, S. Szopa, S. Tyteca, R. Alkama, S. Belamari, A. Braun, L. Coquart et F. Chauvin, 2013 : The CNRM-CM5.1 global climate model: Description and basic evaluation, Climate Dynamics, 40, 2091-2121, doi: 10.1007/s00382-011-1259-y.

- Barrier N., A.-M. Treguier, C. Cassou et J. Deshayes 2012 : Impact of the winter North-Atlantic Weather Regimes on subtropical Sea-Surface Height variability, Climate Dynamics, doi:10.1007/s00382-012-1578-7.

- A. M. Treguier, J. Deshayes, C. Lique, R. Dussin et J.M. Molines, 2012 : Eddy contributions to the meridional transport of salt in the North Atlantic, Journal of Geophysical Research, 117, doi:10.1029/2012JC007927.

- Deshayes J., F. Straneo et M. Spall, 2009 : Mechanisms of variability in a convective basin, Journal of Marine Research, 67, 273-303, doi: 10.1357/002224009789954757.

- Frankignoul C., J. Deshayes et R. Curry, 2009 : The role of salinity in the decadal variability of the North Atlantic meridional overturning circulation, Climate Dynamics, 33, 777-793, doi:10.1007/s00382-008-0523-2.

- Deshayes J., C. Frankignoul, 2008 : Simulated variability of the circulation in the North Atlantic from 1953 to 2003, Journal of Climate, 21, 4919-4933, doi: 10.1175/2008JCLI1882.1.

- Deshayes, J., C. Frankignoul, et H. Drange, 2007 : Formation and export of deep water in the Labrador and Irminger Seas in an ocean model, Deep-Sea Research 1, 54, 510-532, doi: 10.1016/j.dsr.2006.12.014.

- Sirven, J., C. Herbaut, J. Deshayes et C. Frankignoul, 2007 : Origin of the peaks of variability in the response of a 1.5 layer ocean model to stochastic forcing, Journal of Physical Oceanography, 37, 2146-2157, doi: 10.1175/JPO3095.1.

- Herbaut, C., J. Sirven et J. Deshayes, 2006 : Sensitivity of the meridional transport in a 1.5 layer ocean model to localized mass sources, Journal of Marine Research, 64, 819-833, doi:10.1357/ 002224006779698404.

- Deshayes, J. and C. Frankignoul, 2005 : Spectral characteristics of the response of the meridional overturning circulation to deep water formation, Journal of Physical Oceanography, 35 (10), 1813-1825, doi: 10.1175/JPO2793.1.

List of supervised Master and PhD projects

Nicolas Barrier, PhD

Nicolas, a Master student of IUEM, was co-supervised for his PhD by Anne-Marie Treguier, Christophe Cassou and myself, from 2010 to 2013. He combined using conceptual models and high-resolution realistic simulations to clarify the oceanic adjustment to atmospheric forcings in the North Atlantic during the last 50 years. Nicolas wrote three publications as first author during his PhD, which is outstanding, and he additionally contributed substantially to the development of PAGO (described in section 3.2). Also he realized himself all the numerical simulations that he used during his PhD, and became rapidly an expert in python for oceanography (see his webpage `http://nicolasbarrier.fr/`). I admire that duality in his PhD project : publishing novel scientific results as well as developping numerical tools for the community. His expertise is North Atlantic dynamics has been internationally recognized since his first PhD publication, yet rather than pursuing a career as research scientist, he chose to contribute to the development of applications for oceanography and has been hired permanently by IRD as a research engineer in 2017.

Claude Talandier, PhD

Claude has been hired permanently by CNRS as a research engineer in 2006, and began his PhD as continuing education in 2010. I proposed to make use of his pre-existing expertise in NEMO (Claude was an NEMO developper from 2006 to 2010) to develop a global configuration with an AGRIF zoom in ice-covered areas (at that time, only 1 such configuration existed, developed by F. Dupont in Canada). With such configuration, we could finally address the impact of spatial resolution on the MOC in the North Atlantic. Claude's work as a PhD student involved a lot of NEMO developments, that were included in the shared version of the model afterwards. He also contributed to advancing our understanding of the impact on spatial resolution on dense water fomation and circulation, as reported in a publication in 2014. He defended his PhD in 2015, but the last chapter of his PhD, analyzing the potential vorticity budget of the Labrador Sea, has not yet been translated into a publication, because we concluded that online diagnostics were necessary. I hope to continue this study as soon as such diagnostics are available (see section 3.3), via an updated NEMO-AGRIF configuration of the subpolar North Atlantic, possibly with a new PhD student.

other students of IUEM

While at LPO, I contributed to the supervision of other students of IUEM, mostly on the analysis of high resolution simulations produced by the DRAKKAR consortium. I co-

advised some of these students with Guillaume Maze, permanent scientist at IFREMER, focussing on mode water formation in the vicinity of the Gulf Stream, which led to a publication in 2013. I also engaged a collaboration with Laurent Memery, CNRS scientist at LEMAR, specialist in biogeochemistry, through the project of Charlène Feucher, that aimed at analyzing the impact of model biases in the Gulf Stream separation on primary production in the North Atlantic.

Lisa Holton

Lisa Holton is the first UCT student whom I was the primary advisor, during my visit to the department of Oceanography in 2013-2014. As a taught master student, she worked under my supervision for 6 months, inter-comparing simulation outputs of ROMS, NEMO and HYCOM for the Agulhas leakage using PAGO (see section 3.2). This led to a publication in Climate Dynamics and Lisa graduated with honors. Since then, she has been hired by Lwandle in Cape Town, a private company that produces marine services, and regularly supervises master students from UCT.

Marion Bezaud

During my stay at UCT, a joint program between LPO and the department of Oceanography encouraged student exchanges in both directions, and Marion Bezaud, Master 2 at UBO and 3rd yr student at ENSTA-Bretagne, benefited from this program and worked under the supervision of Dr B. Backeberg and myself for 5 months. She undertook an analysis of potential vorticity in HYCOM simulations of the Agulhas Current, which explained how a modification in the choice of density layers at depth influences the dynamics of the upper Agulhas Current. This work led to several presentations in international conferences and workshops, and Dr B. Backeberg wrote a manuscript to describe the results, which was never published as Dr B. Backeberg moved away from his academic position. Afterwards, Marion Bezaud did a PhD in oceanography at IFREMER. Since she graduated, I have employed her as a postdoc, working on high resolution simulations of the Caribbean archipelago.

Sarah Asdar, PhD

Sarah Asdar also benefited from the exchange program between UBO and UCT, and I co-supervised, together with Pr I. Ansorge, her 5 month study of the position of ACC fronts in the vicinity of Prince Edward Islands. She then returned to UCT for a PhD, which I co-supervised with Dr P. Penven, Dr T. Gorgues and Pr I. Ansorge, on the interaction between ACC fronts and hydrography in the same region, using ROMS simulations and observations. She graduated in 2018 and has been working as a postdoc since then, in South Africa and in France.

other students of UCT

I have contributed to the supervision of many other students while at UCT, of Master and PhD level. Kyle Cooper was doing a Master by dissertation, which means that he worked for 2 yr under the supervision of Dr B. Backeberg, Dr J. Hermes and myself, intercomparing ROMS, NEMO and HYCOM simulations of the Agulhas Current (I taught him how to use PAGO for this study). I also assisted Alistair McInnes, a PhD student in the biology department of UCT, to analyse diving behaviours of African penguins in relation with hydrographic observations, which led to a publication (Alistair is now a Seabird Conservation Programme Manager for BirdLife South Africa). Finally I co-supervised the PhD of Mthetho Sovara, funded by UCT and CSIR, on the development the ocean component of a climate model to contribute to CMIP6 - a study that was abandoned as Mthetho gave up on his PhD.

Publications from supervised Master and PhD projects

- Colombo P., B. Barnier, T. Penduff, J. Chanut, J. Deshayes, J.-M. Molines, J. Le Sommer, P. Verezemskaya, S. Gulev, and A.-M. Treguier 2020: Representation of the Denmark Strait overflow in a z-coordinate eddying configuration of the NEMO (v3.6) ocean model: resolution and parameter impacts, Geoscientific Model Development, 13, 3347-3371, doi:10.5194/gmd-13-3347-2020.

- McInnes M. A., P. G. Ryan, M. Lacerda, J. Deshayes, W. S. Goschen, L. Pichegru 2017: Small pelagic fish responses to fine-scale oceanographic conditions: implications for the endangered African penguin, Marine Ecology Progress Series, 569, 187–203, doi:10.3354/meps12089.

- Holton, L., J. Deshayes, B.C. Backeberg, B.R. Loveday, J.C. Hermes and C.J.C. Reason 2017: Spatio-temporal characteristics of Agulhas leakage: a model intercomparison study. Climate Dynamics, 48, 2107-2121, doi:10.1007/s00382-016-3193-5.

- Barrier N., J. Deshayes, A.-M. Treguier et C. Cassou 2015 : Heat budget in the North Atlantic subpolar gyre: Impacts of atmospheric weather regimes on the 1995 warming event, Progress in Oceanography, 130 75–90, doi:10.1016/j.pocean.2014.10.001.

- Talandier C., J. Deshayes, A.-M. Treguier, X. Capet, R. Benshila, L. Debreu, R. Dussin, J.-M. Molines, G. Madec 2014 : Improvements of simulated Western North Atlantic current system and impacts on AMOC, Ocean Modelling, 76, 1-19, doi:10.1016/j.ocemod.2013.12.007.

- Barrier N., C. Cassou, J. Deshayes et A.-M. Treguier 2013 : Response of North Atlantic ocean circulation to atmospheric weather regimes, Journal of Physical Oceanography, 44, 179- 201, doi:10.1175/JPO-D-12-0217.1.
- Maze G., J. Deshayes, J. Marshall, A.-M. Treguier, L. Vollmer et A. Chronis 2013 : Surface vertical PV fluxes and subtropical mode water formation in an eddy-resolving numerical simulation, Deep Sea Research 2, 91, 128-138, doi:10.1016/j.dsr2.2013.02.026.
- Barrier N., A.-M. Treguier, C. Cassou et J. Deshayes 2012 : Impact of the winter North-Atlantic Weather Regimes on subtropical Sea-Surface Height variability, Climate Dynamics, doi:10.1007/s00382-012-1578-7.

Bibliography

Adcroft, A., Anderson, W., Balaji, V., Blanton, C., Bushuk, M., Dufour, C. O., Dunne, J. P., Griffies, S. M., Hallberg, R., Harrison, M. J., Held, I. M., Jansen, M. F., John, J. G., Krasting, J. P., Langenhorst, A. R., Legg, S., Liang, Z., McHugh, C., Radhakrishnan, A., Reichl, B. G., Rosati, T., Samuels, B. L., Shao, A., Stouffer, R., Winton, M., Wittenberg, A. T., Xiang, B., Zadeh, N., and Zhang, R. (2019). The GFDL Global Ocean and Sea Ice Model OM4.0: Model Description and Simulation Features. *Journal of Advances in Modeling Earth Systems*, 11(10):3167–3211.

Anderson, D. L. and Killworth, P. D. (1977). Spin-up of a stratified ocean, with topography. *Deep Sea Research*, 24(8):709–732.

Balaji, V. (2021). Climbing down charney's ladder: machine learning and the post-Dennard era of computational climate science. *Philosophical Transactions of the Royal Society A: Mathematical, Physical and Engineering Sciences*, 379(2194):20200085. _eprint: https://royalsocietypublishing.org/doi/pdf/10.1098/rsta.2020.0085.

Barnier, B., Madec, G., Penduff, T., Molines, J.-M., Treguier, A.-M., Le Sommer, J., Beckmann, A., Biastoch, A., Böning, C., Dengg, J., Derval, C., Durand, E., Gulev, S., Remy, E., Talandier, C., Theetten, S., Maltrud, M., McClean, J., and De Cuevas, B. (2006). Impact of partial steps and momentum advection schemes in a global ocean circulation model at eddy-permitting resolution. *Ocean Dynamics*, 56(5-6):543–567.

Barrier, N., Deshayes, J., Treguier, A.-M., and Cassou, C. (2015). Heat budget in the North Atlantic subpolar gyre: Impacts of atmospheric weather regimes on the 1995 warming event. *Progress in Oceanography*, 130:75–90.

Bauer, P., Stevens, B., and Hazeleger, W. (2021). A digital twin of Earth for the green transition. *Nature Climate Change*, 11(2):80–83.

Bolton, T. and Zanna, L. (2019). Applications of Deep Learning to Ocean Data Inference and Subgrid Parameterization. *Journal of Advances in Modeling Earth Systems*, 11(1):376–399. _eprint: https://agupubs.onlinelibrary.wiley.com/doi/pdf/10.1029/2018MS001472.

Bonnet, R., Swingedouw, D., Gastineau, G., Boucher, O., Deshayes, J., Hourdin, F., Mignot, J., Servonnat, J., and Sima, A. (2021). Increased risk of near term global warming due to a recent AMOC weakening. *Nature Communications*, 12(1):6108.

Boucher, O., Servonnat, J., Albright, A. L., Aumont, O., Balkanski, Y., Bastrikov, V., Bekki, S., Bonnet, R., Bony, S., Bopp, L., Braconnot, P., Brockmann, P., Cadule, P., Caubel, A., Cheruy, F., Codron, F., Cozic, A., Cugnet, D., D'Andrea, F., Davini, P., Lavergne, C., Denvil, S., Deshayes, J., Devilliers, M., Ducharne, A., Dufresne, J., Dupont, E., Éthé, C., Fairhead, L., Falletti, L., Flavoni, S., Foujols, M., Gardoll, S., Gastineau, G., Ghattas, J., Grandpeix, J., Guenet, B., Guez, E., L., Guilyardi, E., Guimberteau, M., Hauglustaine, D., Hourdin, F., Idelkadi, A., Joussaume, S., Kageyama, M., Khodri, M., Krinner, G., Lebas, N., Levavasseur, G., Lévy, C., Li, L., Lott, F., Lurton, T., Luyssaert, S., Madec, G., Madeleine, J., Maignan, F., Marchand, M., Marti, O., Mellul, L., Meurdesoif, Y., Mignot, J., Musat, I., Ottlé, C., Peylin, P., Planton, Y., Polcher, J., Rio, C., Rochetin, N., Rousset, C., Sepulchre, P., Sima, A., Swingedouw, D., Thiéblemont, R., Traore, A. K., Vancoppenolle, M., Vial, J., Vialard, J., Viovy, N., and Vuichard, N. (2020). Presentation and Evaluation of the IPSL-CM6A-LR Climate Model. *Journal of Advances in Modeling Earth Systems*, 12(7).

Böning, C. W., Behrens, E., Biastoch, A., Getzlaff, K., and Bamber, J. L. (2016). Emerging impact of Greenland meltwater on deepwater formation in the North Atlantic Ocean. *Nature Geoscience*, 9(7):523–527.

Böning, C. W., Bryan, F. O., Holland, W. R., and Döscher, R. (1996). Deep-Water Formation and Meridional Overturning in a High-Resolution Model of the North Atlantic. *Journal of Physical Oceanography*, 26(7):1142 – 1164. Place: Boston MA, USA Publisher: American Meteorological Society.

Böning, C. W. and Budich, R. G. (1992). Eddy Dynamics in a Primitive Equation Model: Sensitivity to Horizontal Resolution and Friction. *Journal of Physical Oceanography*, 22(4):361 – 381. Place: Boston MA, USA Publisher: American Meteorological Society.

Caesar, L., McCarthy, G. D., Thornalley, D. J. R., Cahill, N., and Rahmstorf, S. (2021). Current Atlantic Meridional Overturning Circulation weakest in last millennium. *Nature Geoscience*, 14(3):118–120.

Caesar, L., Rahmstorf, S., Robinson, A., Feulner, G., and Saba, V. (2018). Observed fingerprint of a weakening Atlantic Ocean overturning circulation. *Nature*, 556(7700):191–196.

Cessi, P. and Otheguy, P. (2003). Oceanic Teleconnections: Remote Response to Decadal Wind Forcing. *JOURNAL OF PHYSICAL OCEANOGRAPHY*, 33:14.

Cessi, P. and Primeau, F. O. (2001). Dissipative Selection of Low-Frequency Modes in a Reduced-Gravity Basin. *JOURNAL OF PHYSICAL OCEANOGRAPHY*, 31:11.

Chanut, J., Barnier, B., Large, W., Debreu, L., Penduff, T., Molines, J. M., and Mathiot, P. (2008). Mesoscale Eddies in the Labrador Sea and Their Contribution to Convection and Restratification. *Journal of Physical Oceanography*, 38(8):1617–1643.

Chérubin, L. and Richardson, P. (2007). Caribbean current variability and the influence of the Amazon and Orinoco freshwater plumes. *Deep Sea Research Part I: Oceanographic Research Papers*, 54(9):1451–1473.

Couvreux, F., Hourdin, F., Williamson, D., Roehrig, R., Volodina, V., Villefranque, N., Rio, C., Audouin, O., Salter, J., Bazile, E., Brient, F., Favot, F., Honnert, R., Lefebvre, M.-P., Madeleine, J.-B., Rodier, Q., and Xu, W. (2021). Process-Based Climate Model Development Harnessing Machine Learning: I. A Calibration Tool for Parameterization Improvement. *Journal of Advances in Modeling Earth Systems*, 13(3):e2020MS002217. _eprint: https://agupubs.onlinelibrary.wiley.com/doi/pdf/10.1029/2020MS002217.

Curry, R. (2005). Dilution of the Northern North Atlantic Ocean in Recent Decades. *Science*, 308(5729):1772–1774.

Curry, R. G. and Mccartney, M. S. (2001). Ocean Gyre Circulation Changes Associated with the North Atlantic Oscillation. *JOURNAL OF PHYSICAL OCEANOGRAPHY*, 31:27.

Danabasoglu, G., Yeager, S. G., Bailey, D., Behrens, E., Bentsen, M., Bi, D., Biastoch, A., Böning, C., Bozec, A., Canuto, V. M., Cassou, C., Chassignet, E., Coward, A. C., Danilov, S., Diansky, N., Drange, H., Farneti, R., Fernandez, E., Fogli, P. G., Forget, G., Fujii, Y., Griffies, S. M., Gusev, A., Heimbach, P., Howard, A., Jung, T., Kelley, M., Large, W. G., Leboissetier, A., Lu, J., Madec, G., Marsland, S. J., Masina, S., Navarra, A., George Nurser, A., Pirani, A., y Mélia, D. S., Samuels, B. L., Scheinert, M., Sidorenko, D., Treguier, A.-M., Tsujino, H., Uotila, P., Valcke, S., Voldoire, A., and Wang, Q. (2014). North Atlantic simulations in Coordinated Ocean-ice Reference Experiments phase II (CORE-II). Part I: Mean states. *Ocean Modelling*, 73:76–107.

de Jong, M. F. and de Steur, L. (2016). Strong winter cooling over the Irminger Sea in winter 2014-2015, exceptional deep convection, and the emergence of anomalously low SST: IRMINGER SEA COOLING AND CONVECTION. *Geophysical Research Letters*, 43(13):7106–7113.

Debreu, L., Marchesiello, P., Penven, P., and Cambon, G. (2012). Two-way nesting in split-explicit ocean models: Algorithms, implementation and validation. *Ocean Modelling*, 49-50:1–21.

Deshayes, J. (2006). Influence de la formation d'eau profonde sur la variabilité de la circulation méridienne moyenne dans l'océan Atlantique. *PhD dissertation*, page 154.

Deshayes, J., Curry, R., and Msadek, R. (2014). CMIP5 Model Intercomparison of Freshwater Budget and Circulation in the North Atlantic. *Journal of Climate*, 27(9):3298–3317.

Deshayes, J. and Frankignoul, C. (2005). Spectral Characteristics of the Response of the Meridional Overturning Circulation to Deep-Water Formation. *Journal of Physical Oceanography*, 35(10):1813–1825.

Deshayes, J. and Frankignoul, C. (2008). Simulated Variability of the Circulation in the North Atlantic from 1953 to 2003. *Journal of Climate*, 21(19):4919–4933.

Deshayes, J., Frankignoul, C., and Drange, H. (2007). Formation and export of deep water in the Labrador and Irminger Seas in a GCM. *Deep Sea Research Part I: Oceanographic Research Papers*, 54(4):510–532.

Deshayes, J., Straneo, F., and Spall, M. A. (2009). Mechanisms of variability in a convective basin. *Journal of Marine Research*, 67(3):273–303.

Deshayes, J., Tréguier, A.-M., Barnier, B., Lecointre, A., Sommer, J. L., Molines, J.-M., Penduff, T., Bourdallé-Badie, R., Drillet, Y., Garric, G., Benshila, R., Madec, G., Biastoch, A., Böning, C. W., Scheinert, M., Coward, A. C., and Hirschi, J. J.-M. (2013). Oceanic hindcast simulations at high resolution suggest that the Atlantic MOC is bistable: SIMULATED AMOC FRESHWATER TRANSPORT. *Geophysical Research Letters*, 40(12):3069–3073.

Devilliers, M., Swingedouw, D., Mignot, J., Deshayes, J., Garric, G., and Ayache, M. (2021). A realistic Greenland ice sheet and surrounding glaciers and ice caps melting in a coupled climate model. *Climate Dynamics*, 57(9):2467–2489.

Dickson, R. R. and Brown, J. (1994). The production of North Atlantic Deep Water: Sources, rates, and pathways. *Journal of Geophysical Research: Oceans*, 99(C6):12319–12341. _eprint: https://agupubs.onlinelibrary.wiley.com/doi/pdf/10.1029/94JC00530.

Eden, C. (2001). Mechanism of Interannual to Decadal Variability of the North Atlantic Circulation. *JOURNAL OF CLIMATE*, 14:15.

Eden, C. and Boning, C. (2002). Sources of Eddy Kinetic Energy in the Labrador Sea. *JOURNAL OF PHYSICAL OCEANOGRAPHY*, 32:18.

Fox-Kemper, B., Adcroft, A., Böning, C. W., Chassignet, E. P., Curchitser, E., Danabasoglu, G., Eden, C., England, M. H., Gerdes, R., Greatbatch, R. J., Griffies, S. M., Hallberg, R. W., Hanert, E., Heimbach, P., Hewitt, H. T., Hill, C. N., Komuro, Y., Legg, S., Le Sommer, J., Masina, S., Marsland, S. J., Penny, S. G., Qiao, F., Ringler, T. D., Treguier, A. M., Tsujino, H., Uotila, P., and Yeager, S. G. (2019). Challenges and Prospects in Ocean Circulation Models. *Frontiers in Marine Science*, 6:65.

Fox-Kemper, B., Danabasoglu, G., Ferrari, R., Griffies, S., Hallberg, R., Holland, M., Maltrud, M., Peacock, S., and Samuels, B. (2011). Parameterization of mixed layer eddies. III: Implementation and impact in global ocean climate simulations. *Ocean Modelling*, 39(1-2):61–78.

Frankignoul, C., Deshayes, J., and Curry, R. (2009). The role of salinity in the decadal variability of the North Atlantic meridional overturning circulation. *Climate Dynamics*, 33(6):777–793.

Frankignoul, C. and Hasselmann, K. (1977). Stochastic climate models, Part II Application to sea-surface temperature anomalies and thermocline variability. *Tellus*, 29(4):289–305.

Furevik, T., Bentsen, M., Drange, H., Kindem, I. K. T., Kvamsto, N. G., and Sorteberg, A. (2003). Description and evaluation of the bergen climate model: ARPEGE coupled with MICOM. *Climate Dynamics*, 21(1):27–51.

Ganachaud, A. and Wunsch, C. (2003). Large-Scale Ocean Heat and Freshwater Transports during the World Ocean Circulation Experiment. *JOURNAL OF CLIMATE*, 16:10.

Gates, W. L. (1992). AMIP: The Atmospheric Model Intercomparison Project. *Bulletin of the American Meteorological Society*, 73(12):1962–1970.

Gent, P. R. and Mcwilliams, J. C. (1990). Isopycnal Mixing in Ocean Circulation Models. *Journal of Physical Oceanography*, 20(1):150 – 155. Place: Boston MA, USA Publisher: American Meteorological Society.

Griffies, S. M., Biastoch, A., Böning, C., Bryan, F., Danabasoglu, G., Chassignet, E. P., England, M. H., Gerdes, R., Haak, H., Hallberg, R. W., Hazeleger, W., Jungclaus, J., Large, W. G., Madec, G., Pirani, A., Samuels, B. L., Scheinert, M., Gupta, A. S., Severijns, C. A., Simmons, H. L., Treguier, A. M., Winton, M., Yeager, S., and Yin, J. (2009). Coordinated Ocean-ice Reference Experiments (COREs). *Ocean Modelling*, 26(1-2):1–46.

Griffies, S. M., Danabasoglu, G., Durack, P. J., Adcroft, A. J., Balaji, V., Böning, C. W., Chassignet, E. P., Curchitser, E., Deshayes, J., Drange, H., Fox-Kemper, B.,

Gleckler, P. J., Gregory, J. M., Haak, H., Hallberg, R. W., Heimbach, P., Hewitt, H. T., Holland, D. M., Ilyina, T., Jungclaus, J. H., Komuro, Y., Krasting, J. P., Large, W. G., Marsland, S. J., Masina, S., McDougall, T. J., Nurser, A. J. G., Orr, J. C., Pirani, A., Qiao, F., Stouffer, R. J., Taylor, K. E., Treguier, A. M., Tsujino, H., Uotila, P., Valdivieso, M., Wang, Q., Winton, M., and Yeager, S. G. (2016). OMIP contribution to CMIP6: experimental and diagnosticprotocol for the physical component of the Ocean Model Intercomparison Project. *Geoscientific Model Development*, 9(9):3231–3296.

Haine, T. W. N. (2016). Vagaries of Atlantic overturning. *Nature Geoscience*, 9(7):479–480.

Hakkinen, S. (2004). Decline of Subpolar North Atlantic Circulation During the 1990s. *Science*, 304(5670):555–559.

Hallberg, R. (2013). Using a resolution function to regulate parameterizations of oceanic mesoscale eddy effects. *Ocean Modelling*, 72:92–103.

Hatun, H. (2005). Influence of the Atlantic Subpolar Gyre on the Thermohaline Circulation. *Science*, 309(5742):1841–1844.

Hausmann, U., Sallée, J.-B., Jourdain, N. C., Mathiot, P., Rousset, C., Madec, G., Deshayes, J., and Hattermann, T. (2020). The Role of Tides in Ocean-Ice Shelf Interactions in the Southwestern Weddell Sea. *Journal of Geophysical Research: Oceans*, 125(6):e2019JC015847. _eprint: https://agupubs.onlinelibrary.wiley.com/doi/pdf/10.1029/2019JC015847.

Hawkins, E., Smith, R. S., Allison, L. C., Gregory, J. M., Woollings, T. J., Pohlmann, H., and de Cuevas, B. (2011). Bistability of the Atlantic overturning circulation in a global climate model and links to ocean freshwater transport: BISTABILITY OF THE ATLANTIC MOC. *Geophysical Research Letters*, 38(10):n/a–n/a.

Holmes, R. M., Zika, J. D., Griffies, S. M., Hogg, A. M., Kiss, A. E., and England, M. H. (2021). The Geography of Numerical Mixing in a Suite of Global Ocean Models. *Journal of Advances in Modeling Earth Systems*, 13(7).

Holton, L., Deshayes, J., Backeberg, B. C., Loveday, B. R., Hermes, J. C., and Reason, C. J. C. (2017). Spatio-temporal characteristics of Agulhas leakage: a model intercomparison study. *Climate Dynamics*, 48(7-8):2107–2121.

Hourdin, F., Mauritsen, T., Gettelman, A., Golaz, J.-C., Balaji, V., Duan, Q., Folini, D., Ji, D., Klocke, D., Qian, Y., Rauser, F., Rio, C., Tomassini, L., Watanabe, M., and Williamson, D. (2017). The Art and Science of Climate Model Tuning. *Bulletin of the American Meteorological Society*, 98(3):589–602.

Hourdin, F., Williamson, D., Rio, C., Couvreux, F., Roehrig, R., Villefranque, N., Musat, I., Fairhead, L., Diallo, F. B., and Volodina, V. (2021). Process-Based Climate Model Development Harnessing Machine Learning: II. Model Calibration From Single Column to Global. *Journal of Advances in Modeling Earth Systems*, 13(6):e2020MS002225. _eprint: https://agupubs.onlinelibrary.wiley.com/doi/pdf/10.1029/2020MS002225.

Huang, R. X., Cane, M. A., Naik, N., and Goodman, P. (2000). Global adjustment of the thermocline in response to deepwater formation. *Geophysical Research Letters*, 27(6):759–762.

Hutchinson, K., Beal, L. M., Penven, P., Ansorge, I., and Hermes, J. (2018). Seasonal Phasing of Agulhas Current Transport Tied to a Baroclinic Adjustment of Near-Field Winds. *Journal of Geophysical Research: Oceans*, 123(10):7067–7083.

Hutchinson, K., Deshayes, J., Sallee, J.-B., Dowdeswell, J. A., de Lavergne, C., Ansorge, I., Luyt, H., Henry, T., and Fawcett, S. E. (2020). Water Mass Characteristics and Distribution Adjacent to Larsen C Ice Shelf, Antarctica. *Journal of Geophysical Research: Oceans*, 125(4):e2019JC015855. _eprint: https://agupubs.onlinelibrary.wiley.com/doi/pdf/10.1029/2019JC015855.

Jiang, W., Gastineau, G., and Codron, F. (2021). Multicentennial Variability Driven by Salinity Exchanges Between the Atlantic and the Arctic Ocean in a Coupled Climate Model. *Journal of Advances in Modeling Earth Systems*, 13(3).

Johnson, H. L. and Marshall, D. P. (2002). A Theory for the Surface Atlantic Response to Thermohaline Variability. *JOURNAL OF PHYSICAL OCEANOGRAPHY*, 32:12.

Jouanno, J., Sheinbaum, J., Barnier, B., Molines, J.-M., Debreu, L., and Lemarié, F. (2008). The mesoscale variability in the Caribbean Sea. Part I: Simulations and characteristics with an embedded model. *Ocean Modelling*, 23(3-4):82–101.

Katsman, C. A., Spall, M. A., and Pickart, R. S. (2004). Boundary Current Eddies and Their Role in the restratification of the Labrador Sea. *JOURNAL OF PHYSICAL OCEANOGRAPHY*, 34:17.

Kawase, M. (1987). Establishment of Deep Ocean Circulation Driven by Deep-Water Production. *Journal of Physical Oceanography*, 17(12):2294–2317.

Lacasce, J. H. (2000). Floats and <I>f</I>/<I>H</I>. *Journal of Marine Research*, 58(1):61–95.

LaCasce, J. H. and Pedlosky, J. (2004). The Instability of Rossby Basin Modes and the Oceanic Eddy Field*. *Journal of Physical Oceanography*, 34(9):2027–2041.

Large, W. and Yeager, S. (2004). Spectral analysis for physical applications : Multitaper and conventional univariate techniques. *NCAR Technical Note: NCAR/TN-460+STR. CGD Division of the National Center for Atmospheric Research.*

Lavergne, C. d., Falahat, S., Madec, G., Roquet, F., Nycander, J., and Vic, C. (2019). Toward global maps of internal tide energy sinks. *Ocean Modelling*, 137:52–75.

Levier, B., Tréguier, A.-M., Madec, G., and Garnier, V. (2007). Free surface and variable volume in the nemo code. Marine EnviRonment and Security for the European Area or MERSEA research project was co-funded by the European Commission (grant agreement ID 502885), under the 6th Framework Programme in Aeronautics and Space for Ocean and Marine applications on the period 2004-2008.

Lilly, J. M., Rhines, P. B., Schott, F., Lavender, K., Lazier, J., Send, U., and D'Asaro, E. (2003). Observations of the Labrador Sea eddy field. *Progress in Oceanography*, 59(1):75–176.

Longuet-Higgins, M. S. (1968). On the trapping of waves along a discontinuity of depth in a rotating ocean. *Journal of Fluid Mechanics*, 31(3):417–434.

Lorenz, E. N. (1996). Predictability - a problem partly solved, in predictability of weather and climate, ed. tim palmer and renate hagedorn. published by cambridge university press, 2006.

Lozier, M. S., Li, F., Bacon, S., Bahr, F., Bower, A. S., Cunningham, S. A., de Jong, M. F., de Steur, L., deYoung, B., Fischer, J., Gary, S. F., Greenan, B. J. W., Holliday, N. P., Houk, A., Houpert, L., Inall, M. E., Johns, W. E., Johnson, H. L., Johnson, C., Karstensen, J., Koman, G., Le Bras, I. A., Lin, X., Mackay, N., Marshall, D. P., Mercier, H., Oltmanns, M., Pickart, R. S., Ramsey, A. L., Rayner, D., Straneo, F., Thierry, V., Torres, D. J., Williams, R. G., Wilson, C., Yang, J., Yashayaev, I., and Zhao, J. (2019). A sea change in our view of overturning in the subpolar North Atlantic. *Science*, 363(6426):516–521.

Lévy, M., Mémery, L., and Madec, G. (1998). The onset of a bloom after deep winter convection in the northwestern Mediterranean sea: mesoscale process study with a primitive equation model. *Journal of Marine Systems*, 16(1-2):7–21.

Lévy, M., Resplandy, L., and Lengaigne, M. (2014). Oceanic mesoscale turbulence drives large biogeochemical interannual variability at middle and high latitudes. *Geophysical Research Letters*, 41(7):2467–2474.

Mahadevan, A., D'Asaro, E., Lee, C., and Perry, M. J. (2012). Eddy-Driven Stratification Initiates North Atlantic Spring Phytoplankton Blooms. *Science*, 337(6090):54–58.

Mailler, S., Pennel, R., Menut, L., and Lachâtre, M. (2021). Using the Després and Lagoutière (1999) antidiffusive transport scheme: a promising and novel method against excessive vertical diffusion in chemistry-transport models. *Geoscientific Model Development*, 14(4):2221–2233.

Mak, M. and Cai, M. (1989). Local Barotropic Instability. *Journal of Atmospheric Sciences*, 46(21):3289 – 3311. Place: Boston MA, USA Publisher: American Meteorological Society.

Marshall, J., Hill, C., Perelman, L., and Adcroft, A. (1997). Hydrostatic, quasi-hydrostatic, and nonhydrostatic ocean modeling. *Journal of Geophysical Research: Oceans*, 102(C3):5733–5752. _eprint: https://agupubs.onlinelibrary.wiley.com/doi/pdf/10.1029/96JC02776.

Marshall, J. and Schott, F. (1999). Open-ocean convection: Observations, theory, and models. *Reviews of Geophysics*, 37(1):1–64.

Mathiot, P., Jenkins, A., Harris, C., and Madec, G. (2017). Explicit representation and parametrised impacts of under ice shelf seas in the $z^\ast$ coordinate ocean model NEMO 3.6. *Geoscientific Model Development*, 10(7):2849–2874.

Maze, G., Deshayes, J., Marshall, J., Tréguier, A.-M., Chronis, A., and Vollmer, L. (2013). Surface vertical PV fluxes and subtropical mode water formation in an eddy-resolving numerical simulation. *Deep Sea Research Part II: Topical Studies in Oceanography*, 91:128–138.

McManus, J. F., Francois, R., Gherardi, J.-M., Keigwin, L. D., and Brown-Leger, S. (2004). Collapse and rapid resumption of Atlantic meridional circulation linked to deglacial climate changes. *Nature*, 428(6985):834–837.

Mignot, J. and Frankignoul, C. (2005). The Variability of the Atlantic Meridional Overturning Circulation, the North Atlantic Oscillation, and the El Niño–Southern Oscillation in the Bergen Climate Model. *Journal of Climate*, 18(13):2361–2375.

Mignot, J., Hourdin, F., Deshayes, J., Boucher, O., Gastineau, G., Musat, I., Vancoppenolle, M., Servonnat, J., Caubel, A., Chéruy, F., Denvil, S., Dufresne, J., Ethé, C., Fairhead, L., Foujols, M., Grandpeix, J., Levavasseur, G., Marti, O., Menary, M., Rio, C., Rousset, C., and Silvy, Y. (2021). The Tuning Strategy of IPSL-CM6A-LR. *Journal of Advances in Modeling Earth Systems*, 13(5).

Mignot, J., Swingedouw, D., Deshayes, J., Marti, O., Talandier, C., Séférian, R., Lengaigne, M., and Madec, G. (2013). On the evolution of the oceanic component of the IPSL climate models from CMIP3 to CMIP5: A mean state comparison. *Ocean Modelling*, 72:167–184.

Moat, B. I., Smeed, D. A., Frajka-Williams, E., Desbruyères, D. G., Beaulieu, C., Johns, W. E., Rayner, D., Sanchez-Franks, A., Baringer, M. O., Volkov, D., Jackson, L. C., and Bryden, H. L. (2020). Pending recovery in the strength of the meridional overturning circulation at 26n. *Ocean Science*, 16(4):863–874.

Penven, P., Herbette, S., and Rouault, M. (2011). Ocean modelling in the agulhas current system. In *Proc. Nansen-Tutu Conf*, pages 17–21.

Pickart, R. S. and Spall, M. A. (2007). Impact of Labrador Sea Convection on the North Atlantic Meridional Overturning Circulation. *Journal of Physical Oceanography*, 37(9):2207–2227.

Primeau, F. (2002). Long Rossby Wave Basin-Crossing Time and the Resonance of Low-Frequency Basin Modes. *Journal of Physical Oceanography*, 32(9):2652 – 2665. Place: Boston MA, USA Publisher: American Meteorological Society.

Rahmstorf, S. (1996). On the freshwater forcing and transport of the Atlantic thermohaline circulation:. *Climate Dynamics*, 12(12):799–811.

Rahmstorf, S., Box, J. E., Feulner, G., Mann, M. E., Robinson, A., Rutherford, S., and Schaffernicht, E. J. (2015). Exceptional twentieth-century slowdown in Atlantic Ocean overturning circulation. *Nature Climate Change*, 5(5):475–480.

Renault, L., McWilliams, J. C., and Penven, P. (2017). Modulation of the Agulhas Current Retroflection and Leakage by Oceanic Current Interaction with the Atmosphere in Coupled Simulations. *Journal of Physical Oceanography*, 47(8):2077–2100.

Reverdin, G. (2003). North Atlantic Ocean surface currents. *Journal of Geophysical Research*, 108(C1):3002.

Robson, J., Ortega, P., and Sutton, R. (2016). A reversal of climatic trends in the North Atlantic since 2005. *Nature Geoscience*, 9(7):513–517.

Roquet, F., Madec, G., Brodeau, L., and Nycander, J. (2015). Defining a Simplified Yet "Realistic" Equation of State for Seawater. *Journal of Physical Oceanography*, 45(10):2564–2579.

Rousset, C., Vancoppenolle, M., Madec, G., Fichefet, T., Flavoni, S., Barthélemy, A., Benshila, R., Chanut, J., Levy, C., Masson, S., and Vivier, F. (2015). The Louvain-La-Neuve sea ice model LIM3.6: global and regional capabilities. *Geoscientific Model Development*, 8(10):2991–3005.

Sabine, C. L., Feely, R. A., Gruber, N., Key, R. M., Lee, K., Bullister, J. L., Wanninkhof, R., Wong, C. S., Wallace, D. W. R., Tilbrook, B., Millero, F. J., Peng, T.-H., Kozyr,

A., Ono, T., and Rios, A. F. (2004). The Oceanic Sink for Anthropogenic CO $_2$. *Science*, 305(5682):367–371.

Sarafanov, A., Falina, A., Mercier, H., Sokov, A., Lherminier, P., Gourcuff, C., Gladyshev, S., Gaillard, F., and Daniault, N. (2012). Mean full-depth summer circulation and transports at the northern periphery of the Atlantic Ocean in the 2000s: NORTHERN ATLANTIC CIRCULATION IN 2000s. *Journal of Geophysical Research: Oceans*, 117(C1).

Schott, F. A., Fischer, J., Dengler, M., and Zantopp, R. (2006). Variability of the Deep Western Boundary Current east of the Grand Banks. *Geophysical Research Letters*, 33(21):L21S07.

Smeed, D. A., Josey, S. A., Beaulieu, C., Johns, W. E., Moat, B. I., Frajka-Williams, E., Rayner, D., Meinen, C. S., Baringer, M. O., Bryden, H. L., and McCarthy, G. D. (2018). The North Atlantic Ocean Is in a State of Reduced Overturning. *Geophysical Research Letters*, 45(3):1527–1533.

Smeed, D. A., McCarthy, G. D., Cunningham, S. A., Frajka-Williams, E., Rayner, D., Johns, W. E., Meinen, C. S., Baringer, M. O., Moat, B. I., Duchez, A., and Bryden, H. L. (2014). Observed decline of the Atlantic meridional overturning circulation 2004–2012. *Ocean Science*, 10(1):29–38.

Spall, M. A. (2004). Boundary Currents and Watermass Transformation in Marginal Seas. *JOURNAL OF PHYSICAL OCEANOGRAPHY*, 34:17.

Stommel, H. and Arons, A. (1959). On the abyssal circulation of the world ocean—I. Stationary planetary flow patterns on a sphere. *Deep Sea Research (1953)*, 6:140–154.

Straneo, F. (2006a). Heat and Freshwater Transport through the Central Labrador Sea. *Journal of Physical Oceanography*, 36(4):606 – 628. Place: Boston MA, USA Publisher: American Meteorological Society.

Straneo, F. (2006b). On the Connection between Dense Water Formation, Overturning, and Poleward Heat Transport in a Convective Basin. *Journal of Physical Oceanography*, 36(9):1822–1840.

Swingedouw, D., Braconnot, P., Delecluse, P., Guilyardi, E., and Marti, O. (2006). The impact of global freshwater forcing on the thermohaline circulation: adjustment of North Atlantic convection sites in a CGCM. *Climate Dynamics*, 28(2-3):291–305.

Talandier, C., Deshayes, J., Treguier, A.-M., Capet, X., Benshila, R., Debreu, L., Dussin, R., Molines, J.-M., and Madec, G. (2014). Improvements of simulated Western North Atlantic current system and impacts on the AMOC. *Ocean Modelling*, 76:1–19.

Treguier, A. M., Deshayes, J., Lique, C., Dussin, R., and Molines, J. M. (2012). Eddy contributions to the meridional transport of salt in the North Atlantic: EDDY TRANSPORT OF SALT. *Journal of Geophysical Research: Oceans*, 117(C5):n/a–n/a.

Voldoire, A., Sanchez-Gomez, E., Salas y Mélia, D., Decharme, B., Cassou, C., Sénési, S., Valcke, S., Beau, I., Alias, A., Chevallier, M., Déqué, M., Deshayes, J., Douville, H., Fernandez, E., Madec, G., Maisonnave, E., Moine, M.-P., Planton, S., Saint-Martin, D., Szopa, S., Tyteca, S., Alkama, R., Belamari, S., Braun, A., Coquart, L., and Chauvin, F. (2013). The CNRM-CM5.1 global climate model: description and basic evaluation. *Climate Dynamics*, 40(9-10):2091–2121.

von Schuckmann, K., Le Traon, P.-Y., Smith, N., Pascual, A., Brasseur, P., Fennel, K., Djavidnia, S., Aaboe, S., Fanjul, E. A., Autret, E., Axell, L., Aznar, R., Benincasa, M., Bentamy, A., Boberg, F., Bourdallé-Badie, R., Nardelli, B. B., Brando, V. E., Bricaud, C., Breivik, L.-A., Brewin, R. J., Capet, A., Ceschin, A., Ciliberti, S., Cossarini, G., de Alfonso, M., de Pascual Collar, A., de Kloe, J., Deshayes, J., Desportes, C., Drévillon, M., Drillet, Y., Droghei, R., Dubois, C., Embury, O., Etienne, H., Fratianni, C., Lafuente, J. G., Sotillo, M. G., Garric, G., Gasparin, F., Gerin, R., Good, S., Gourrion, J., Grégoire, M., Greiner, E., Guinehut, S., Gutknecht, E., Hernandez, F., Hernandez, O., Høyer, J., Jackson, L., Jandt, S., Josey, S., Juza, M., Kennedy, J., Kokkini, Z., Korres, G., Kõuts, M., Lagemaa, P., Lavergne, T., le Cann, B., Legeais, J.-F., Lemieux-Dudon, B., Levier, B., Lien, V., Maljutenko, I., Manzano, F., Marcos, M., Marinova, V., Masina, S., Mauri, E., Mayer, M., Melet, A., Mélin, F., Meyssignac, B., Monier, M., Müller, M., Mulet, S., Naranjo, C., Notarstefano, G., Paulmier, A., Gomez, B. P., Gonzalez, I. P., Peneva, E., Perruche, C., Andrew Peterson, K., Pinardi, N., Pisano, A., Pardo, S., Poulain, P.-M., Raj, R. P., Raudsepp, U., Ravdas, M., Reid, R., Rio, M.-H., Salon, S., Samuelsen, A., Sammartino, M., Sammartino, S., Sandø, A. B., Santoleri, R., Sathyendranath, S., She, J., Simoncelli, S., Solidoro, C., Stoffelen, A., Storto, A., Szerkely, T., Tamm, S., Tietsche, S., Tinker, J., Tintore, J., Trindade, A., van Zanten, D., Vandenbulcke, L., Verhoef, A., Verbrugge, N., Viktorsson, L., von Schuckmann, K., Wakelin, S. L., Zacharioudaki, A., and Zuo, H. (2018). Copernicus Marine Service Ocean State Report. *Journal of Operational Oceanography*, 11(sup1):S1–S142.

Von Storch, J.-S. (2000). Variability of Deep-Ocean Mass Transport: Spectral Shapes and Spatial Scales. *JOURNAL OF CLIMATE*, 13:20.

Weaver, A. J., Sedláček, J., Eby, M., Alexander, K., Crespin, E., Fichefet, T., Philippon-Berthier, G., Joos, F., Kawamiya, M., Matsumoto, K., Steinacher, M., Tachiiri, K., Tokos, K., Yoshimori, M., and Zickfeld, K. (2012). Stability of the Atlantic meridional overturning circulation: A model intercomparison. *Geophysical Research Letters*, 39(20):2012GL053763.

Williamson, D., Goldstein, M., Allison, L., Blaker, A., Challenor, P., Jackson, L., and Yamazaki, K. (2013). History matching for exploring and reducing climate model parameter space using observations and a large perturbed physics ensemble. *Climate Dynamics*, 41(7):1703–1729.

Williamson, D. B., Blaker, A. T., and Sinha, B. (2017). Tuning without over-tuning: parametric uncertainty quantification for the NEMO ocean model. *Geoscientific Model Development*, 10(4):1789–1816.

Worthington, E. L., Moat, B. I., Smeed, D. A., Mecking, J. V., Marsh, R., and McCarthy, G. D. (2021). A 30-year reconstruction of the Atlantic meridional overturning circulation shows no decline. *Ocean Science*, 17(1):285–299.

Wu, P. and Wood, R. (2008). Convection induced long term freshening of the subpolar North Atlantic Ocean. *Climate Dynamics*, 31(7-8):941–956.

Yashayaev, I. and Loder, J. W. (2016). Recurrent replenishment of Labrador Sea Water and associated decadal-scale variability: 2015 Convection in Labrador Sea. *Journal of Geophysical Research: Oceans*, 121(11):8095–8114.

Zhang, R., Sutton, R., Danabasoglu, G., Kwon, Y., Marsh, R., Yeager, S. G., Amrhein, D. E., and Little, C. M. (2019). A Review of the Role of the Atlantic Meridional Overturning Circulation in Atlantic Multidecadal Variability and Associated Climate Impacts. *Reviews of Geophysics*, 57(2):316–375.

Østerhus, S., Woodgate, R., Valdimarsson, H., Turrell, B., de Steur, L., Quadfasel, D., Olsen, S. M., Moritz, M., Lee, C. M., Larsen, K. M. H., Jónsson, S., Johnson, C., Jochumsen, K., Hansen, B., Curry, B., Cunningham, S., and Berx, B. (2019). Arctic Mediterranean exchanges: a consistent volume budget and trends in transports from two decades of observations. *Ocean Science*, 15(2):379–399.